Experimental Investigation of the Effect of Axial Vibration Generated By Pressure Pulses on Drilling Performance

By

© Ahmed Elnahas

A Thesis submitted to the

School of Graduate Studies

in partial fulfillment of the requirements for the degree of

Master of Engineering

Faculty of Engineering and Applied Sciences

Memorial University of Newfoundland

October 2014

St. John's Newfoundland

ABSTRACT

Considering the fact that improving drilling efficiency contributes to the industry success, many academic organizations, industrial research organizations and companies have invested in research that leads to better drilling experience, time wise and efficiency wise. This thesis is a research based study that aims to find new methods to improve drilling efficiency. The study investigates the effect of vibration generated using periodic pressure pulses created at the bit by a down-hole tool on the drilling efficiency, and in fact demonstrates that the technology can improve drilling efficiency. The study is based on various sets of laboratory experiments, which were conducted to characterize the functionality of a Pressure Pulses Generating (PPG) down-hole tool, and to test the effect of the down-hole tool output on actual drilling experiments. Two different setups were used to conduct the experiments in laboratory environment. In the drilling experiments synthetic rock was used as test specimens with highly controlled properties and strength. The drilling experiments were conducted at different simulated down-hole condition, including bottom hole pressures, and different fluid flow rates.

The study also highlighted the effect of varying the drill string compliance on the overall effect of induced down-hole axial vibration. Finally the study sets base for further investigation and experiment that will be conducted using a bigger scale setup similar to land drill rigs.

ACKNOWLEDGEMENTS

I would like to express my genuine gratitude to my supervisor professor Stephen Butt for his valuable guidance, constant encouragement, and support, without which I could not have completed this program. I would also like to thank the project managers and engineers, Farid Arvani, and Brock Gillis, for their assistance with various technical issues, equipment ordering and useful suggestions and comments regarding the project.

I would like to thank my mother, my wife and my two little boys for giving me the strength to complete my studies and giving me the support I needed to do all what I could do to complete my program. I would like to thank all current and previous members of the Advanced Drilling Group for their cooperation, support and friendly environment. Special thanks to Hossein Khorshidian, Sadegh Babapour, Yousef Gharibiyamchi, Pushpinder Singh Rana, Masoud Khademi and Qian Gao for assistance with experiments and data analysis.

Finally I want to thank all Technical Services personnel, David Snook and Ron Monks, for their help, advice and assistance.

This research was conducted at the Advanced Drilling Technology Laboratory at Memorial University of Newfoundland and was funded by the Atlantic Canada Opportunities Agency (AIF Contract no. 781-2636-1920044), the Research and Development Corporation of Newfoundland and Labrador, Husky Energy, and Suncor Energy.

Table of Contents

List of Tables

List of Figures

List of Symbols, Nomenclature or Abbreviations

ADG	Advanced Drilling Group
AGT	Axial oscillation Generating Tool
BHA	Bottom Hole Assembly
BHC	Bottom Hole Cleaning
BP	British Petroleum
CPF	Cost Per Foot
DAQ	Data Acquisition
DOC	Depth Of Cut
EOR	Enhanced Oil Recovery
FPD	Feet Per Day
INPT	Invisible Non Productive Time
LPM	Liter Per Minute
LVDT	Linear Variable Displacement Transducer
LWD	Logging While Drilling
MSE	Mechanical Specific Energy
MWD	Measurement While Drilling
NOV	National Oil Well Varco
NPT	Non Productive Time
OD	Outside Diameter
PDC	Poly Crystalline Diamond Compact
POOH	Poll Out Of Hole

PPG	Pressure Pulses Generator
PQ	Performance Qualifiers
RIH	Run In Hole
ROP	Rate of Penetration
ROPav	average Rate of Penetration
ROPi	instantaneous Rate Of Penetration
RPM	Revolutions Per Minute
TD	Total Depth
UCS	Unconfined Compressive Strength
USGPM	United States Gallon Per Minute
VARD	Vibration Assisted Rotary Drilling
WOB	Weight On Bit

Note on the Used Units

Two measurement unit systems were used in this thesis: S.I. and traditional (Imperial and American). In some cases traditional units were chosen due to several reasons:

- This study is oriented to the drilling engineering branch of the petroleum industry in North America, where imperial units are commonly used by engineers;
- many American Petroleum Institute (API) standards contain non-S.I. units, as well as industrial drilling equipment specifications presented in imperial units, such as drill string components and drill bits;
- the majority of reviewed publications in the drilling engineering field present results in imperial units.

Considering mentioned points, it was decided to give preference to imperial units; however, in some cases S.I. units were used, where this system was more applicable. The table of conversion presents conversion factors for non-S.I. units used.

Table of conversion: imperial to metric

Imperial	Multiplying factor	Metric
US-GPM	0.0000631	m^3/s
psi	6895	Pa
in	0.0254	M
feet	0.3048	M
lbs (mass)	0.4536	Kg

List of Appendices

1 Introduction

1.1 Introduction

Oil and gas have been indispensible sources of energy for centuries. The first oil wells were drilled in China in the 4th century, they used oil to evaporate brine and produce salt. The Chinese drilled wells that had depths up to 243 meters by using bamboo poles and bits attached to them. In the modern era, the first oil well was drilled in 1848 by the Russian engineer F.N Semoyonov, on the Aspheron peninsula north-east of Baku, followed by Poland's Ignacy Lukasiewicz who discovered a means of refining kerosene from petroleum oil in 1852.

These discoveries spread all over the world; consequently the first commercial oil well was drilled in North America in Oil Springs, Ontario, Canada in 1858, dug by James Miller Williams.

The Americans started their petroleum industry with Edwin Drake's discovery of oil near Titusville, Pennsylvania. The oil industry grew slowly in the 19th century driven by the need of kerosene to operate kerosene lamps. However, when the internal combustion engine was introduced in the early 1900s, the oil industry started growing rapidly to provide the world with the fuel and industrial materials that develop the modern civilization [1].

British Petroleum (BP) published a recent report named 'Energy outlook 2030' describing the current and future demand for oil and gas products, they expected a 36% increase of world need of oil and gas between 2011 and 2030 [2].

Major players in the industry keep trying to enhance the current technologies and introduce new technologies in different fields to fulfill the growing demand, that includes efforts such as increasing the volume of hydrocarbon recovered from reservoirs using Enhanced Oil Recovery methods (EOR), investing in infrastructure for Liquefied Natural Gas (LNG) and certainly increasing the drilling efficiency to produce more hydrocarbons using the same available resources.

By taking a closer look on the drilling operation, it's easy to realize how costly it is and just like any industry, cost is the main factor that drives operations and sets their limits. Rigzone [3] gives an idea about the daily rate of offshore drilling rigs, which is so far the biggest part of the overall cost associated with drilling operations. The source indicated that the daily rate of a small jack up rig capable of drilling in water depth of 200' ranges between $75,000 to $100,000 per day, while the average rate of a semisubmersible rig capable of drilling in water depth of 4000' is about $440,000 a day. It's clear that reducing drilling time consequently decreases the overall drilling cost and a better understanding of managing rig time leads to a better drilling efficiency.

Rig Time can be classified into three main times, drilling time which is the time consumed when the bit is penetrating the formation to intersect a geological target at a certain depth, non drilling time which is the time consumed while tripping in or out of the well or when performing an operation like cementing or casing as an example, and Non

Productive Time (NPT) which is the time creditable to events in drilling that delay the progress of the planned activities, that includes unnecessary trips to change bits , failed down-hole tools, a rig mechanical failure or other events that are not supposed to happen in the first place.

Non productive time can be unnoticeable sometimes and hard to recognize, in such case it's called Invisible Non Productive Time (INPT), an example for INPT is the time lost when drilling extremely abrasive formation using an improper drilling method, using a wrong type of drill bits or applying improper drilling parameters which lead to excessive wear of the bit and bit failure.

As shown if Figure 1.1, Vieira [4] explained the effect of INPT on the drilling time and the overall drilling cost of a well drilled in the Middle East. Clearly, identifying NPT and introducing methods to eliminate it serves reducing the overall cost of wells and consequently directing the extra spending to develop other wells or exploring other fields.

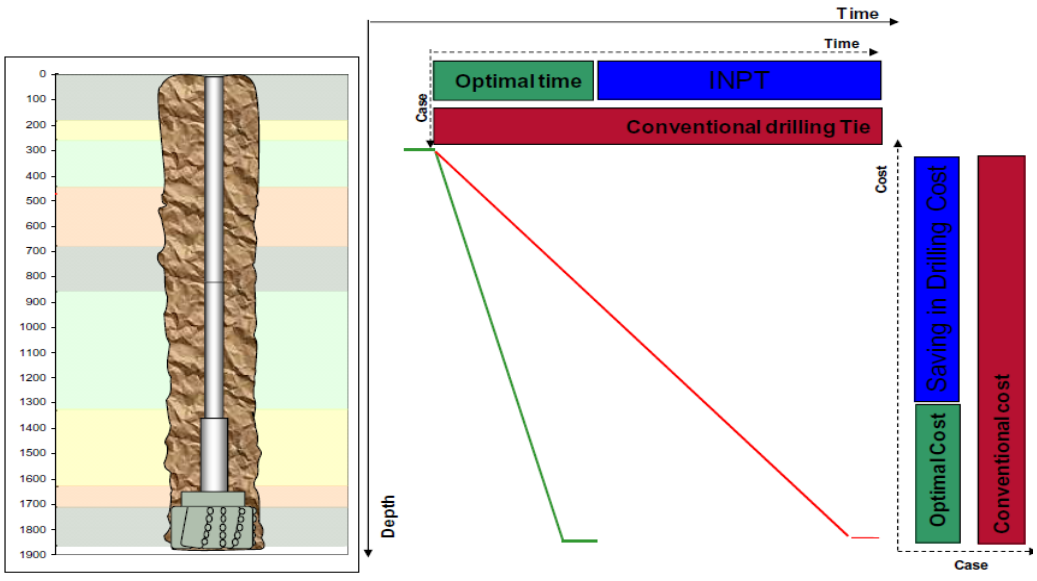

Figure 1.1- Effect of INPT on drilling Time and Well cost after Vieira [4]

Research has been done and is currently on going in many countries to optimize drilling time and eliminate NPT. One way of optimizing drilling time is to develop technologies and theories to enhance the rate of penetration in the drilling phase of the well.

This thesis is a contribution from the author to the efforts done in that field of research as a part of a group that has several publications and work done in the drilling optimization area of research, these publications are discussed in Chapter 2 of the thesis.

1.2 Research Scope and objective

In 2008, the Memorial University of Newfoundland started a project under the supervision of Prof. Stephen Butt to study the promising technology of utilizing vibrations to increase drilling rate of penetration.

Prof. Butt formed the Advanced Drilling Group (ADG) to investigate and introduce the Vibration Assisted Rotary Drilling (VARD) Technology, and several publications were published by graduate students from the group under the supervision of Prof. Butt.

This thesis investigates the effect of pressure pulses generated by a down-hole tool as a source of vibration when integrated to the drilling assembly right behind the drill bit. Tools similar to the Pressure Pulse Generator (PPG) have been used in other applications to reduce the friction within the Bottom Hole Assembly (BHA), but for the first time the PPG is used as a source of vibration, utilizing the generated sinusoidal forces from the pressure pulses coupled with a compliant element in the BHA to convert the axial force into axial displacement.

Previous work done by the ADG and others has shown that axial vibration displacement has had a positive effect on increasing the drilling efficiency in general.

The objective of this thesis is to investigate the effect of the vibrations generated by the PPG on the drilling performance by conducting laboratory experiments using a sophisticated experimental setup which can help to clearly observe the effect of the tool on drilling performance.

1.3 Significance of Research

As mentioned earlier, the research mainly benefits the efforts to minimize drilling time and in turn minimize the overall cost of drilling.

The work presented in this thesis shows that the existent pressure pulses generating technology could be used to introduce new applications and benefits to the drilling operation. Also, the laboratory drilling experiments consider and verify the role of a very important drilling parameter which is the near bit drill-string compliance, a parameter that was extensively studied by the ADG in past literature and experiments but never been addressed to the author's knowledge in research or literature before the VARD project was launched.

1.4 Thesis Outline

The thesis consists of 6 chapters in which all the work done by the author is presented.

In Chapter 2, the research done in areas related to the thesis topic is discussed to give the reader an overall view of the objective of this study. Also the existent down-hole systems that utilize vibration and dynamic forces are presented to give the reader an idea about the progress of the technology, and both the positive and negative sides of each concept.

In Chapter 3, The Pressure Pulse Generator (PPG) concept and operational mechanism are presented. The chapter also includes details about an experimental setup that was used to analyse the tool's performance and the forces generated at different modes of operation, in addition to the experiments matrix and procedures followed .

In Chapter 4, the results of the experiments done to characterize the PPG are discussed thoroughly. In Chapter 5, Laboratory drilling experiments are discussed in details, including the experimental setup, sensors, the synthetic rock used for drilling, variable parameters like WOB, flow rate, BHP and compliance levels and also the constant parameters used in the experiments. In Chapter 6, the results of the drilling experiments are discussed in detail showing the contribution of each parameter to the drilling process.

In Chapter 7, a summary of the whole study is presented, showing conclusions and the positive and negative impressions about the experimental results, and the recommended future work to achieve a full awareness of the effect of the pressure pulses as a source of vibration to enhance the drilling experience.

2 Literature Review

In this chapter, publications from different sources are briefly presented to help the reader get a full picture of the thesis topic and objectives. At first the relationship between the drilling efficiency and the Rate of Penetration (ROP) is defined, and then the factors that affect ROP are discussed. Literature related to the area of vibration drilling that involve the use of axial forces to enhance drilling efficiency are summarized, that includes research done by the ADG of the Memorial University of Newfoundland. In the last section of the chapter, some of the existing down-hole systems that utilize vibration energy to enhance ROP are presented to give the reader an idea about the technology progression.

2.1 The Relationship between Drilling Efficiency and ROP

In most cases as shown by Taylor et al [5], discussions relating to drilling efficiency have focused on ROP. As a result, ROP is either equated to drilling efficiency, or considered as the parameter that establishes drilling efficiency. These assumptions are highly inconsistent with several field results. ROP must not be equated to drilling efficiency. Rather, ROP should be seen as one of various parameters that influence drilling efficiency. Wilmot et al [6], addressed the distinction between ROP and drilling efficiency; they stated that drilling efficiency depends on a set critical operational parameters, referred to as Performance Qualifiers (PQ) that include footage drilled per BHA, down-hole tool life, vibration control, durability, steering efficiency, directional responsiveness, borehole quality and ROP. Although important, ROP improvement must not compromise other PQs.

ROP is defined as drilling advancement per unit time, while the drill bit is on bottom and drilling ahead. Most of the factors that affect ROP have influencing effects on the other PQs. These factors can be grouped into categories such as planning, environment, and execution.

a) Hole size, casing depths, well profile, bit drive mechanism, BHA, drilling fluid type and rheological properties, flow rate, hydraulic horse power per square inch (HSI), and hole cleaning belong to the planning group.

b) Lithology types, formation drillability (hardness, abrasiveness), pressure conditions and deviation tendencies are the environmental factors.

c) Weight on bit (WOB), RPM, and drilling dynamics belong to the execution category.

There are also two main types of ROP, instantaneous (ROPi) and average (ROPav). Instantaneous ROP is measured over a finite time or distance, while drilling is still in progress. Average ROP is measured over the total interval drilled, from Running In Hole (RIH) to Pull Out Of Hole (POOH).

Wilmot et al, stated that by increasing the magnitude of some of the factors that affect ROP, the effect can be noticeably positive on instantaneous ROPi but not necessarily positive on Average ROPav and the effect might have negative influence on the equipment instead. Figure 2.1, shows an example of possible effects of WOB on ROP. Well A (green line), with less WOB, drilled slower initially but remained consistent to TD. Well B (red line), With more WOB, drilled faster initially but required a BHA trip for a bit change.

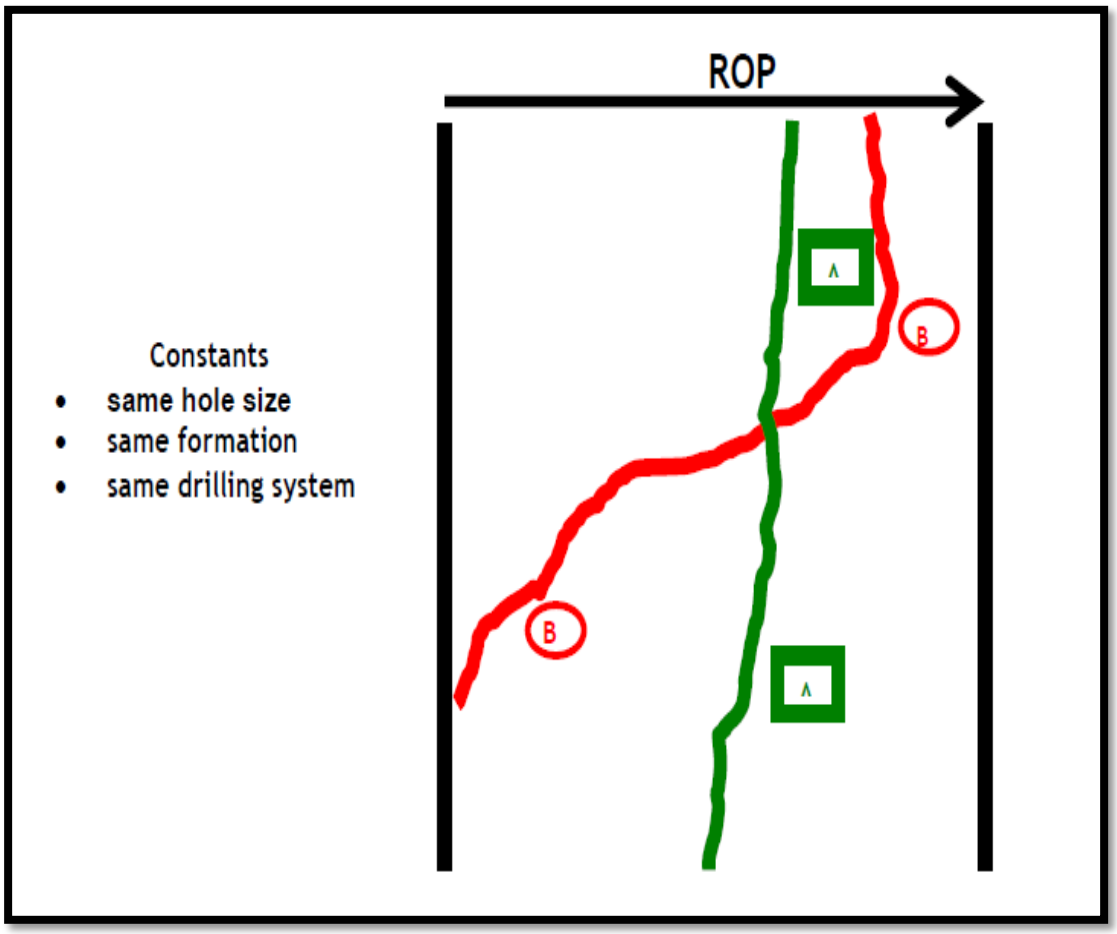

Figure 2.1- Effects of WOB on ROP in two different wells [6]

Wilmot et al, considered the industry's most common performance quantifying metrics for drilling efficiency including Cost Per Foot (CPF), Feet Per Day (FPD), Mechanical Specific Energy (MSE) that are strongly influenced by ROP as shown in the equations governing these metrics.

$$CPF = \frac{1}{ROP}\left[\frac{BC}{t} + RR\ \left(1+\frac{Tt}{T}\right)\right] \qquad (2.1)$$

Where "BC" is the bit cost, "RR" is the rig rate, "t" is time and "Tt" is the Trip Time.

$$MSE = \frac{WOB}{AB} + \left[\frac{120 \times \Pi \times RPM \times T}{AB \times ROP} \right] \quad (2.2)$$

Where "AB" is the Bit area, "RPM" is rev/min of the bit and "T" is the Torque.

$$FBD = ROPav \times 24 \quad (2.3)$$

However, as it's clear in the equations, ROP is not the only factor and other factors should be considered when aiming for a better drilling efficiency.

Pessier et al [7], studied the strong interdependence among ROP, MSE and power at the surface and at the bit. They stated that "It is the magnitude of mechanical power delivered to the bit that defines the capacity of the drilling system and directly affects efficiencies, operating practices and performance".

In many cases it is shocking how little power is left for the drill bit that in the end controls the ROP. The oil industry, unlike others, rarely focuses on the power requirements for the rotating drilling system and its effect on drilling performance. An explanation might be the fact that for more than 100 years roller cone bits have been the preferred drilling bits. Roller cone bits require little torque due to their low aggressiveness and due to the limited load capacity of their bearings; in fact they act as perfect torque limiters. The rotating power system therefore utilizes only a small fraction of the total applied power of a rotary drill rig and lack of power has not been considered a limiting factor. This has gradually changed with the introduction of Polycrystalline Diamond Compact (PDC) bits which have now replaced roller cone bits in many applications.

On average, PDC bits have three times the ROP numbers, resulting in a step change in drilling performance and lower CPF. However, this step change did not come because PDC bits are more efficient than roller cone bits. PDC bits are simply more aggressive, drag type tools which draw more power to fracture and disintegrate the rock at a faster rate. Pessier et al, introduced a graphical method to analyze the relationship between ROP, MSE and power (P) called the power graph.

They showed the relationship between ROP, MSE and P by plotting them in a single graph that covers a whole drilled section.

The distribution of the data suggests a simple mathematical relationship in the form of:

$$ROP = c / MSE \qquad (2.4)$$

The constant "c" is the product of ROP and MSE. The product of ROP x MSE represents the area specific mechanical power MPSI which is the total available power (P) divided by the borehole area (A)

$$MPSI = ROP \times MSE / 1.98 \times 106 = P / A / 1.98 \times 106 \qquad (2.5)$$

The unit for MPSI is horsepower per square inch. It is obtained by dividing the product of MSE x ROP by the constant 1.98 x 106 to convert [ft-lb/hr] to [HP].

$$P = MPSI \times A \text{ [HP]} \qquad (2.6)$$

Then they used a large data set from a field research facility to explore and validate the effectiveness of the Power Graph .The data was generated in a project to study stick slip as a function of PDC bit design and therefore covered a broad range of operating parameters.

Their study covered the effect of changing drilling parameters like WOB and RPM and variables like bit type, lithology change and bit wear conditions.

The Power Graph gave an overview of the performance and capacity of an entire drilling system and its individual components. Also it displayed the complex relationship between ROP, MSE and available power.

Figure 2.2 shows The Power Graph of a well and the effect of varying WOB while keeping rotational speed of the bit at 60 RPM and the effect of that on the power transmitted to the bit.

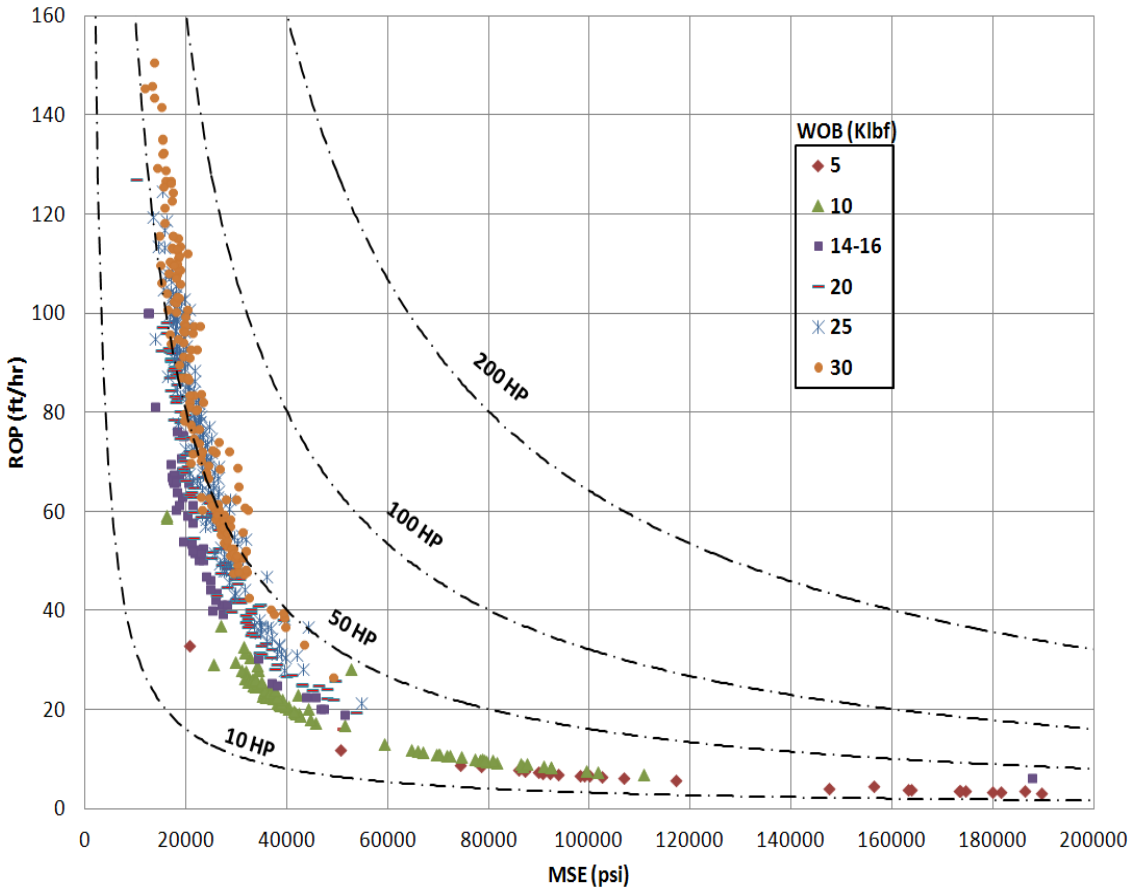

Figure 2.2- Power Graph of a Well with constant 60 RPM and Variable WOB [7]

Figure 2.3, shows the Power Graph of a well with varying both the RPM and WOB and the effect of that on the power transmitted to the bit.

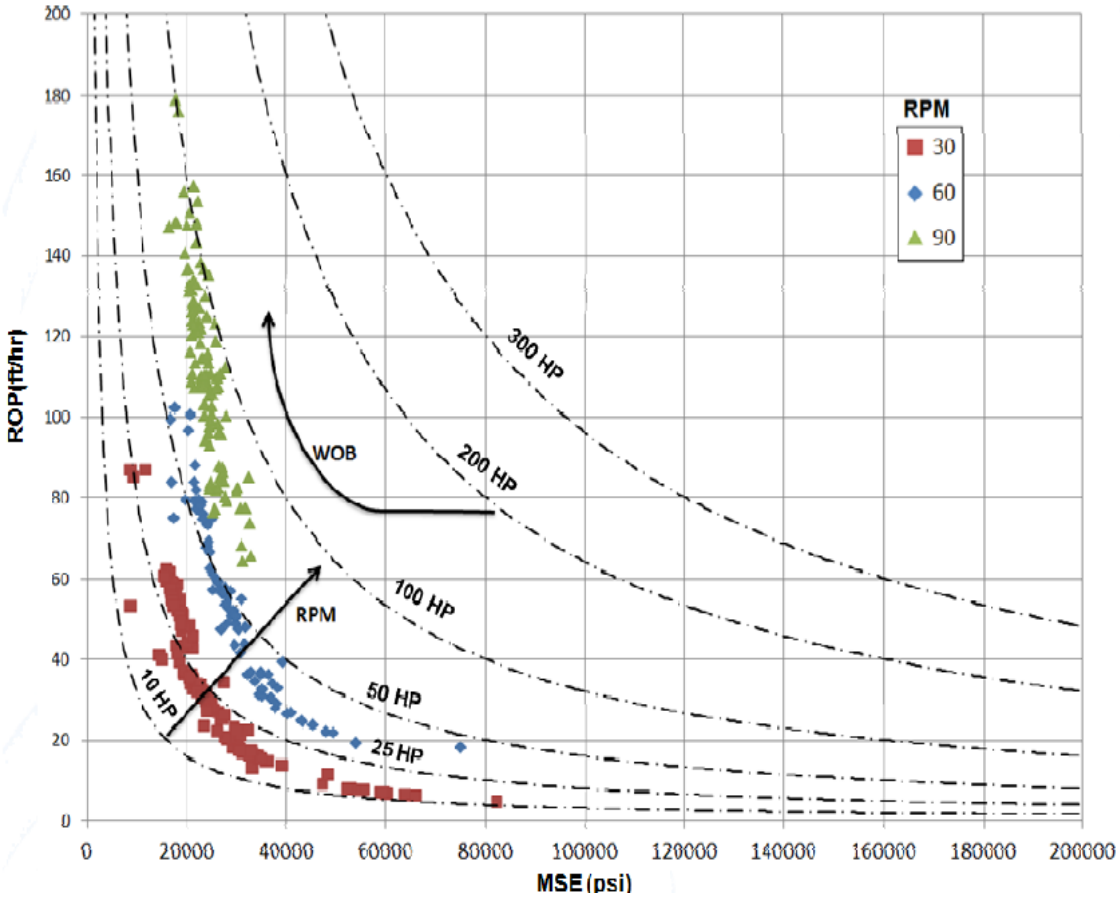

Figure 2.3- Power Graph of a well With Varying Both the RPM and WOB [7]

2.2 Factors Affecting the Rate of Penetration (ROP)

Known as the most important factor affecting drilling efficiency for decades, ROP and the factors affecting it have been studied by several researchers. Some of their work is summarized in the next few pages showing factors affecting ROP like varying surface drilling parameters and bottom hole parameters like Bottom Hole Pressure (BHP) and Bottom Hole Cleaning (BHC).

2.2.1 Surface Drilling Parameters

Brantly et al [8], studied four factors controlling ROP, which they thought were the most effective. They conducted a study using data from 500 wells drilled in several states across the United States of America in the late 1930s.

The factors they studied were Personnel and Equipment, WOB, Rotary Speed and Circulation Fluid Volume. For Personnel and Equipment, Brantley used the data from 14 wells drilled over a period of 3 years by the same drilling practice. The average pressure, fluid volume, drill-pipe size, mud characteristic, WOB, rotating speed, size of bits and formations were the same for each of the 14 wells. However, it was noticed that the wells although drilled using the same drilling practice, varied in their ROP records. The analysis showed a noticed trend of "penetration rate increase" over the period of 36 months. The conclusion was that the increased ROP was due to increased efficiency of personnel and equipment. Another analysis of data coming from the records of a different number of wells tracking the Rotary Speed of the String showed a trend of ROP increase with the increase of rotary table speed when all the other variables were constant. The third group of wells was studied to determine the effect of fluid volume upon the ROP, wells from four fields were selected which showed constant table speeds and weight on the bit for each field, but which had been drilled with varying fluid volumes. The resulting analysis accounted for a direct relationship between ROP and fluid volume increase.

The fourth set of data was selected to represent wells drilled by constant parameters except for varying WOB. It was noted that increased WOB was more effective in hard formations than in soft ones. In one field in which experimental work was carried on, it was observed that increased WOB at the same rotating speed resulted in no noticeable increase in ROP, but, by increasing the speed of rotation, the ROP increased almost directly in proportion to increased speed for twice the usual WOB.

2.2.2 Bottom Hole Pressure (BHP)

Garnier and Van Lingen [9] studied the effect of Bottom Hole Pressure (BHP) on the ROP of different types of rocks. They observed that when drilling permeable rocks like Obernkirchener Sandstone and Vaurian Limestone, the change in BHP caused no significant effect on ROP when using water as the drilling fluid. However, increasing BHP when drilling a low permeable rock like Belgian Limestone with water and mud a the drilling fluids decreased the ROP. It was also observed that increasing BHP could decrease the ROP to a specific reduction factor after which it could no longer influence the ROP.

Garnier and Van Lingen claimed that in permeable rocks, due to negligible difference between BHP and pore pressure, the chip hold-down effect which tends to reduce ROP is less significant. However, ROP is likely to slow down in less permeable rocks due to the pressure difference between the BHP and the formation pressure, which can be noticed obviously when drilling deep wells.

Figure 2.4 shows the results of the experiment for the influence of BHP on ROP done by Garnier and Van Lingen [9].

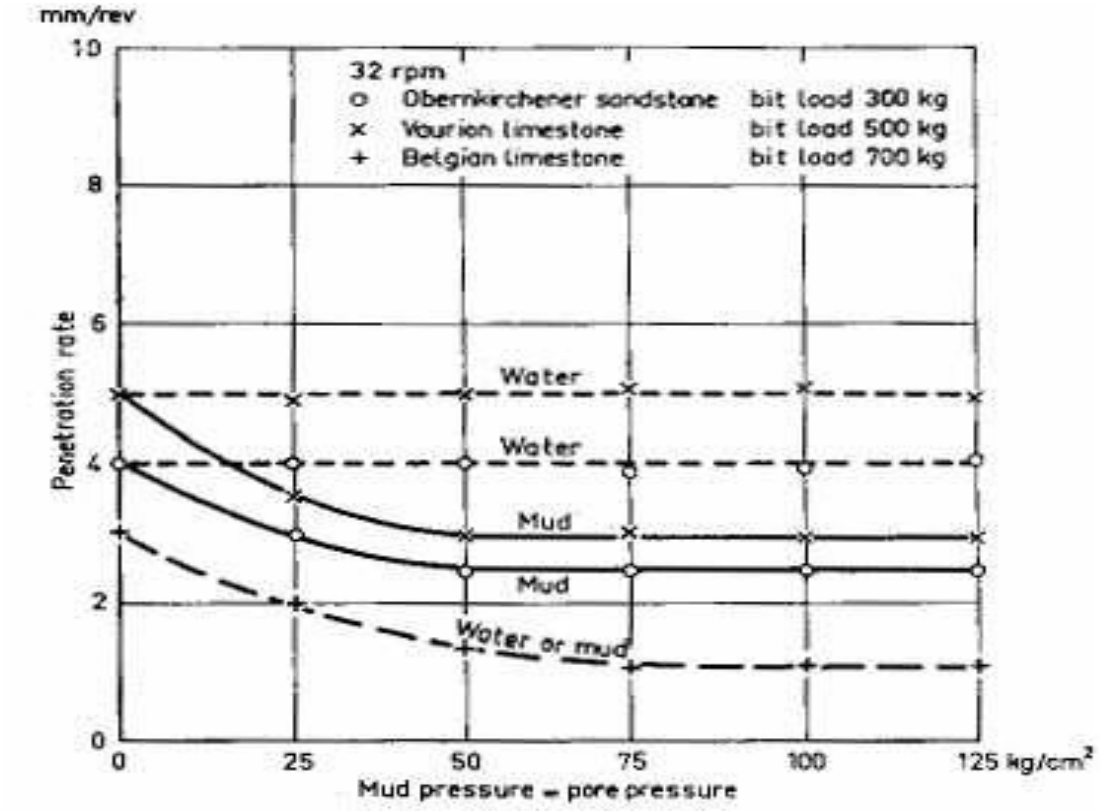

Figure 2.4- The results of the experiment for the influence of BHP on ROP [9]

Garner [10] studied the performance of a diamond cutter bit in the penetration of shale and limestone, under increased BHP with no fluid circulation. The results showed that the volume of the cut was significantly reduced by an increase in BHP. Black et al. [11] studied the effect of mud filtration on ROP. The study was conducted to observe the effect of the rate of filtration on the reduction of the nominal effective stress which is defined as the difference between the pore pressure and the BHP.

The results showed an increases of ROP when the nominal effective strength was minimum.

2.2.3 Bottom Hole Cleaning (BHC)

Maurer [12] studied the effect of Bottom Hole Cleaning (BHC) on ROP. In this study, ROP was considered a function of WOB, rotary speed (RPM), bit diameter and the rock strength. However while drilling with high WOB and rotary speed, the increasing trend of ROP was stopped eventually. Maurer suggested that the phenomenon was due to decreasing BHC which caused bit tumbling in surrounding rock cuttings which decrease the interaction area between the bit and the rock.

Figure 2.5 shows the results of Maurer's study on the relation between rate of penetration (R), Weight on Bit (W), Rotary Speed (N) and Bottom Hole Cleaning (BHC).

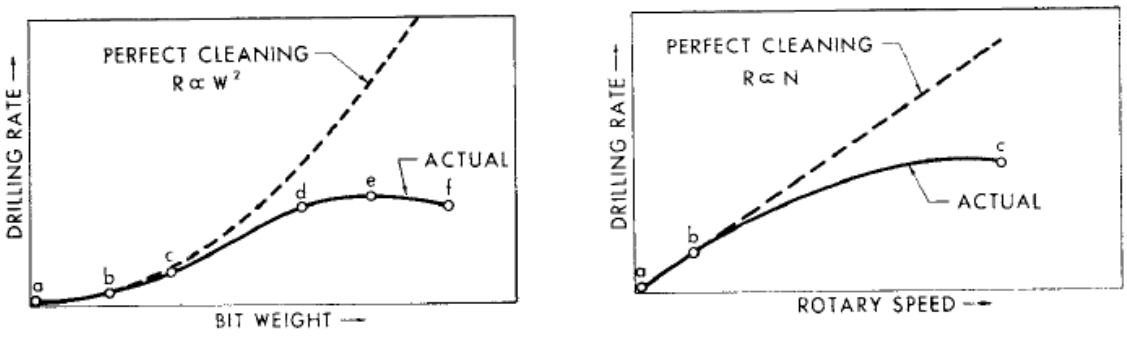

Figure 2.5- Response of ROP Bottom-hole Cleaning condition [12]

Wells et al. [13] studied another aspect of BHC when they studied the effect of increasing WOB when drilling shale with a PDC Bit. They observed that an increase in WOB under a constant bit hydraulic horsepower caused the balling of junk slots on the sides of the bit resulting in a significant drop in ROP and an increase in the torque of the bit.

2.3 The Role of Vibration in Rock Penetration

It's been common understanding in the drilling industry that down-hole vibrations are usually not desirable and have destructive influence on the bit and the Bottom Hole Assembly (BHA). That is certainly true when considering some forms of down-hole vibrations like lateral vibration (most destructive) or torsional vibration, but in fact not all vibrations are harmful to the drilling process. Researchers have shown that in some cases, axial vibrations can be useful and boost the ROP, and some of their work is presented in this section.

2.3.1 Definition of Down-Hole Vibration

Feenstra et al [14], defined 4 known forms of Down-Hole vibrations which are:

1- *Axial Vibrations* (also known as “Bit Bounce"): Generally caused by large variations in weight on bit (WOB). The bit repeatedly lifts off bottom and impacts the formation. Axial Vibrations are characterized by up and down motion of the drill string/BHA. The surface indicators could be top drive or kelly shaking axially and fluctuating WOB on the weight gauge. This can result in premature bit and BHA component failure and reduced ROP when the amplitude of bouncing is high ,as shown by Yaveri et al [15].

2- *Torsional Vibrations* (also known as "Stick-Slip"): they can be observed at the surface as fluctuations in the current through the electric motor that drives the rotating table/ top drive. When the rock can no longer withstand the building up torque, the energy is suddenly released and the bit starts spinning. The bit spins so fast that the drill string unwinds and the torque drops. As a result, the bit slows down again until it finally stops completely, after which the entire process of winding and unwinding is repeated.

3- *Lateral Vibrations*: Are widely recognized as the leading cause of drill string and BHA failures. Whirls are severe forms of lateral vibrations; and is defined as an eccentric rotation of the bit. Instead of rotating around its center, the bit rotates eccentrically as a result of its interaction with the wellbore. It generally occurs in vertical wells, in laminated layers of soft and hard formations, and with PDC bits with aggressive side cutters. Surface detection is nearly impossible but the bit will have noticeable characteristics when it's pulled out.

4- *Eccentered Vibration*: is the motion that a bit makes when it does not rotate about its center. This may manifest itself in out of round holes and severe bit damage. Generally a poor drilling performance. Figure 2.6 after Ashley et al [16], shows the variable major forms of vibration that occur down-hole.

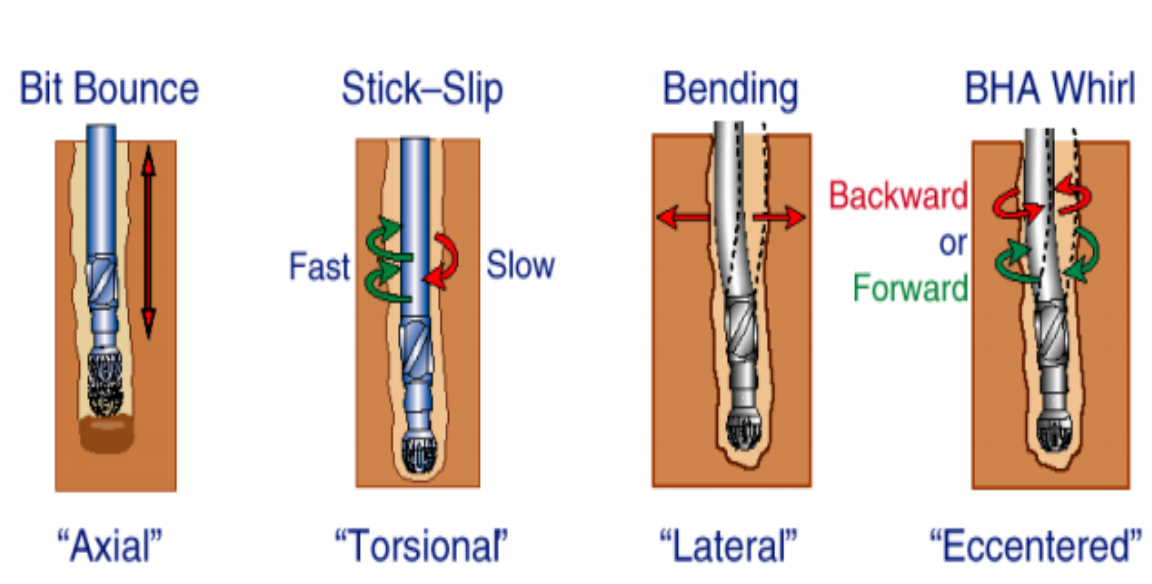

Figure 2.6- Forms of Vibration after Ashley et al [16]

2.3.2 Initial Research on Vibration effect on ROP

All forms of vibrations have been extensively studied by researchers to eliminate the harm and use the energy gone to vibration to help increase drilling efficiency.

Eskin et al [17] showed that the Russians took the lead when they started studying the effect of vibration on ROP in the 1950s and introduced methods to utilize vibration, before others get satisfactory results to rely on vibration in enhancing ROP.

Barkap et al. [18] in 1957, presented the results of experimental studies which were conducted while drilling in red granite in a laboratory environment with the drill bit rotating at speeds of 37 to 254 rpm and with the superposition of mechanical axial vibrations at frequencies of 4000 to 5000 per minute. These experiments demonstrated the possibility of increasing the drilling rate while reducing the rotary speed of the drill bit and the axial static load (WOB) in presence of vibration.

In 1979, the All Union Drilling Institute (VNII) in Moscow conducted bench studies of drilling using cutter drill bits with superposition of additional dynamic forces, as mentiond by baidyuk et al [19]. Drilling was carried out in Urals "Koelga" Marble which has a uniaxial compressive strength of 79 MPa with a 33-mm diameter cutter drill bit. The drill bit was rotated at a rotary speed of 42 rpm. Extra forces of both pulsed and vibration types with various combinations of frequency and amplitude were superimposed on the drill bit. The applied force amplitude to static load ratio was ranged from 0 to 0.6, and the ratio of the introduced vibration frequency to the rotation frequency ranged changed from 1 to 24. The results demonstrated that pulsed loading always gives a positive effect, with

the biggest increase in penetration rate obtained when load pulse frequency coincides with the frequency of contact between the bottom hole and the peripheral cutter rim teeth. Figure 2.7, shows the experimental results of the penetration per drill bit turn "h" obtained with several values of static load “Gc", when superimposing an extra vibration load of amplitude ΔG.

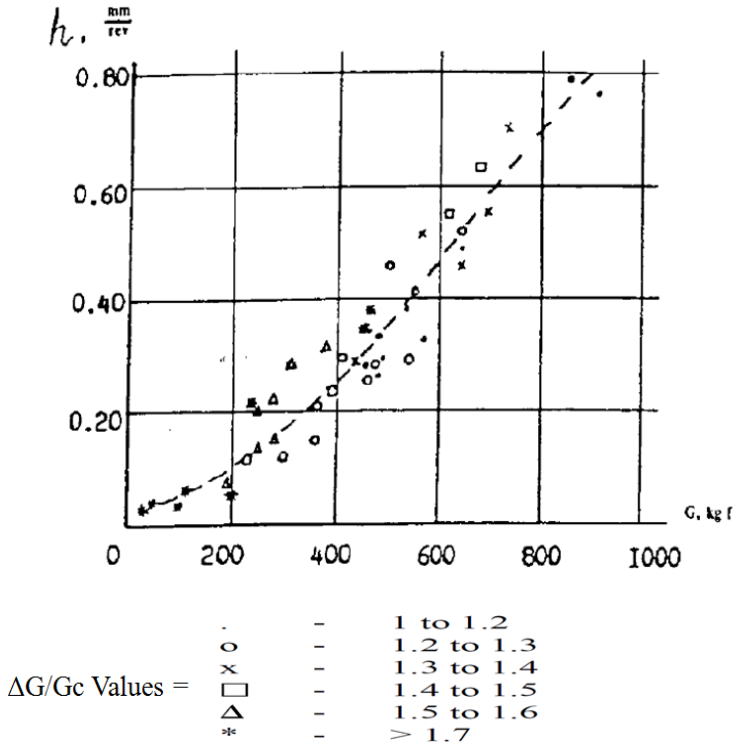

Figure 2.7- Experimental drilling results when applying extra vibration load [19]

The Russians also introduced several special mechanical vibrators developed to increase drill string vibrations and thereby increase the power delivered to the drill bit, drilling rate, and drilling efficiency.

Some were surface mechanical vibrators acting at the top of the drill string, like the Vibropercussion device which was proposed for spudding in wells with hard rock in the year 1980 as shown by Izosimov et al [20]. Others were Down hole Vibrators, like the drilling shock wave device which was proposed by Sintsov et al [21] in 1985 which focuses shock waves on the drill bit edge to increase bit efficiency in blast holes and deep wells. Western researchers also conducted major investigations by an industry consortium in the 1950s, Drilling Research Investigation Ltd (DRI). Pennington [22] released some of the results in 1953. The DRI project was looking into possible improvement in ROP by utilizing vibration and percussion drilling techniques. The researchers assumed that drilling could be greatly accelerated by these means; however, they also observed a decrease in ROP enhancement with the increase of down-hole pressure and depth. Eventually, the researchers abandoned the project as they could not obtain drilling improvement at greater depths.

2.3.3 Recent Research on Vibration effect on ROP

Li et al [23], investigated the effect of vibration on the bit performance and on the improvement of ROP. They used a VARD laboratory scale experimental setup to monitor and record the effects. This setup was an electrical coring drill rig that underwent some modifications by Li [24] to meet the experimental requirements. During the experiments, coring and full face drilling were done at various combinations of rotary speed and vibration amplitude. Vibration frequency was kept constant and a sufficient fluid flow rate for each rotary speed was maintained. Figure 2.8 shows the experimental results of the coring bit.

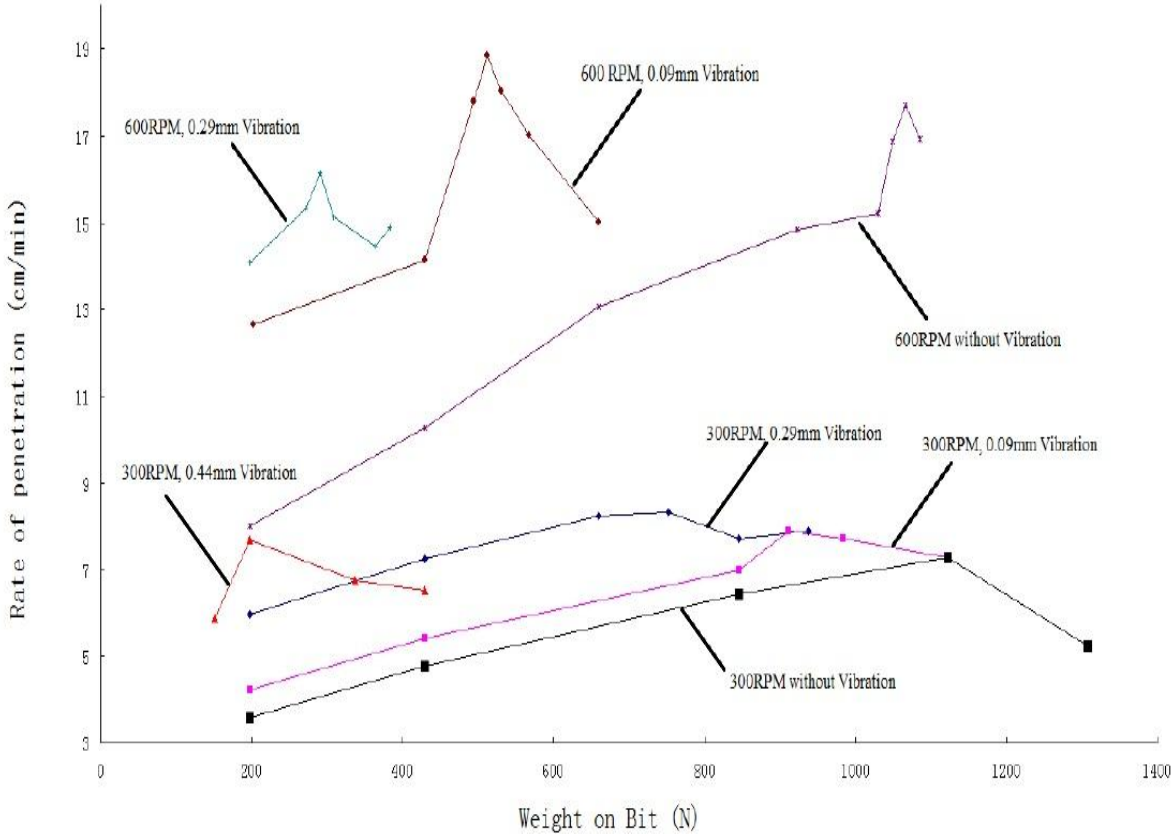

Figure 2.8- Li's coring experimental results [24]

They concluded that vibration amplitude has a non-linear relationship with ROP and some optimum performance could be achieved by varying the amplitude. However, it was found a linear trend of ROP in relation to amplitude when drilling with constant WOB and rotary speed. Figure 2.9 shows Li's results when drilling with constant WOB and rotary speed, and the observed linear relationship between ROP and Vibration amplitude.

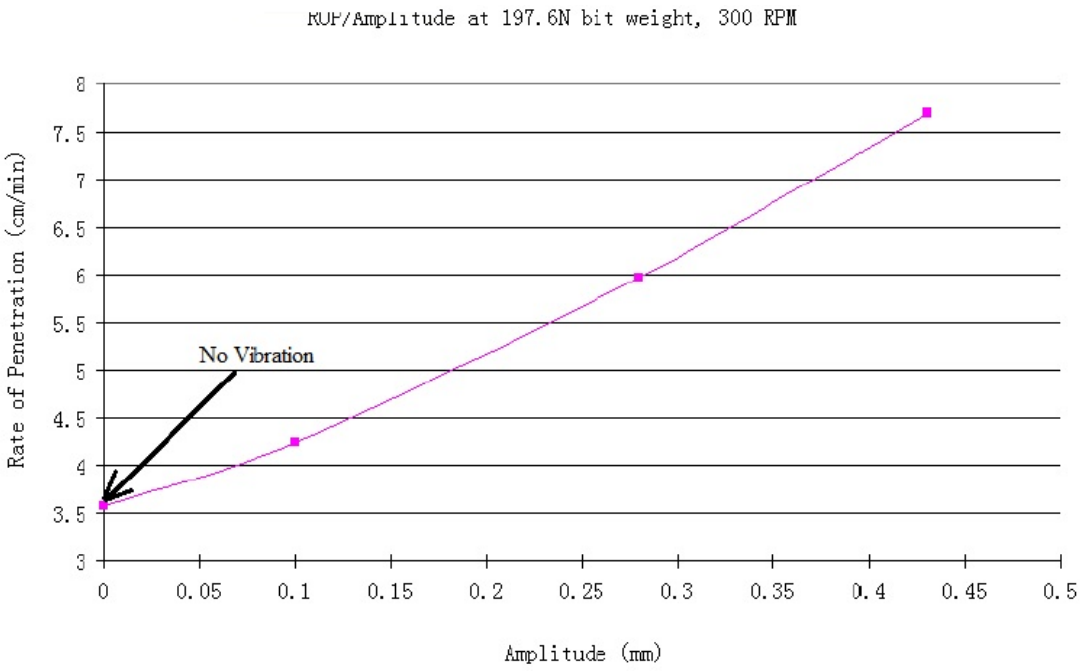

Figure 2.9- Li's coring results with constant WOB and RPM [24]

Li et al, observed similar results with drilling experiments using a full face bit and concluded that ROP was enhanced when vibrations were introduced to the system.

In the end, the following was concluded:

- The Vibration Assisted Rotary Drilling technology (VARD) could significantly enhance the ROP;
- As vibration amplitude increases, the ROP, WOB relationship curves are shifted, meaning that less WOB can be applied to achieve a higher ROP;
- ROP significantly increases with the increase of vibration amplitude until the founder point is reached, after which the increase of WOB doesn't lead a proportional increase of ROP;
- Vibration amplitude is proportional to the increase in ROP.

Figure 2.10, shows the drilling results of the experiments with a full face diamond impregnated bit.

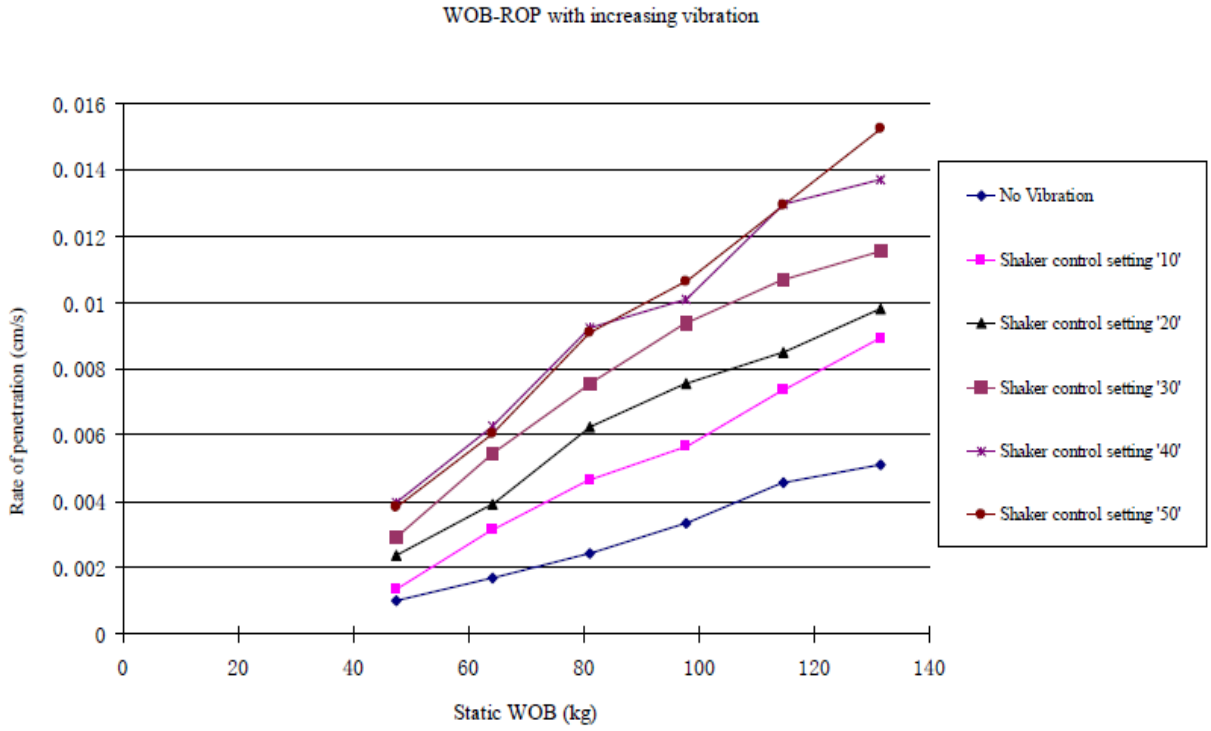

Figure 2.10- Li's drilling experimental results with the full face bit [24]

Yusuf Babatunde et al [25], used a modified vibration table from Li's experimental setup in order to be able to control the vibration frequency. and the second round of experiments utilized a PDC Bit with two cutters to drill through synthetic concrete in addition to the full face diamond drag bit. they used three levels of vibration amplitude (low, medium and high) and three levels of frequency (45, 55 and 65 Hz) for the experiments. First experimental runs were conducted with full face diamond drag bit.

They observed improvement in ROP up to more than 100% at any mode of vibration. These results lead to the following conclusions:

- ROP can be significantly increased with the use of vibrations;
- ROP increase range varies from 25% to more than 100%;
- Amplitude of vibration is proportional to ROP.

A second series of experiments was conducted using a PDC with two cutters and two nozzles. The results were similar and the experiments data showed ROP improvement in all runs where vibration assisted drilling was utilized compared to conventional drilling. This second series of experiments made Babatunde conclude that:

- ROP was improved more by vibration in the PDC bit case;
- Optimum frequency of vibration was 65 Hz for lower WOB and 55 Hz for higher WOB.

Another conclusion was made by Babatunde [26], when the spectral analysis of the load cell data were conducted, which was that frequency peak of the vibration was achieved at 9 Hz, that was assumed as the mechanical interaction of rock and the two cutter PDC bit at the motor speed. Optimum frequencies were harmonics of the 9 Hz, so it was assumed that maximum ROP increase occurs at some resonance of excited and natural vibrations.

Khorshidian et al [27] from the ADG studied the influence of vibrations on the penetration mechanism of a PDC Single cutter using the Distinct Element Method (DEM). They adjusted the DEM parameters to match the macro properties of Carthage Limestone which were obtained from calibrations done according to real UCS tests. Based on the results it was found that there are two effects of the cutter vertical vibration

on the penetration mechanism. The first one is the positive effect that can be significant when the cutter imposes a sufficient impact on the rock for cratering. On the other hand, exceeding the optimal point of vibration increases the required MSE which is the second and negative effect . Also it was observed that excessive fluctuations in vertical position of the cutter can result in no penetration in direction of the cut, as the cutter tends to slide instead of chipping or crushing. Therefore, he concluded that there is an optimal condition for vertical oscillations which should be controlled with respect to the other drilling parameters such as the horizontal velocity and rock strength.

They, also concluded that the main reasons of the improvement in the penetration mechanism of the PDC cutter due to vertical oscillation are both the reduction of the required horizontal force for cutter advancement and the generation of larger chips after imposing an impact. Figure 2.11 shows the generation of the cutting in front of the PDC cutter under a low vertical force oscillation (normal chipping). Figure 2.12 shows the generation of the cutting under a high amplitude vertical force oscillation.

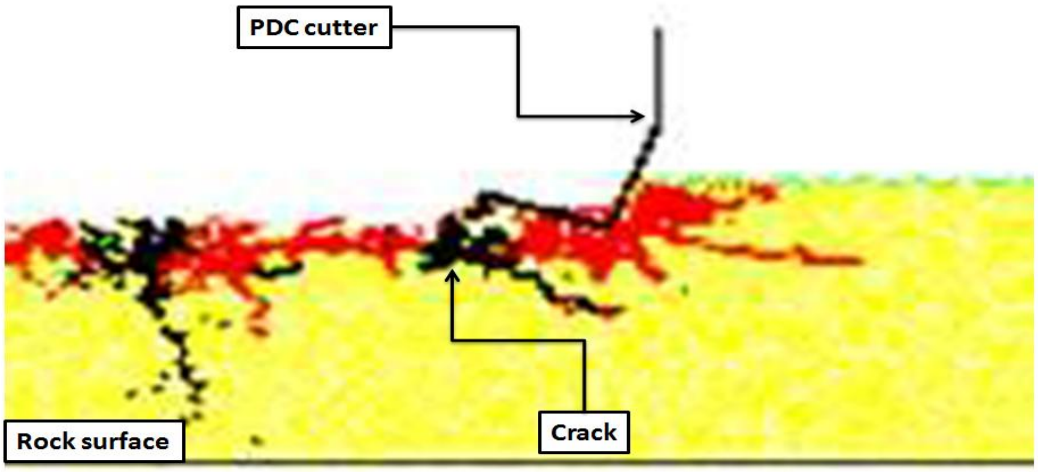

Figure 2.11 - Normal chipping in front of the PDC cutter [27]

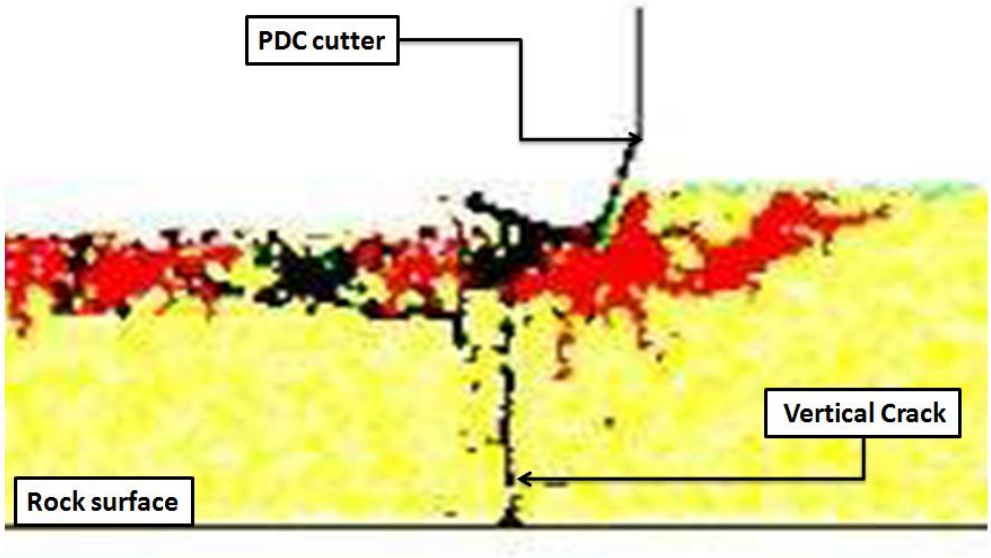

Figure 2.12- Combination of chipping and cratering after impact of PDC cutter [27]

In Figure 2.13, the vertical crack underneath the cutter is due to introducing a high energy impact to the rock. In addition to above conclusions, Khorshidian considered that the effect of a cutter vertical oscillation on the penetration mechanism can be dependent on drilling conditions such as rock strength, rock elasticity, bottom-hole pressure, cutter geometry, DOC, bit wear and specifically, the drill string stiffness.

Therefore, by considering all conditions of a drilling operation, optimizing the vertical Oscillations can provide enhancements in the performance of PDC bits.

Gharibiyamchi [28] studied and characterized two types of hydraulic pulse tools that generate down-hole vibrations, the Axial oscillation Generating Tool (AGT) and the Hydropulse tool. He designed a simulation scenario to simulate these tools in a DEM environment, and then this scenario was combined with simulations of drilling operations to simulate the drilling process with both tools.

For the simulations of the AGT and Hydropulse tool, Gharibiyamchi used the rock that was developed and calibrated by Ledgerwood [29] (UCS= 55MPa) and considered a 6" diameter (150 mm) bit in the simulations. Overall 20 runs were conducted to investigate the performance of the AGT in drilling with different down-hole hydrostatic pressures and 9 runs were conducted for the Hydropulse tool.

Gharibiyamchi evaluated the drilling performance of the two tools using three indicators which are the Material Removal Rate (MRR), ROP, and the MSE based on the simulation results. In the AGT simulations, the MRR values were much lower with conventional drilling than that of drilling with vibrations. Particularly at higher pressures, a more than 100 % increase was obtained when using the AGT in the drilling process.

Figure 2.13 shows the graphical results of MRR values obtained from the simulations at same BHP with best results obtained when applying high amplitude dynamic force of 19250 N and worst results observed when not using the AGT at all.

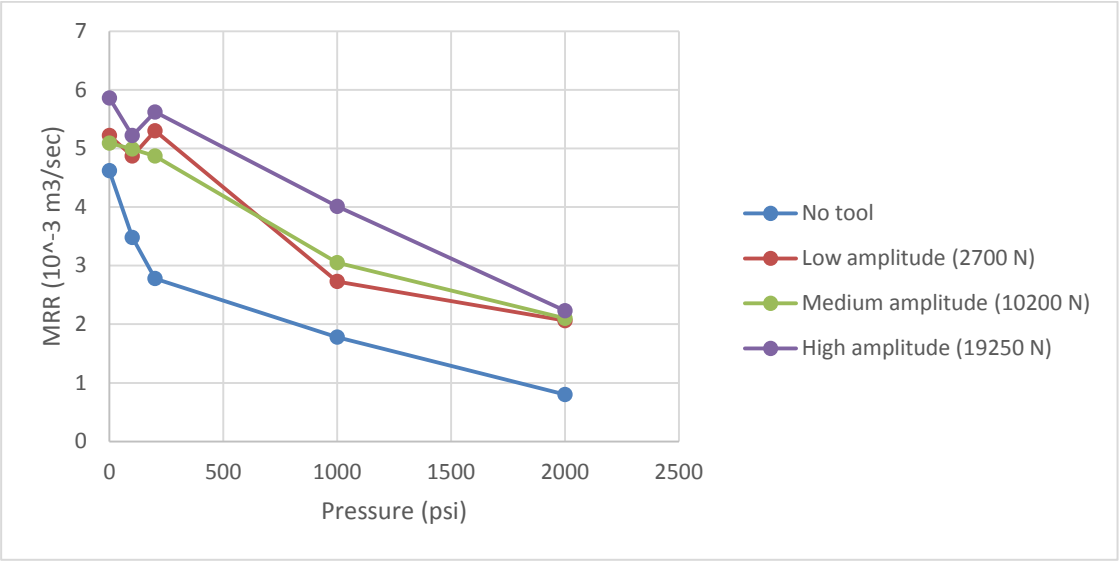

Figure 2.13- Graphical illustration of MRR results for the simulation of the AGT [28]

Considering ROP, the results showed the best ROP when using a high amplitude vibration force of 19250 N and worst when drilling with no AGT.

Figure 2.14, shows the graphical results of ROP obtained from simulations

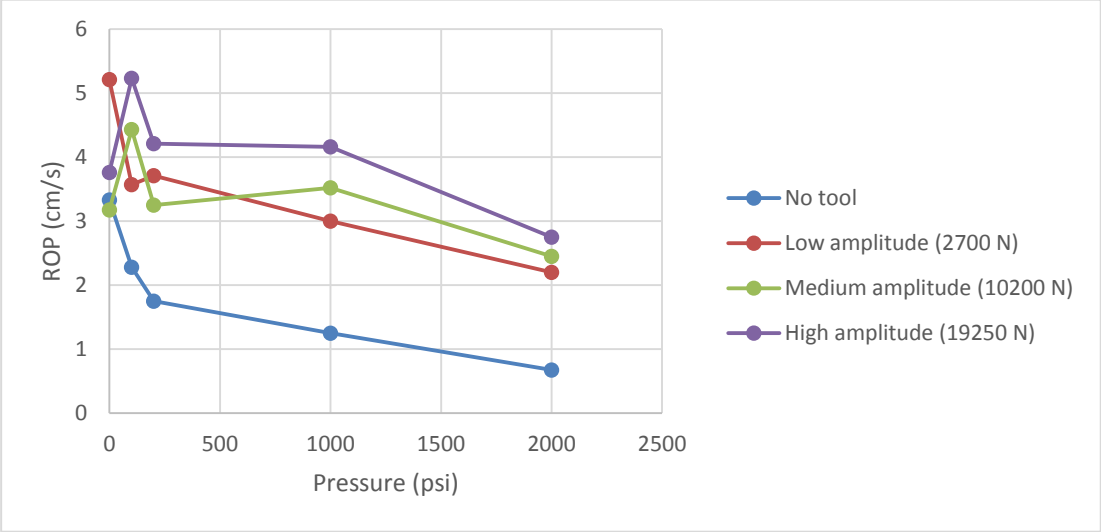

Figure 2.14- Graphical illustration of ROP results for the simulation of the AGT [28]

Analyzing the MSE results from the AGT simulations, Gharibiyamchi found that high amplitude vibrations also increase drilling performance from the MSE prospective. In other words, through the analyses of MSE results, it was found that the high amplitude of vibrations consumes less energy to drill a unit volume of rock among the other drilling scenarios. An approximately 50 % decrease in MSE value was found in the bottom-hole pressure of 2000 psi by using the AGT and accompanying shock tool. Figure 2.15, shows the Graphical illustration of MSE results for the simulation of the AGT

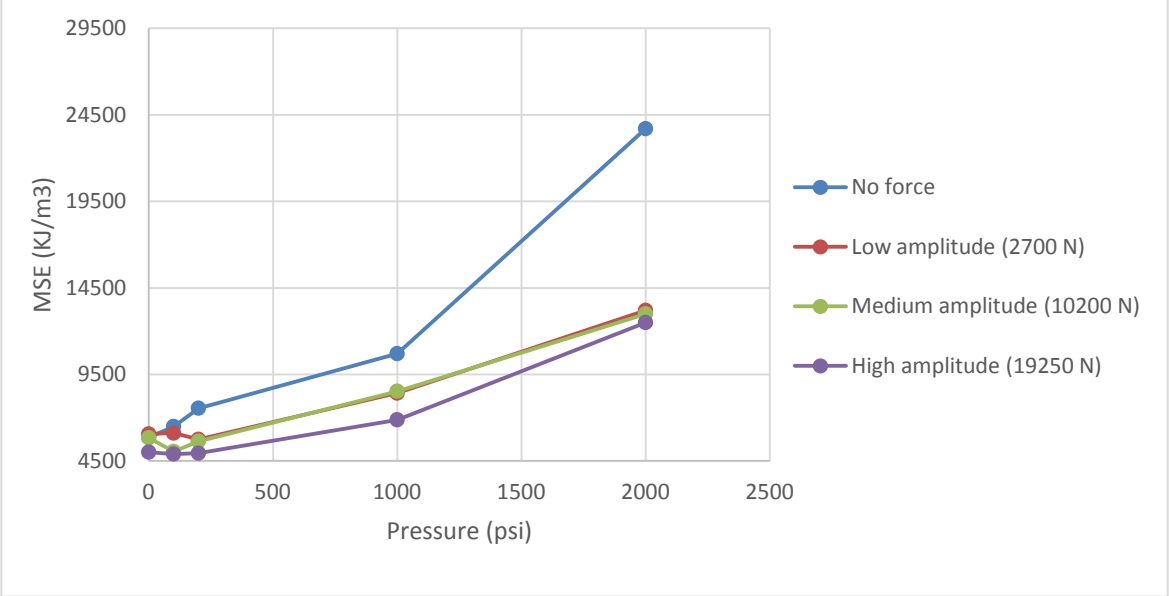

Figure 2.15- Graphical illustration of MSE results for the simulation of the AGT [28]

Considering the Hydropulse simulations and according to the calculations, high amplitude suction pulses which correspond to the flow rate (250 GPM) and causes a 198.5 KN dynamic vibration force could result in an MRR increase of 55 to 65 % depending on the BHP. Figure 2.16, shows the graphical illustration of MRR results of the Hydropulse simulations

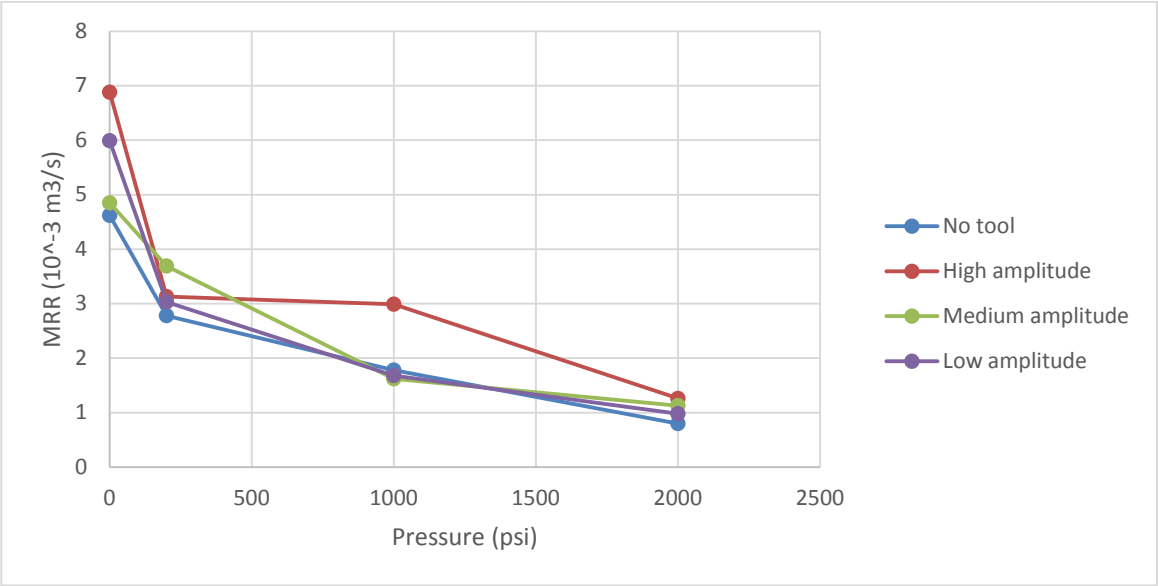

Figure 2.16- Graphical illustration of MRR results of the Hydropulse simulations [28].

The ROP values were also calculated for the simulation runs. These values are shown graphically in Figure 2.17.

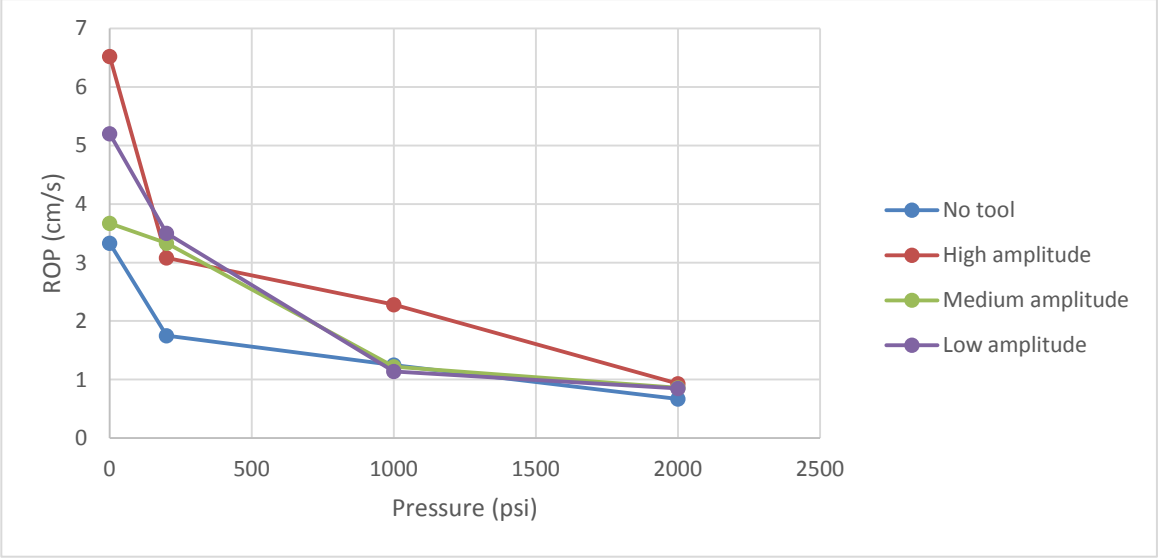

Figure 2.17- Graphical illustration of ROP results of the Hydropulse tool simulations [28].

The ROP results were consistent with the results obtained by calculating MRR values and show the same trend. It can be seen that high amplitude of pulsation has the best performance. For MSE analysis, high amplitude of pulsation had better performance compared to others. It causes the MSE values to be decreased by 50 %. However, similar to the MRR and ROP results, the medium and low amplitudes of pulsations do not have significant effect on drilling performance. Figure 2.18, shows Graphical illustration of MSE results of the Hydropulse tool simulations

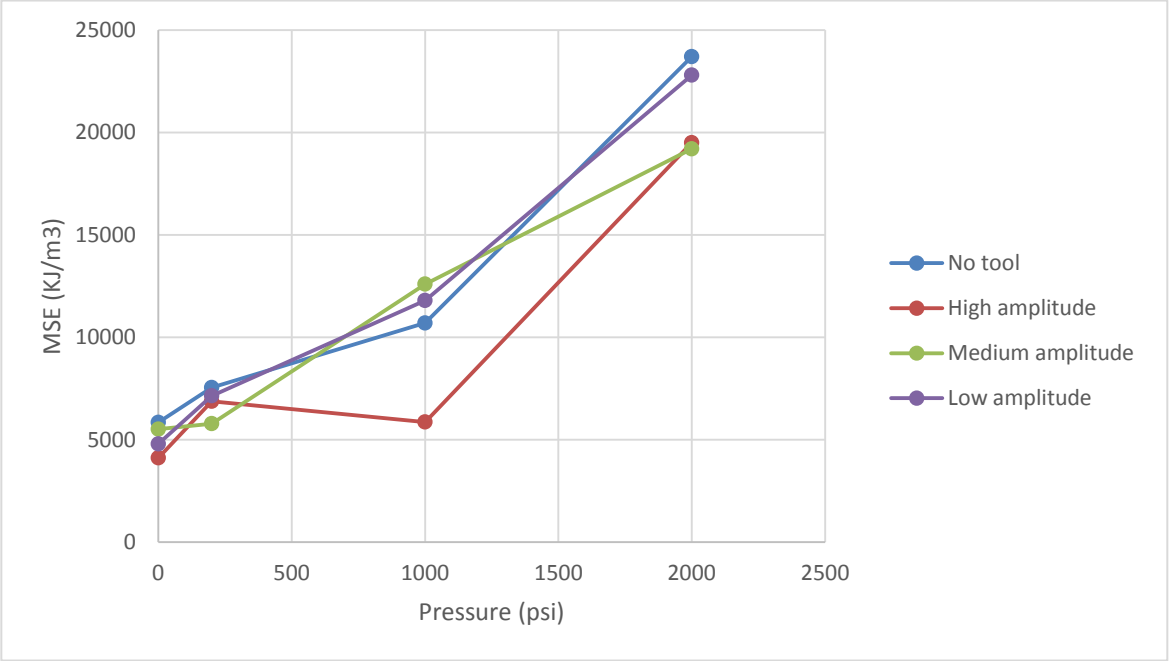

Figure 2.18- Graphical illustration of MSE results of the Hydropulse tool simulations [28]

Gharibiyamchi also observed the effect of compliance presented by the shock tool by running simulations of both tools with and without the shock tool installed. Comparing the drilling performance of the both tools with and without shock tool, he concluded that shock tool could increase ROP by more than 100 %. For example, the MRR value for the

high amplitude impact force of the Hydropulse tool at the bottom-hole pressure of 1000 psi was about 2.28× $10^{-3}m^3/s$ while at the same condition with shock tool, the MRR value of 4.88 × $10^{-3}m^3/s$ was obtained. The effect of shock tool is even more significant for the AGT because of the nature of its force profile. Negative forces applied by the tool to the cutter are normally damped by the shock tool but in the absence of the shock tool, these forces caused the whole assembly to bounce. Finally Gharibiyamchi conclusions can be listed as follows;

- Results of the simulations showed great increase in drilling performance when the AGT was used.
- The results showed that the AGT tool with shock tool above it had better performance than the integrated Hydropulse tool and drilling bit.
- Results of additional simulations revealed the effect of compliance introduced by the shock tool on drilling performance. These results showed that when the AGT is deployed without the shock tool, it could affect the drilling rate negatively.
- The simulations suggested the use of shock tool with the Hydropulse assembly as the drilling performance was significantly improved when the shock tool was used in combination with the Hydropulse tool. It was observed from the simulation results that the drilling performance of the Hydropulse tool was increased by more than 100 % when shock tool was used in the assembly.

Another approach by the ADG members was to design a down-hole source of vibration to make use of the good results that were achieved in the previous experiments and simulations, and to validate the results in down-hole conditions. Babapour et al [30], studied a method to enhance drill cuttings cleaning and ROP using cavitation pressure pulses. The study is based on previous research done by Pronin [31] utilizing the fact that a fluid passing a convergent or a divergent venturi, demonstrates significant pressure fluctuations due to the cavitation phenomenon. As the fluid passes the vena-contracta, according to the Bernoulli's principle, the fluid velocity increases and hence the pressure decreases. If pressure drops below the fluid vapor pressure, cavitation occurs and bubbles are created. Babapour et al, used CFD Simulation software packages such as Flow3D and Autodesk CFD to choose the proper sizes of venturis to be used in a cavitation tool prototype. The simulations resulted in 3 selections of venturi sizes (4, 8 and 12 mm diameter venturis) that could generate cavitation pulses compatible with the range of flow used and the prototype dimensions. Figure 2.19, shows the formation of a cavitation pulses during simulations flow passes through the venturi.

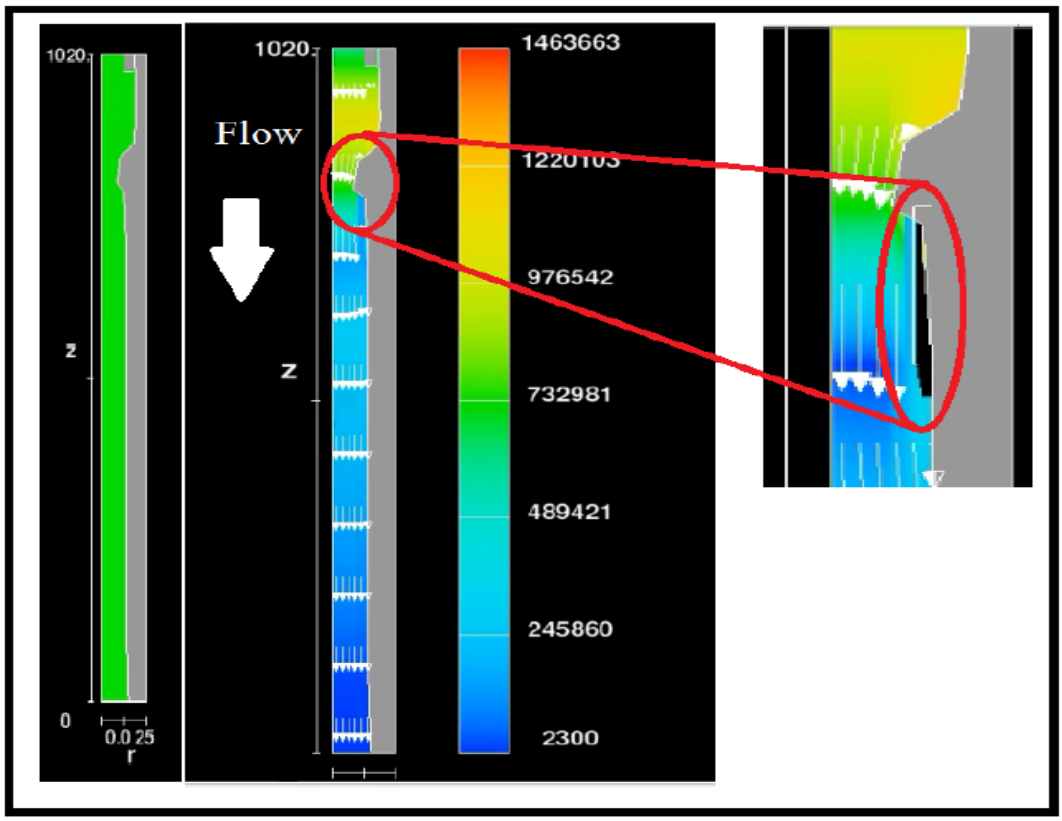

Figure 2.19- 2D presentation of fluid passing venturi and initiation of bubbles growth [30].

They then conducted a set of experiments using an experimental setup consisting of two pressure sensors at upstream and downstream locations, 3 load cells in a triangular combination, and a flow meter to study the output of each venturi and the force output of the generated pulses. The flow rate ranged from 10 to 70 USGPM.

The 12 mm venturi showed a better performance in the preliminary flow tests and was producing larger bubble clusters compared to the other sizes. The force output of the system agreed with the calculations done based on theories of fluid jet impacting on a plane with an average of 103 lbs at 60 USGPM. Also the pressure pulses patterns were in

agreement with the simulations. By applying back pressure, the intensity of the cavitation was reduced and the tool stopped performing efficiently.

The last set of experiments was conducted to study the effect of venturi and axial compliance in drilling through synthetic rock made to simulate a formation of medium strength (UCS=50MPa). The compliant element used in these experiments consisted of two plates with rubber mounts embedded between these two plates in an equilateral configuration. The rubber mounts enabled the displacement of the upper plate on the lower plate. An 8 mm venturi was also mounted on the drill string behind the bit as the cavitation pulses source that is compatible with the available flow rate generated by the test pump.

The experiments results showed that the tool started to cavitate and produced vibrations with maximum performance at 22.6 USGPM within a flow rate ranged from 8 to 30 USGPM. The tool was operated with compliance and without compliance to observe the effects of the compliant element. Results showed that when the rigid setup was used, the vibrations produced, did not have any significant effect on the ROP. However, with the addition of the complaint element, the vibrations produced by the tool, intensified the natural vibration of the compliant element and the penetration rate was increased.

Figure 2.20, shows the effect of compliance on ROP obtained from the experiments.

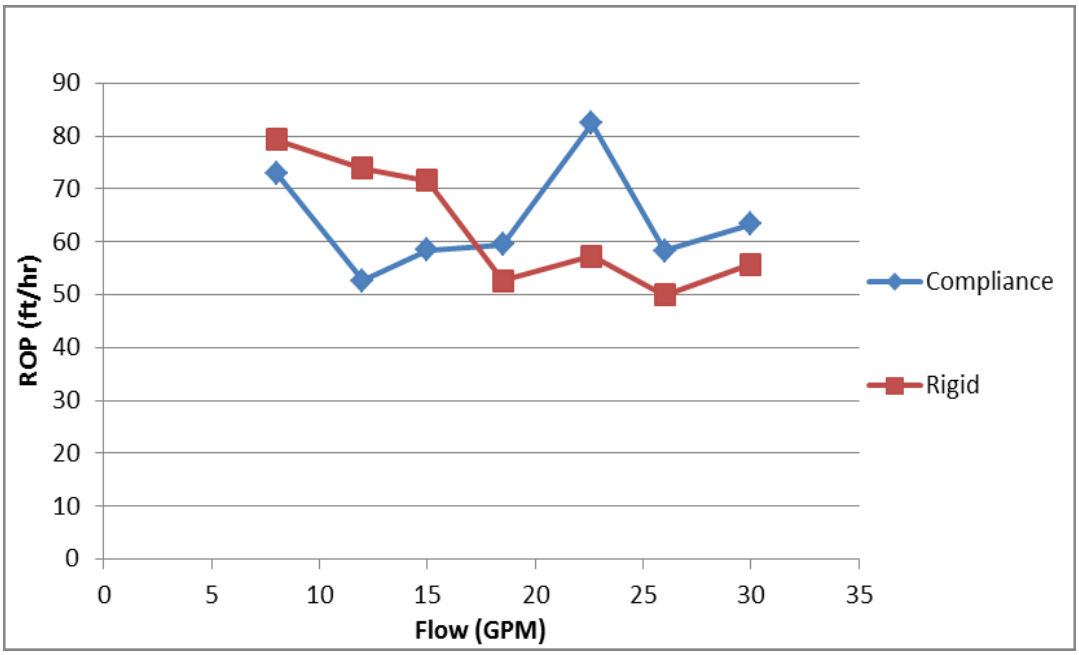

Figure 2.20- ROP for venturi with and without compliant element at different flow rates [30].

Figure 2.21 shows the effect of compliance on transforming cavitation pulses into axial forces.

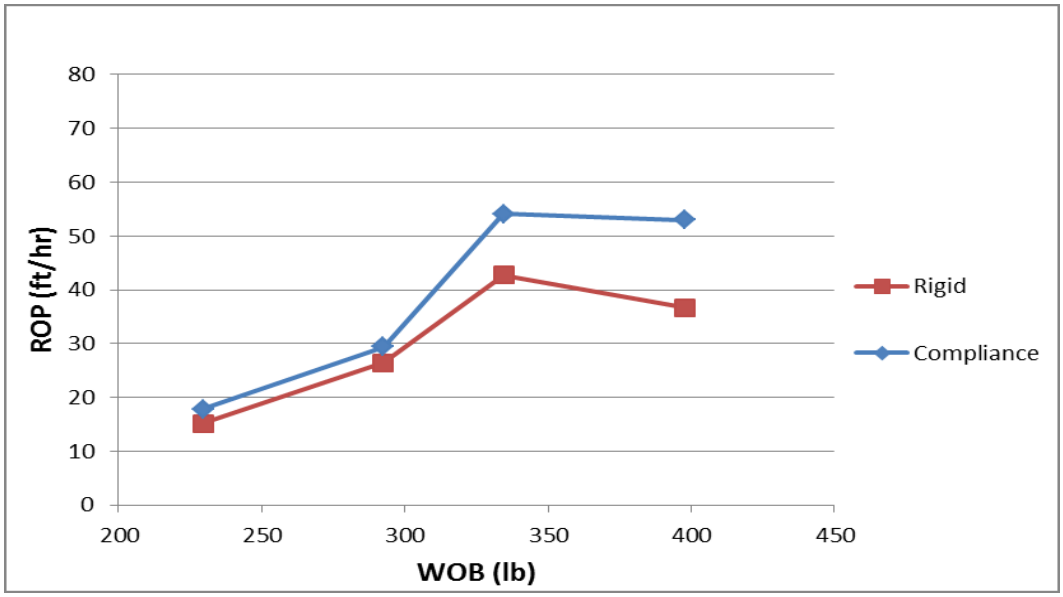

Figure 2.21-- ROP of venturi insert with and without compliance [30]

Finally the following results were concluded:

- Cavitation phenomenon could be used to generate pressure pulses that help enhance the ROP
- Vibration Forces are only useful when a compliant element is integrated to the drill string to transform the forces into an effective displacement
- The tested prototype did not perform efficiently in the existence of high back pressure
- The cavitation tool needs a combination of certain flow rate and BHP to perform well which limits its use in the field conditions

2.3.4 Percussion Drilling Impact forces

Other forms of utilizing axial impact forces and the accompanying generated axial vibration are used to penetrate through rock, these are percussion drilling and its derivative "Rotary Percussion Drilling", which were found very useful especially in hard rock drilling and shallow wells, where applying high WOB is practically difficult due to the limited drill string length.

In early 1970's, significant research and investigation on percussion drilling was done by Hustrulid and Fairhurst [32]. They studied percussion drilling theoretically and experimentally. They also studied the energy transfer, drill steel-piston interface, thrust force requirements. Han et al. [33] described the rock failure mechanisms under both conventional rotary drilling and percussion drilling conditions. The basic differences between these two drilling methods in terms of rock defragmentation are shown in Figure 2.22.

The figure shows that in conventional rotary drilling the rock fails because of axial load (WOB) and drill bit rotation. The bit penetrates the rock in the axial direction then shears a conchoidal chip as it rotates. In percussion drilling a hammer tool produces a short duration high amplitude impact longitudinal force along the direction of bit movement. When the impact force exceeds the compressive strength of the rock, it crushes the rock below the bit and creates fractures forming a narrow wedge along the outer boundaries of the bit inserts.

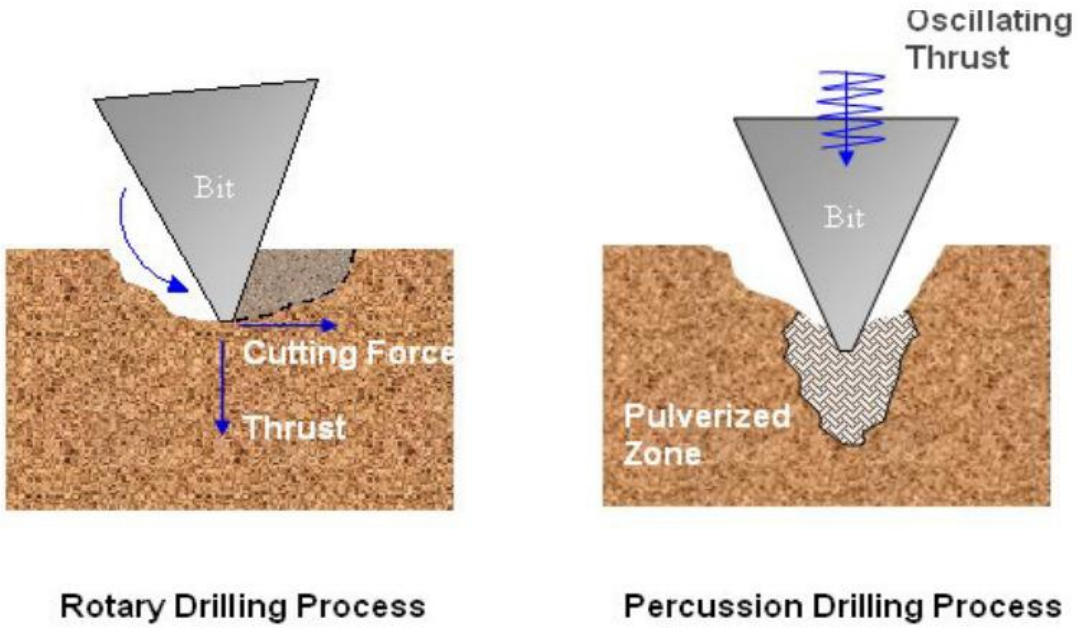

Figure 2.22- Rock failure process in rotary and percussion drilling [33]

Rotary Percussion simply combines both mechanisms to suit the drilling environment in deep oil and gas wells where hard formations are encountered and drilling further with conventional methods is considered INPT.

2.4 Existing Down-hole Vibration and Percussive Systems

Many research and development teams, companies and industry corporations have made an approach to develop down-hole vibration or pressure pulsating systems that can enhance Drilling efficiency and drilling speed in challenging down-hole conditions. In this section, the discussed tools are powered by drilling fluids, which are pumped into the drill string from the surface all the way to the bottom hole.

2.4.1 Self-oscillation Pulse Percussive Rotary Tool

The self-oscillation Pulse Rotary Percussive Tool is a hydraulic pulsing tool that generates high frequency and low amplitude pulses by using a two-stage self-oscillator [34]. Figure 2.23 shows a schematic view of the tool. From the figure, the tool consists of two stage self-oscillators that create pressure waves using the acoustic theory concept. These pressure waves travel down and act on the effective area of bit driving a piston and cause axial force behind the bit. Hydraulic compliance is used in order to convert mechanical forces into the displacement. The pressure profile produced by this tool along time is shown in Figure 2.24.

The Self-oscillation Pulse Percussive Rotary tool has been evaluated in various wells in China. It was tested for the first time in Songoliao Basin (North China) which is known as one of the most challenging zone in Northern China. Results showed a 20 % increase in ROP compared to offset wells. The tool was deployed in the Sichuan and Tarim basins and ROP improved by 20 % to 36 % was compared to the offset wells.

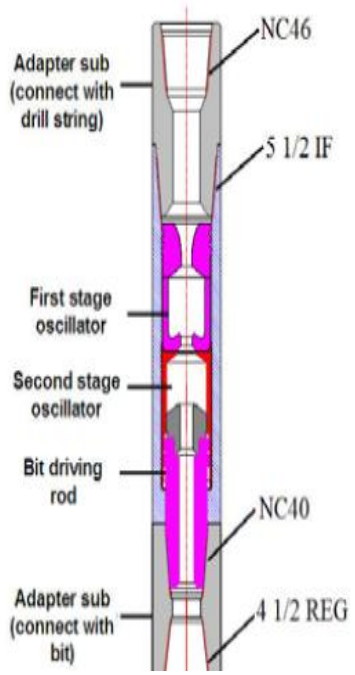

Figure 2.23- Schematic of the Self-Oscillating Tool [34]

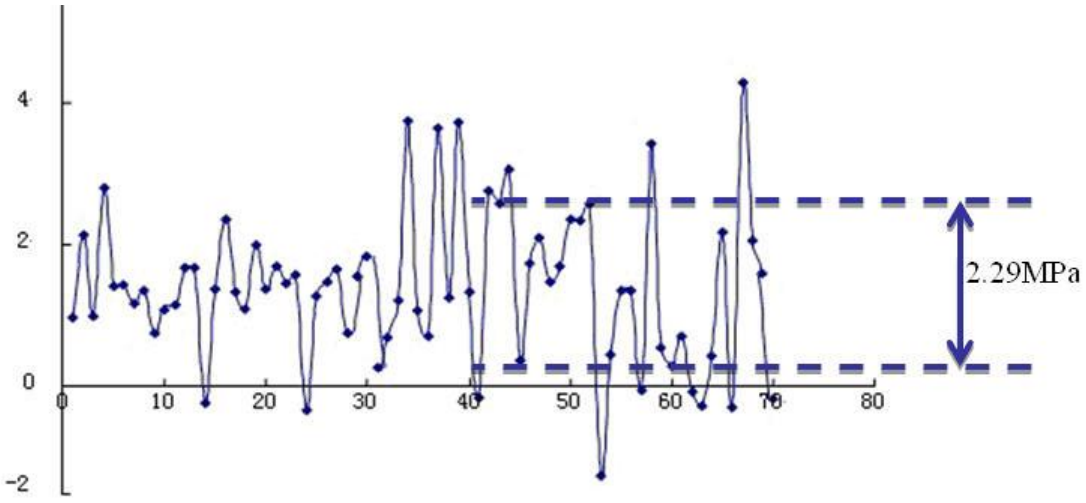

Figure 2.24- The pressure profile produced by Self-Oscillating Tool along time [34]

2.4.2 Hydro Pulse Tool by Tempress

The Hydropulse tool is a down-hole drilling vibrator which is used in over-pressurized formations to enhance ROP. Introduced by Tempress Technology Inc, this tool works by producing suction pulses behind the bit that are converted into impact forces when they act on the bit interaction area with the rock. Figure 2.25 shows the schematics of the Hydropulse tool and the generated suction pulses.

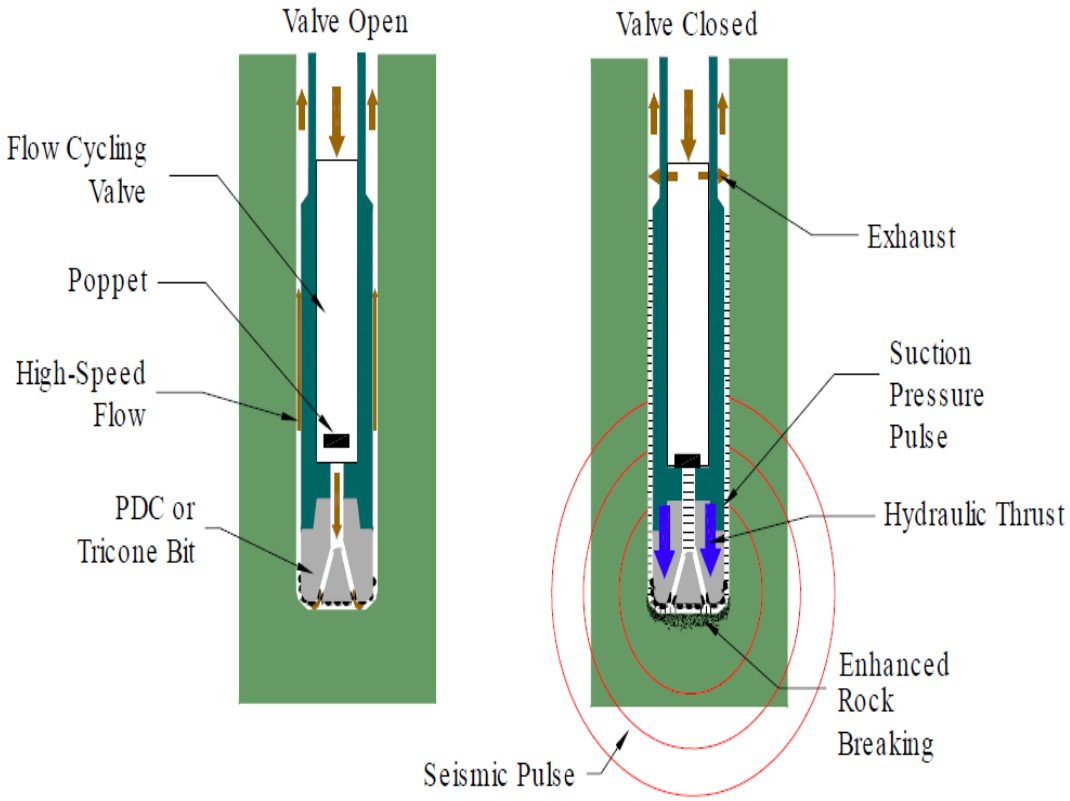

Figure 2.25- Hydropulse Schematic Drawing [35]

Figure 2.25 shows a poppet valve which periodically stops the flow through the flow path. That generates intense suction pulses behind the bit that go through the nozzles and

cause sudden pressure drop instantly for a very short time. This pressure drop causes upward tensile stresses in the rock surface which helps weaken the rock and eventually helps breaking it. Also, the suction pulses can be converted into percussive mechanical forces if proper compliance between the tool and the bit is installed, These percussive forces can create significant displacement below the bit and can also be used as seismic pulses for Seismic While Drilling (SWD) applications as indicated by Kolle [35].

Figure 2.26 shows the typical pressure profiles generated by the Hydropulse tool. The pulse width is proportional to the length of the flow path. The two way travel time of the acoustic wave within the flow path is normally about 3 milliseconds at most of the applications but it can vary by varying the length of the flow path, which depends on the tool size .

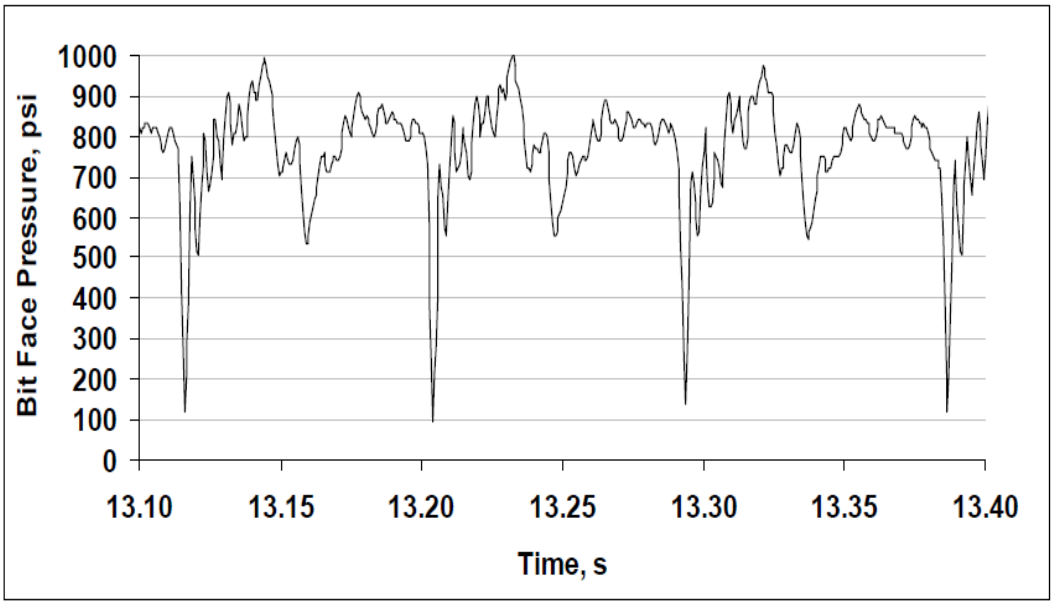

Figure 2.26- Pressure profile generated by Hydropulse (Flow rate: 400 GPM, water, 8 3/4" tool) [37]

Full field scale experiments were conducted by Tempress Technology Inc. at Terra Tek facilities in the USA, using Mancos shale and Crab Orchard sandstone to evaluate the tool performance. An 8 1/8" insert bit along with the first tool were used in the experiments. The results of the experiments showed 50 % to 200 % increase in ROP in Mancos shale when the Hydropulse tool was deployed. Figure 2.29 shows the drilling performance of the Hydropulse tool in comparison with baseline conventional drilling in Mancos shale.

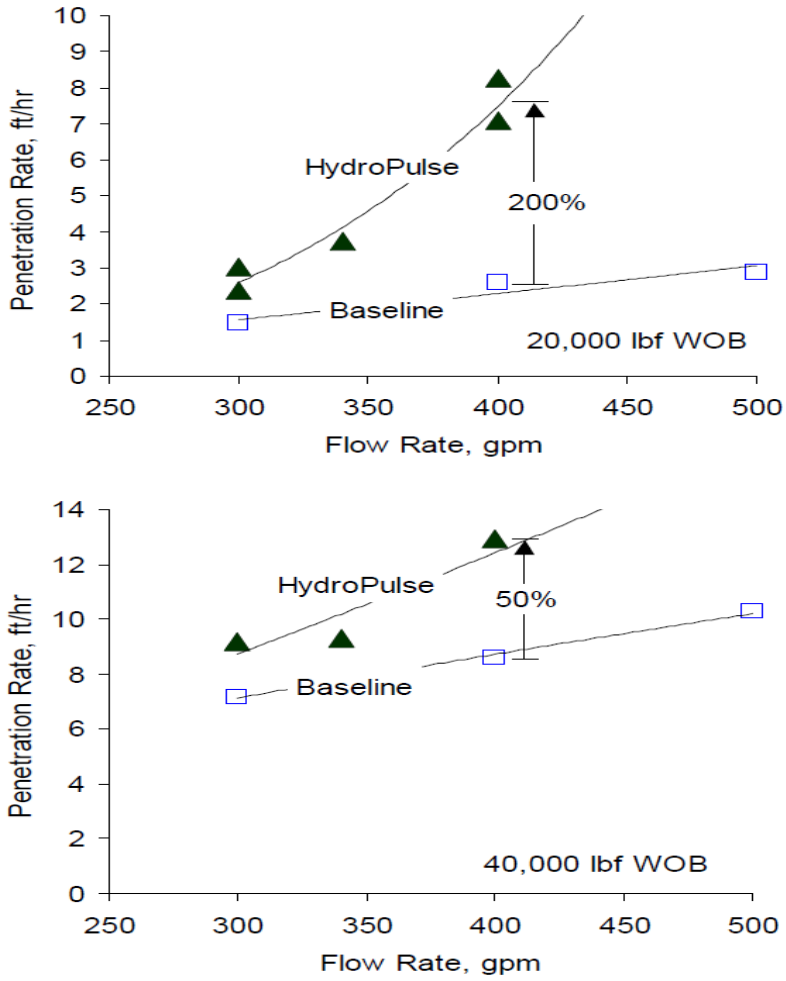

Figure 2.272.26- Mancos shale ROP comparison [35]

2.4.3 NOV Agitator Tool

The Agitator tool was basically designed and introduced to reduce the friction between the drill string and the borehole by means of axial vibration oscillations. NOV stated that the agitator provides BHA excitement to improve weight transfer to the bit while drilling, especially in highly deviated well profiles, which consequently leads to an increase in ROP, as shown by McCarthy et al [36].

The Agitator tool is driven by a positive displacement power section similar to that of a PDM mud motor, the rotor is connected to a valve assembly which creates a cyclic motion that produces pressure pulses within the tool by restricting the mud flow path. The frequency of the pulses is related to rotor speed which in turns depends on the mud flow rate. The Agitator itself only creates pressure pulses; so in order to transform this hydraulic energy into a mechanical force, a shock tool is placed above the Agitator tool in the BHA when traditional drill pipes are used. In coiled tubing operations only the Agitator is required; the coiled tubing expands and contracts as the pressure pulses act on it due to its low stiffness.

The shock tool which is made of a series of compliant elements designed as separate discs contains a sealed mandrel that is spring loaded axially, when internal pressure is applied to the shock tool the mandrel extends due to pressure acting on the sealing area within the tool. When the pressure is removed, the springs return the mandrel to its original position. When used directly above the Agitator, the pressure pulses cause the shock tool to extend and retract, thus producing axial oscillations.

The agitator tool has advantages such as, being fully compatible with MWD/LWD tools; significantly decreases stick slip severity and can fit on several types of BHA and suit different well profiles.

One disadvantage of the Agitator tool is that it has a number of mechanical components that are rotating and sliding; this could lead to a short lifetime of the tool.

Several case studies have been done over the last few years to investigate the Agitator role in reducing friction and enhancing drilling performance. Skyles et al [37] conducted a case study using the Agitator in the drilling of Barnett shale in Tarrant County, Texas. They observed a 20 % increase in ROP when the Agitator was used in the curve section and more than 60 % improvement when the tool was deployed in the curve, lateral and build sections of the well. Robertson et al [38] conducted a series of field tests in the Ullrig test facilities in Norway. The results showed an improvement of 70 to 90 % in weight transfer. Rasheed [39] conducted a case study on the effect of the agitator in maintaining stable tool face orientation, increasing weight transfer, and reducing motor stalling. He observed that there was an increase in ROP from 1.5 m/hr to 4.5 m/hr as well as improvement in the steer ability of motor. Figure 2.28 shows a schematic of the Agitator Tool made by NOV.

Figure 2.28- Agitator tool by NOV [39]

After reviewing the research done since the 1950s, in the area of enhancing the ROP and the drilling efficiency in general, using vibration. It is clear that there's a window to invest more time and effort in order to utilize the VARD technology to boost the drilling speed and efficiency. In the next chapters, a new VARD mechanism is introduced and tested to show that the axial vibration can be used in a new way to enhance drilling efficiency.

3 Pressure Pulses Generator (PPG)

In order to investigate the effect of vibration introduced by periodic pressure pulses on drilling performance, a source of pressure pulses was needed. A selection was then made to use a pressure pulse generating down-hole tool that uses periodic restriction of fluid flow passing through it to generate cyclic pulses of pressure. The tool was designed and manufactured by a sponsoring company, as a friction reducing down-hole tool used in highly deviated wells, and installed in the upper part of the BHA hundreds of feet above the bit. However, in this study the purpose is to use the generated pressure pulses right at the bit by installing the PPG directly above the bit. In this chapter, a description of the Pressure Pulses Generator (PPG) operational mechanism along with an experimental setup to test its performance are presented. The testing results will be then presented in Chapter 4.

3.1 The PPG Description

In this study, the idea is to use the design of the PPG to fluctuate the forces at the bit-rock interface by fluctuating the fluid pressure acting on a fixed area. The main interest to fluctuate the forces generated at the bit in order to generate axial vibration when a compliant element is added above the bit or the PPG in the BHA.

The PPG consists of two sections, the power section and the valve assembly section. The power section is mainly similar to that of the Positive Displacement Mud Motor; it essentially converts hydraulic power from the drilling fluid into mechanical power to drive the valve. The power section is comprised of two components; the stator and the rotor. The stator consists of a steel tube that contains a bonded elastomer insert with a

lobed, helical pattern bore through the centre. The rotor is a lobed, helical steel rod. When the rotor is installed into the stator, the combination of the helical shapes and lobes form sealed cavities between the two components. When drilling fluid is forced through the power section, the pressure drop across the cavities causes the rotor to turn inside the stator. This is how the valve inside the valve assembly is turned. By the nature of the design, the stator always has one more lobe than the rotor and in the PPG case, the stator has two lobes and the rotor is made up of only 1 lobe. Figure 3.1, shows a schematic of the PPG power section with the flow passing through it, where Figure 3.1 A is a 2D side view section and Figure 3.1 B is a 3D Top view section through the power section of the PPG

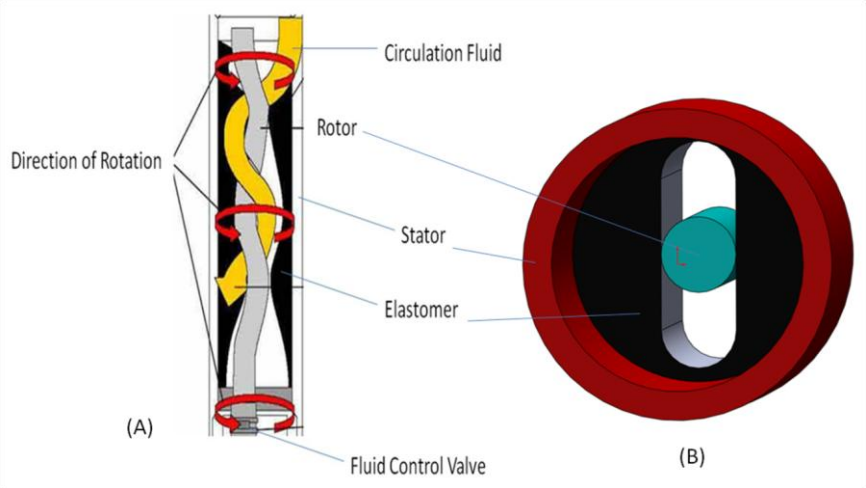

Figure 3.1- A schematic figure for the PPG power section

It is also shown in the figure that the one lobe rotor has three possible positions to move to within the two lobes stator. The rotor is connected to the fluid control valve through a set of bearings which convert the erratic movements of the rotor into a steady cyclic motion that is then used to drive the fluid control valve.

Inside the valve section there is a fixed plate that has an inside diameter similar to the valve's diameter, and is used a partial fluid restrictor when the centers are not coincided. Figure 3.2, shows a drawing that describes the fixed plate and the valve dimensions.

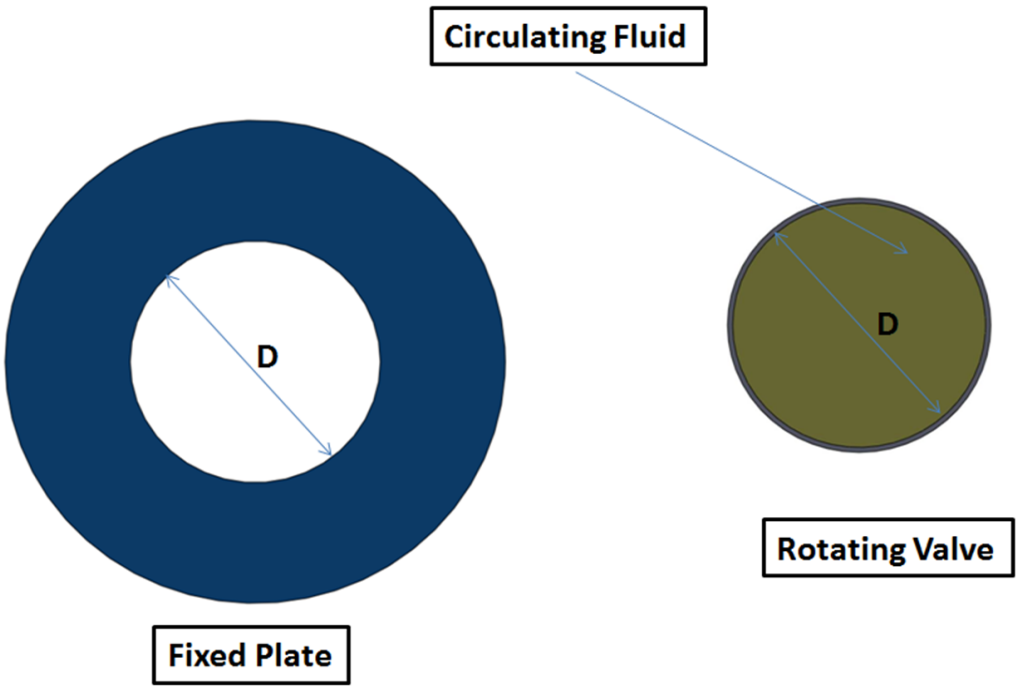

Figure 3.2- A drawing for the rotating valve and the fixed plate inside the valve section

As mentioned earlier the rotor drives the rotating valve into three different positions, the flow area is maximized when both the centers of the rotating valve and the fixed plate coincide, meaning the pressure drop across the tool is minimum. On the other hand when the rotating valve is located in the other two positions, extreme right or extreme left the flow area is minimized leading to an increase in the pressure drop across the tool. The fluctuation in pressure values can be then seen as pressure pulses with a frequency that depends on the rate of the flow passing through the tool.

Figure 3.3, shows a schematic of the pressure fluctuations when the rotating valve position varies relative to the fixed plate, where P is the pressure drop across the tool in psi and t is time in seconds.

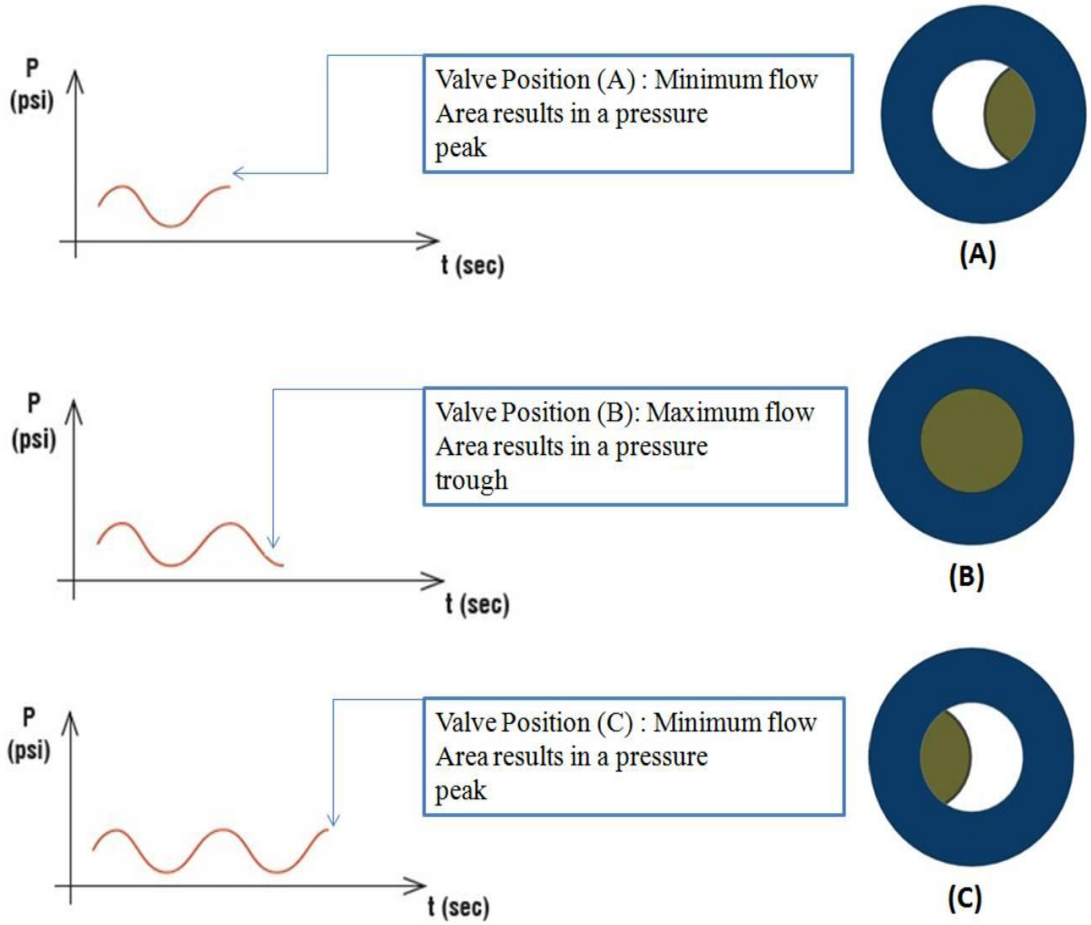

Figure 3.3- A Schematic of the pressure drop fluctuation in response to the valve position

3.2 The PPG Tool Testing

Prior to conducting any drilling tests to evaluate the effect of the generated pressure pulses on drilling performance when the pulses act as vibration forces, it was necessary to understand the tool's performance at various flow rates. A set of experiments was conducted to evaluate the pressure pulses generated at different flow rates along with the forces generated when those pulses acted on a fixed area. In this section the experimental testing setup and the experimental procedures used to test the PPG are presented, while the results are discussed in Chapter 4.

3.2.1 Experimental Setup

The experimental setup consisted mainly of a testing frame, a mobile Data AcQuisition (DAQ) system, a group of sensors and a pumping unit. Each of the setup components is described thoroughly as follows;

3.2.1.1 Testing Frame

The testing frame was built to install the 6 feet long PPG tool (OD= 2 1/8") on one side of the frame and provide a network of pipes and valves to control the flow passing through the PPG tool and attach some of the required sensors on the other side of the frame. As shown in Figure 3.4, the PPG was installed vertically in a position at which the flow travels upward through the tool. The lateral motion of the PPG tool was restricted by three V-shaped restraints on both sides of the tool. Beneath the PPG a triangular plate was installed as shown in figure to ensure the forces exerted by the PPG are equally transferred to the load cells used to record these forces. At the outlet of the tool a T-Piece

pipe was installed, which represents an area upon which the pressure pulses act when the pulses leave the PPG tool.

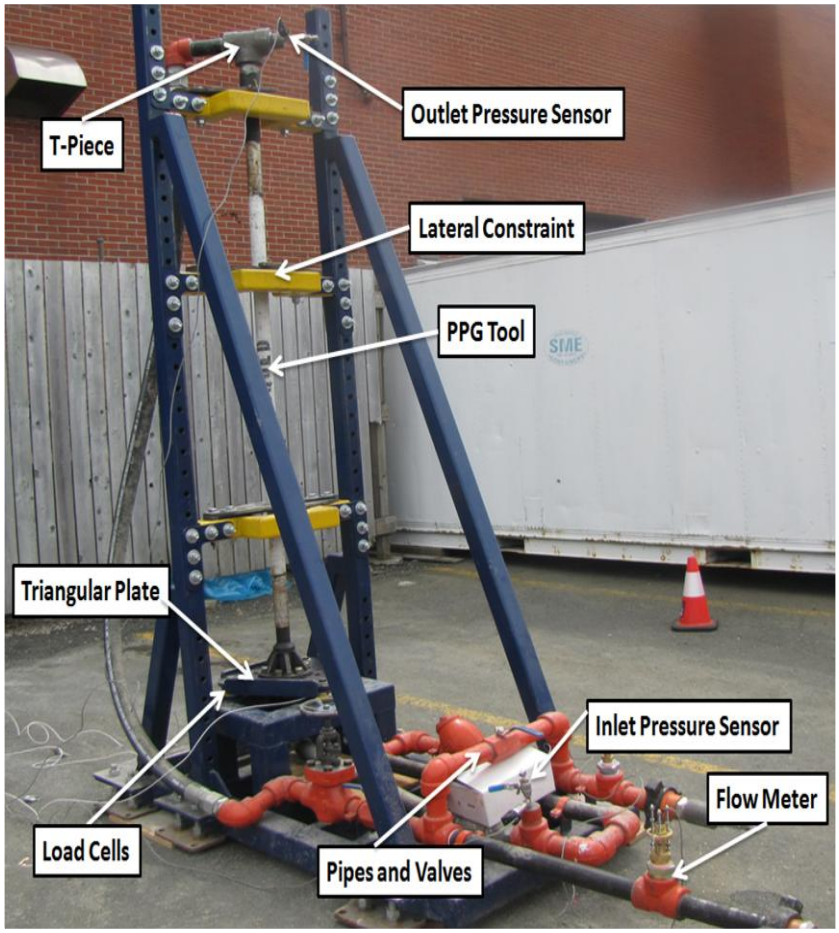

Figure 3.4- Testing Frame for the PPG evaluation experiments

The pipes network also contained a pressure relief valve to release the pressure by diverting the flow directly to the outlet pipe if the pressure exceeded a pre-set value for safety reasons, a Y strainer to filter the water prior passing the PPG tool, a manual bypass valve to divert flow to the outlet pipe if needed and an analogue pressure gauge to monitor pressure.

3.2.1.2 Data Acquisition (DAQ) system

Sensors on the testing frame were connected to a multi-channel DAQ system, which was designed to be portable in order to operate outside the laboratory and tough in order to withstand tough weather conditions and possible harsh transportation. The power supply system for the DAQ is waterproof when sealed and water resistant when open. The DAQ system has a custom cable to plug in to the power supply of 110 V input as well as three different voltage outputs from the system. These three outputs are 24, 9-12 and 5 Volts.

This DAQ has a NI9188 Chassis built in with 16 channels and a NI9237 card for acquiring the data . The DAQ is connected to a laptop using an Ethernet connection. Figure 3.5, shows a photograph taken for the DAQ system in operation.

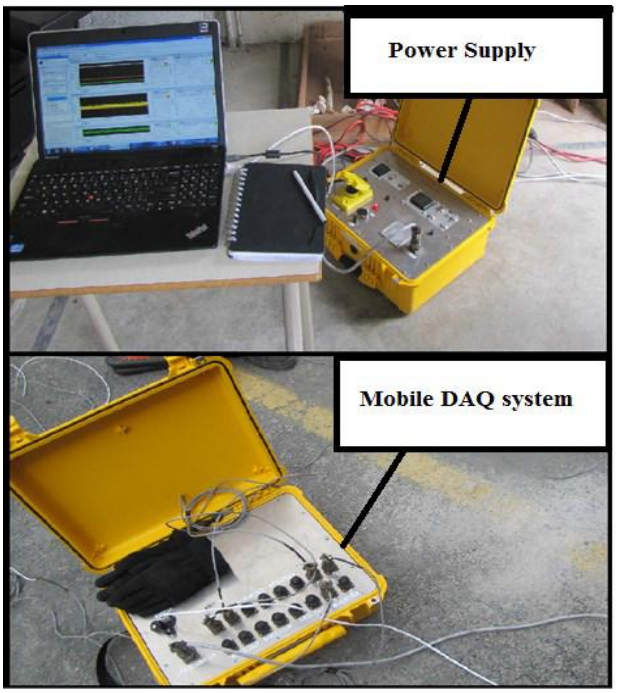

Figure 3.5- Mobile DAQ system and its power supply.

3.2.1.3 Sensors

To conduct the experiments, 6 sensors were required. Two pressure sensors to measure the inlet or the upstream pressure and outlet or downstream pressure fluctuations. Three load cells in a triangular configuration were used to monitor and record the forces generated by the tool, and a flow meter was also used to measure and control the flow rate according to the experimental plan. To measure the outlet pressure, a pressure transducer with operating range of 0 to 1500 psi was used. For the inlet pressure fluctuations, operating range of the pressure transducer was from 0 to 4000 psi. Each load cell had a capacity range of 5000 lbs. Therefore, when they were added together, the load capacity of the system became 15000 lbs. As shown in Figure 3.6, the PPG tool is placed in the center of the plate and the generated force is divided among three load cells. Adding measured loads from each load cell, the total force generated by the tool was calculated.

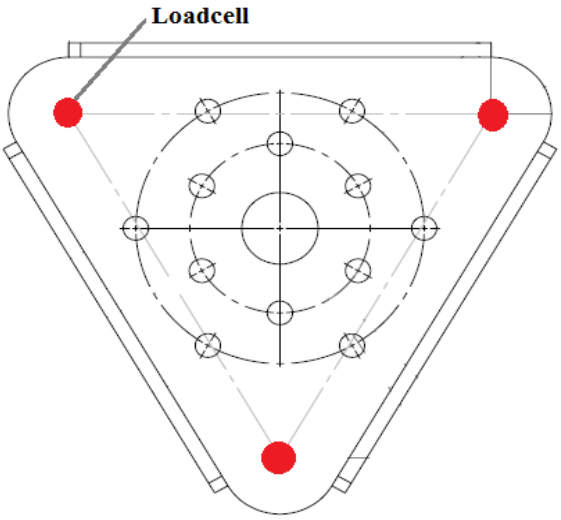

Figure 3.6- Triangular configuration for load cells.

3.2.1.4 Pumping Unit

Input flow was supplied by a mobile pumping unit as shown in Figure 3.6. The unit has the capability to deliver up to 70 USGPM with a maximum pressure of 2500 psi. It utilizes a jet Rodder water pump with a jack hammer action. This water pump is designed to be driven hydraulically and has a one-to-one hydraulic to water ratio. For every gallon of hydraulic oil pumped, one gallon of water is pumped

Figure 3.7- Pumping Unit

The pump is simple to operate and requires only five moving parts. It has a hydraulic cylinder on one side of a sealed center block and a water cylinder on the other side, as shown in Figure 3.8.

A single shaft with specially constructed piston heads is slowly driven back and forth. Hydraulic oil is pumped into the hydraulic section, driving the piston the length of the water barrel. As that occurs, water enters the water barrel behind the moving piston through a check valve. When the piston reaches the end of its stroke, a sensing device reverses the piston, sending it back to its original position and at the same time expelling the water through the directional check valve. As this occurs, water is being introduced into the water barrel on the other side of the piston. The pump is constantly loading and expelling hydraulic oil and is constantly loading and expelling an equal amount of water.

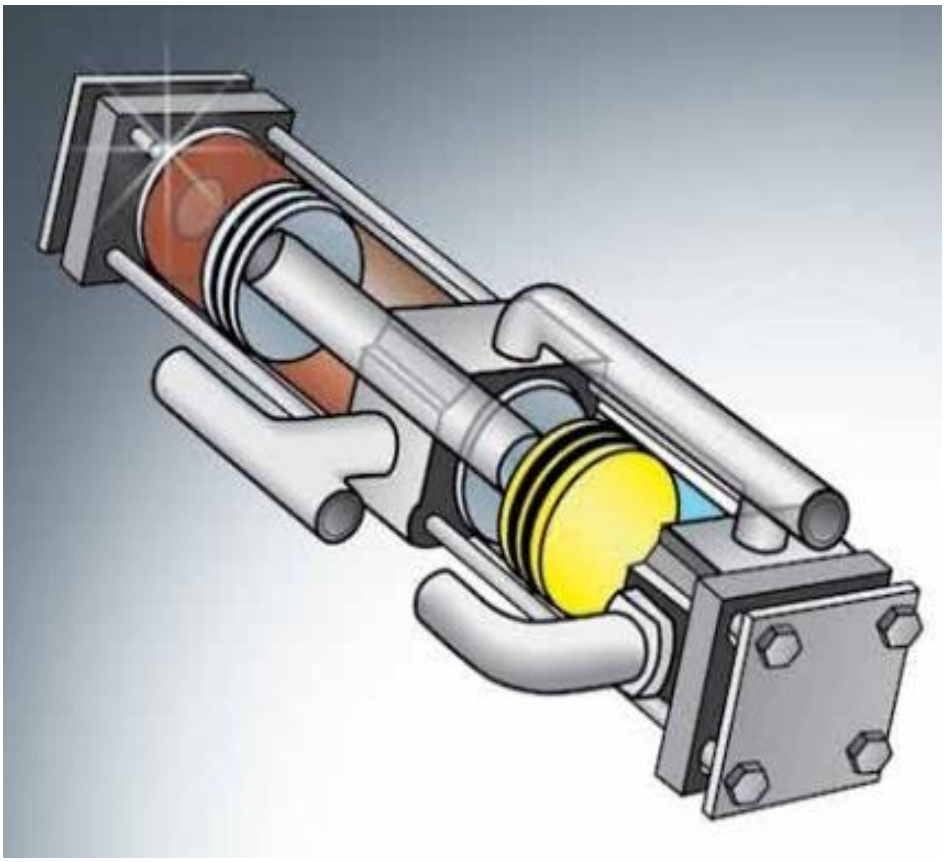

Figure 3.8- Jet Rodder Water Pump as sketched using SolidWorks

3.2.2 Experimental Plan and Procedures

In order to evaluate the performance of the PPG tool, which in the frame of these testing experiments refers to the ability of the tool to generate pressure pulses and consequently vibration forces, it was necessary to test it with a range of fluid flow rates upon which the magnitude and frequency of the generated pressure pulses are dependant. Water was used as the testing fluid, because the pump used was not designed to handle other fluids. Using only water would not affect the experimental results, considering that similar behavior could be obtained with heavier fluids if a more powerful pump is used. Ten runs including five repeats were conducted to test the PPG, the maximum flow rate was 70 US-GPM considering the maximum pumping capacity of the pumping unit, while the minimum was considered 30 GPM to investigate the tool's output at a slightly lower flow rate than the recommended 40 US-GPM by the PPG manufacturer. Prior to conducting the runs, the PPG tool was replaced by an empty pipe to measure the influence of the pumping unit on the recorded readings, also ten runs were conducted on the empty pipe, including five repeats to ensure the accuracy of the recorded data.

After taking into account the effect of the pumping unit the PPG was then installed on the frame. prior to recording data, flow was bypassed to the outlet directly using the manual bypass valve to ensure the desired flow rate was reached and the flow was steady enough, Then the inlet and outlet valves of the frame were opened and the bypass valve was closed to let the water pass through the tool. After the tool operated for about one minute, recording started for 20 seconds with sampling rate of 3000 Hz.

Once the desired time for the recording was reached and enough data was recorded, the bypass valve was opened and the tool was isolated again. For the next flow rate level, the same procedures were repeated. Table 3.1, shows the summary of the conducted runs on both the empty pipe and the PPG tool.

Table 3.1- Experimental runs for testing the PPG tool

Run Number	Tested Tool	Flow Rate (LPM)	Back Pressure	Circulation Fluid
1 2	Empty Pipe	113	Atmospheric Pressure	Water
3 4		151		
5 6		190		
7 8		227		
9 10		265		
11 12	Pressure Pulse Generator (PPG)	113		
13 14		151		
15 16		190		
17 18		227		
19 20		265		

4 The PPG Testing Results

In this chapter the results obtained from the experiments conducted to test the PPG are presented. As mentioned in Chapter 3, the purpose was primarily to measure the amplitude and frequency of the pressure pulses generated by the PPG tool, and measure the forces generated when these pulses act on a fixed area within the BHA. The results are presented in two sections, the pressure data analysis section, and the forces data analysis section. Both sections also contain the spectral analysis of the pressure pulses and the generated forces. The results from the empty pipe runs are presented first, then followed by the results from the PPG tool runs.

4.1 Pressure Data analysis

The first task in the pressure analysis job was to determine the effect of the pumping unit on the recorded data. It was found that the pump caused short time fluctuations in pressure due to its mechanism, these pressure fluctuations were dependant on the flow rate used, and the back pressure applied to the pump when the PPG tool was installed. As a result the pump effect was similar in the empty pipe case and the PPG tool case trend wise, but the amplitude and the duration of these effects differed in each case. These effects are described thoroughly in the next section. The other tasks included analyzing the amplitude and frequency of the pressure pulses generated when the PPG was operated at the flow rate range used, and finding a relationship between the flow rate, amplitude and the frequency of the pressure pulses.

4.1.1 Empty Pipe Pressure Data Analysis

Starting with 113 Liters Per Minute (LPM) flow rate the pumping unit effect was clearly seen in the pressure data as shown in Figure 4.1. A pressure drop of 8.5 psi occurred for 0.4 second before the pressure stabilized and got back to normal, this effect was repeated in the pressure data every 4.35 seconds.

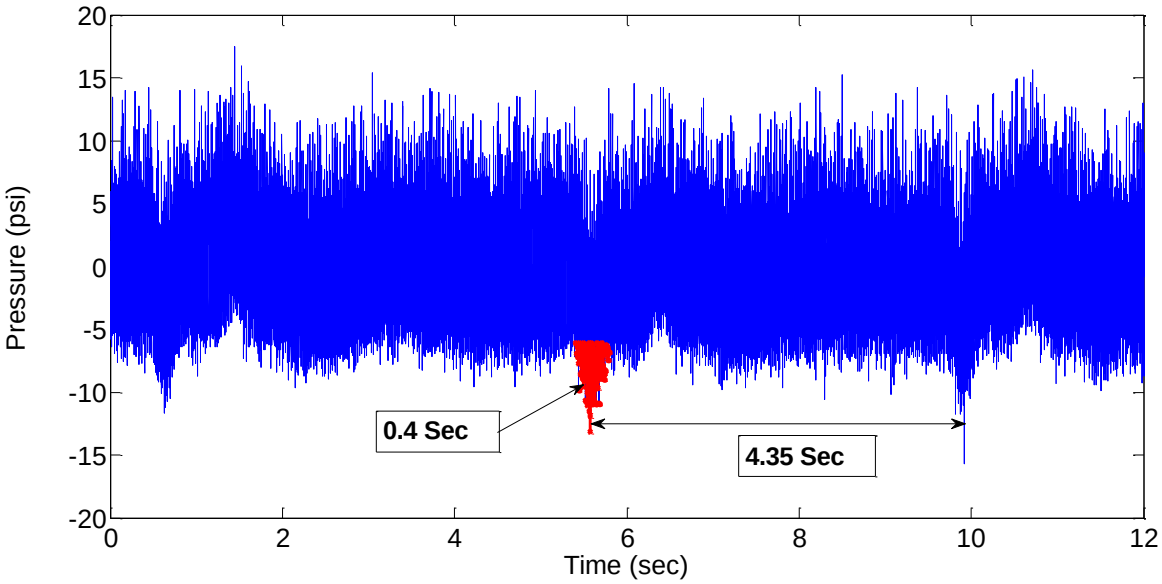

Figure 4.1- Empty pipe pressure data at 113 LPM

At 151 LPM, the pumping unit caused a 9.6 psi pressure drop for a duration of 0.38 second before the pressure stabilizes and went back to normal, the effect was encountered every 3.15 seconds, as shown in Figure 4.2.

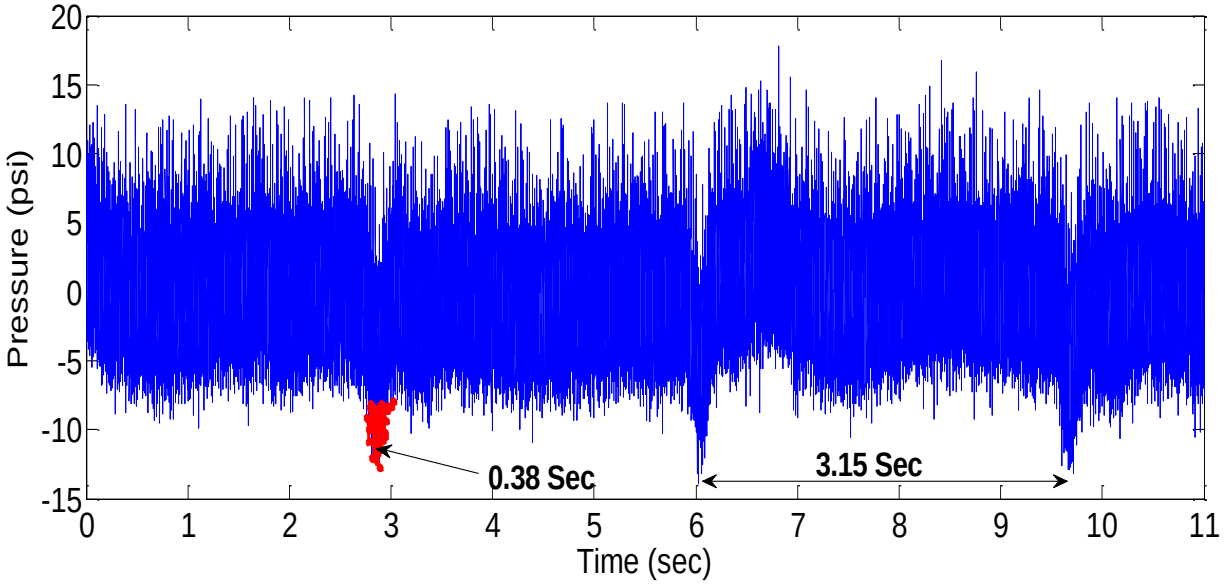

Figure 4.2- Empty pipe pressure data at 151 LPM

At 190 LPM the pumping unit caused a 13.4 psi pressure drop for a duration of 0.34 seconds, and the effect could be seen every 3.1 seconds as shown in Figure 4.3.

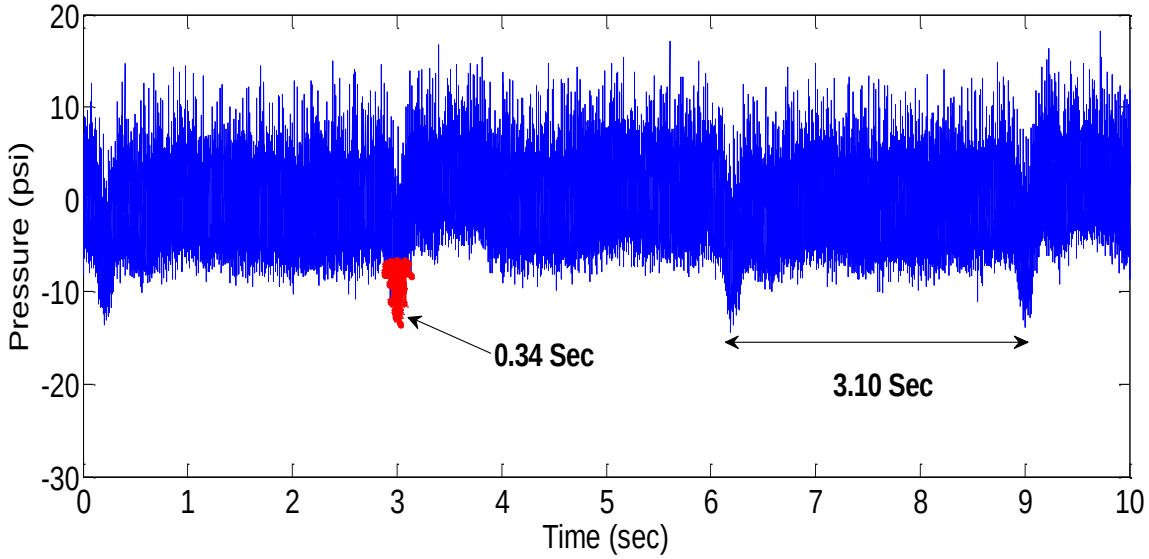

Figure 4.3- Empty pipe pressure data at 190 LPM

At 227 LPM the pumping unit caused a 16 psi pressure drop for a duration of 0.29 seconds, and the effect could be seen every 2.3 seconds as shown in Figure 4.4.

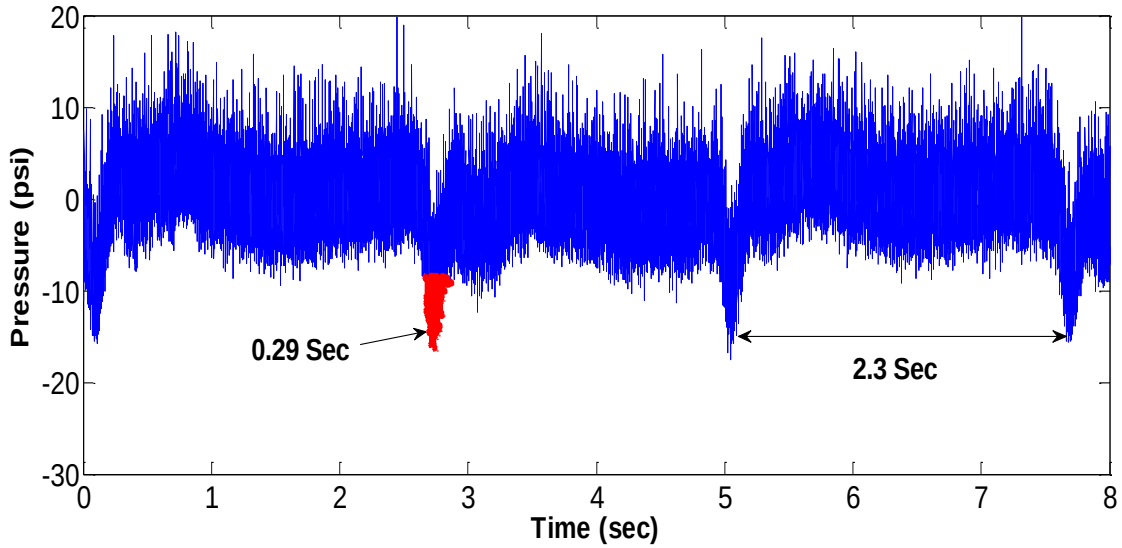

Figure 4.4- Empty pipe pressure data at 227 LPM

At 265 LPM the pumping unit caused a 18 psi pressure drop for a duration of 0.25 seconds, and the effect could be seen every 2 seconds as shown in Figure 4.5.

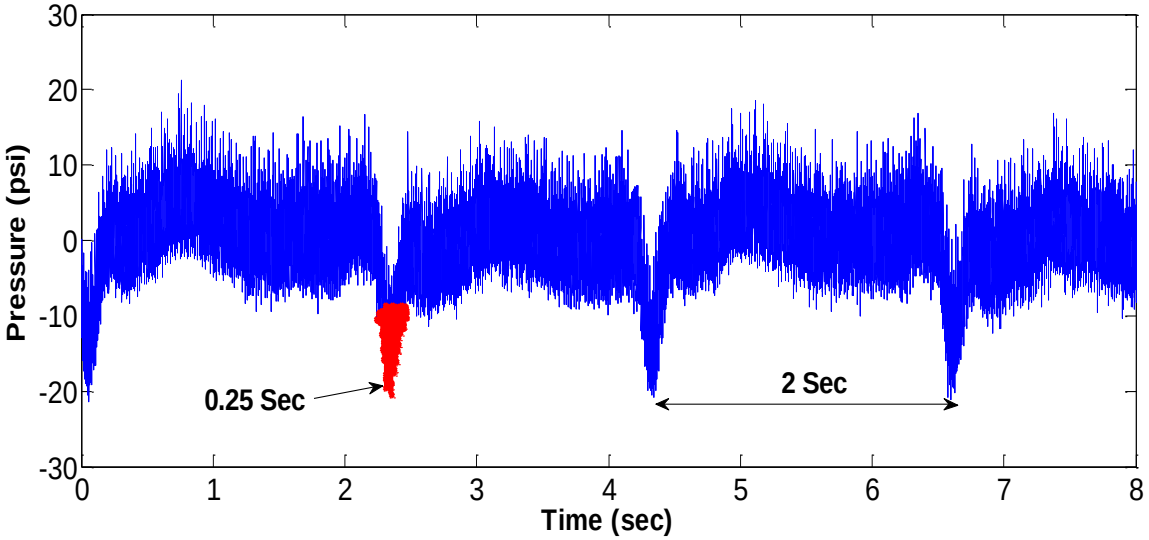

Figure 4.5- Empty pipe pressure data at 265 LPM

The spectral analysis for the pressure data using all the flow rates is shown in Figure 4.6. The data shows a signal with a frequency of 462 Hz. That signal was believed to be a high frequency cavitation occurring in the system.

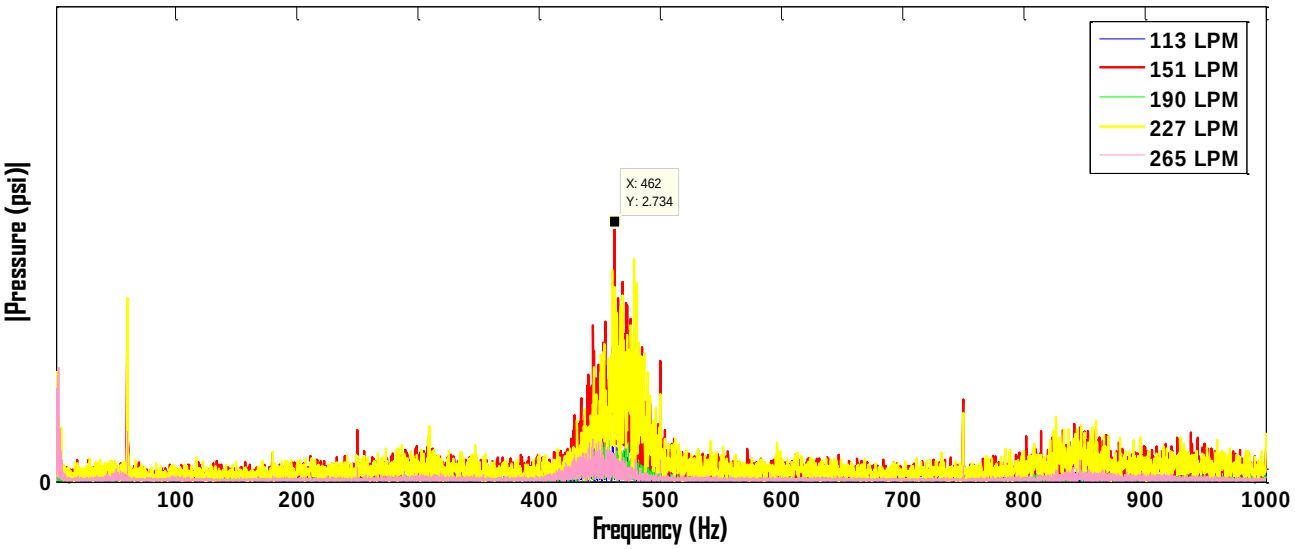

Figure 4.6- Spectral analysis for the empty pipe signal at 5 different flow rates

The summary of the pumping unit effects encountered are summarized in Table 4.1, shown below.

Table 4.1- Summary of the pumping unit effect on the empty pipe pressure data

Flow Rate	Pressure Drop	Duration	Occurrence time
LPM	psi	sec	sec
113	8.5	0.4	4.35
151	9.6	0.38	3.15
190	13.4	0.34	3.10
227	16	0.29	2.3
265	18	0.25	2

4.1.2 PPG Pressure Data Analysis

When the PPG was installed, it was observed that the outlet pressure sensor was reading lower pressure values than the inlet pressure although the frequency and the pressure behaviors were quite similar. Three reasons could explain the difference, the first is that the outlet pressure sensor was installed on the side of the T-Piece upon which the pressure pulses act and the pressure pulses were dispersed once they act on the front area. The second is that the outlet on the side of the T-Piece was connected directly to atmospheric pressure, which could effectively weaken the pressure pulses as they leave the tool, and the third was that in order to connect the T-Piece a cross-over connection was installed, which changed the diameter of the flow path from 1 inch to 2 inches, contributing to weakening the pressure pulses at the outlet.

The experiments started with 113 LPM flow rate, and the PPG tool started pulsing once the system pressure became stable. By analyzing the inlet pressure sensor data it was observed that the pressure pulses amplitude was 180 psi as shown in Figure 4.7, the pumping unit effect was also encountered with a pressure drop of 44 psi for a duration of 0.32 second, and this effect occurred every 5 seconds.

On the other hand it was found that the outlet pressure sensor data showed a pulse amplitude of 40 psi and the pumping unit effect was much weaker than its effect on the inlet sensor pressure data. The pressure data from the outlet pressure sensor are shown in Figure 4.8, followed by the spectral analysis of the signal of both sensors in Figure 4.9.

For the rest of the analysis the inlet pressure sensor data will be presented as a more accurate source for the reasons mentioned above.

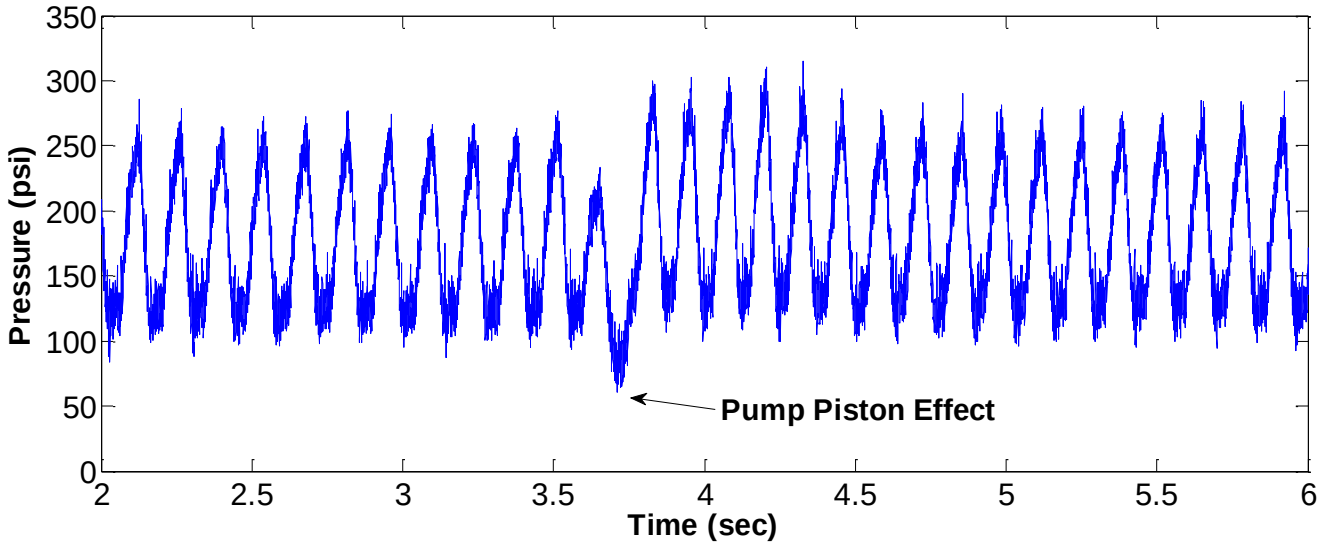

Figure 4.7- Inlet Pressure Data for the PPG tool at 113 LPM

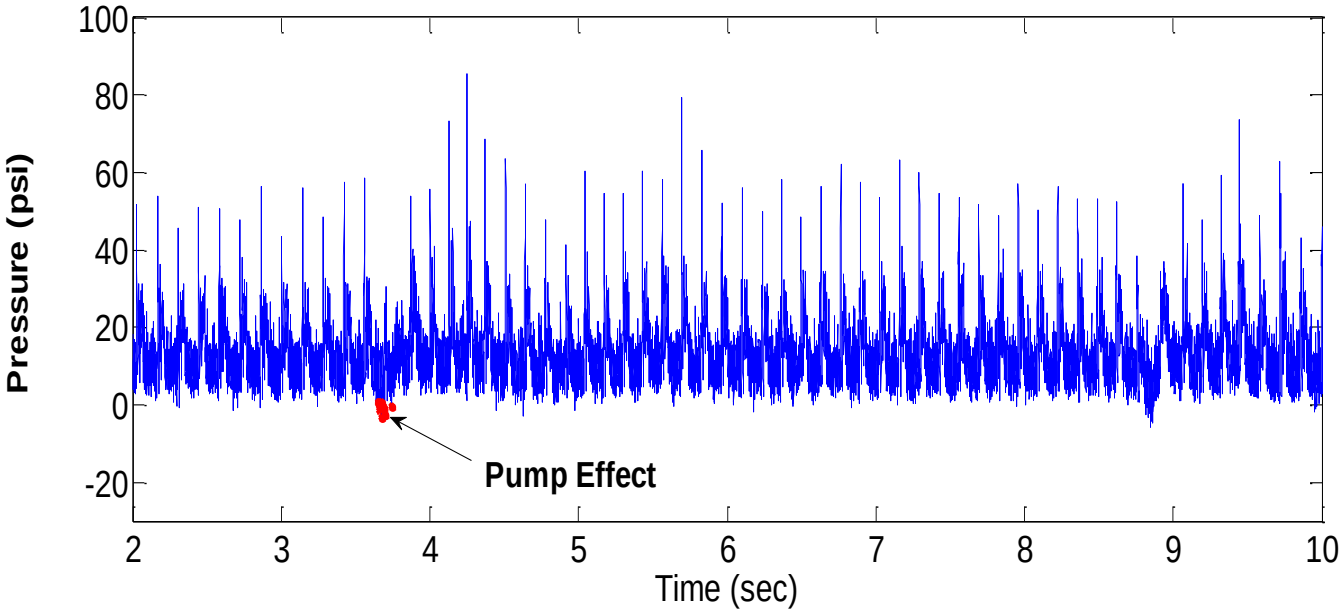

Figure 4.8- Outlet Pressure Data for the PPG tool at 113 LPM

The spectral analysis of the pressure data at 113 LPM showed that the dominant frequency of the pulses was 7.3 Hz while other frequencies were harmonics of the dominant frequency. Signals from both sensors had the same frequency response as shown in Figure 4.9

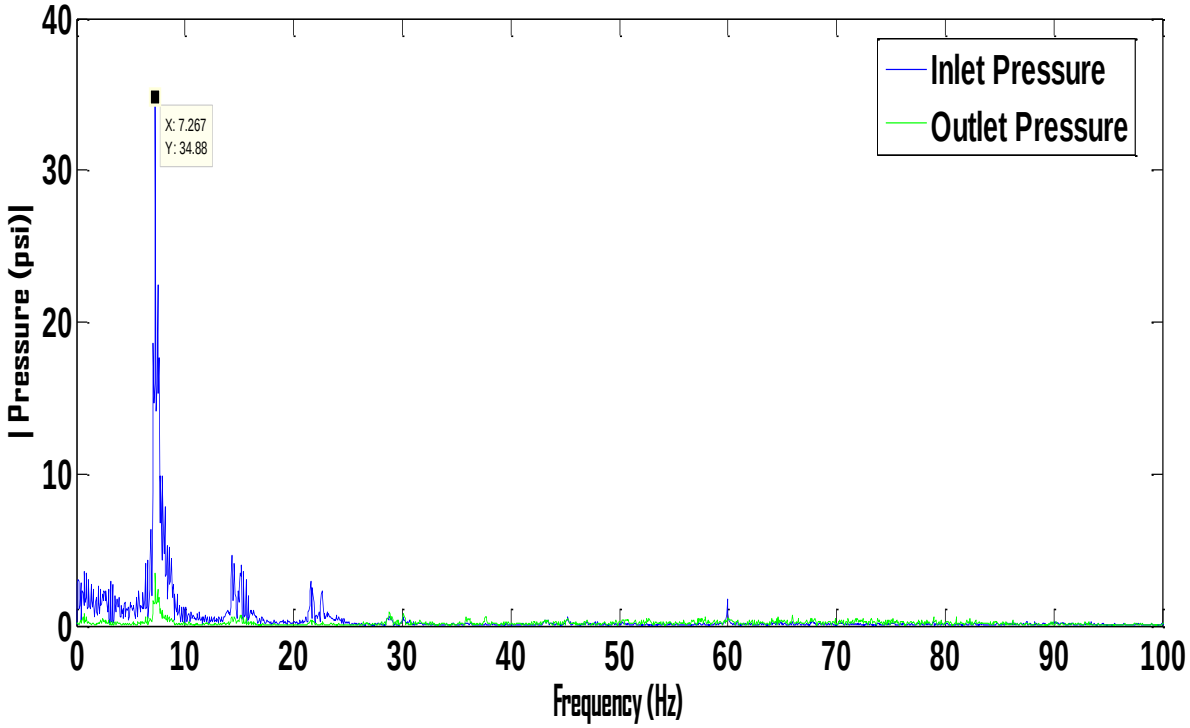

Figure 4.9- Spectral analysis of the pressure signals at 113 LPM

At 151 LPM, the pulse pressure increase was 250 psi peak to peak pressure as shown in Figure 4.10, the pumping unit effect was encountered with a pressure drop of 100 psi for a duration of 0.31 second and this effect occurred every 3.84 seconds.

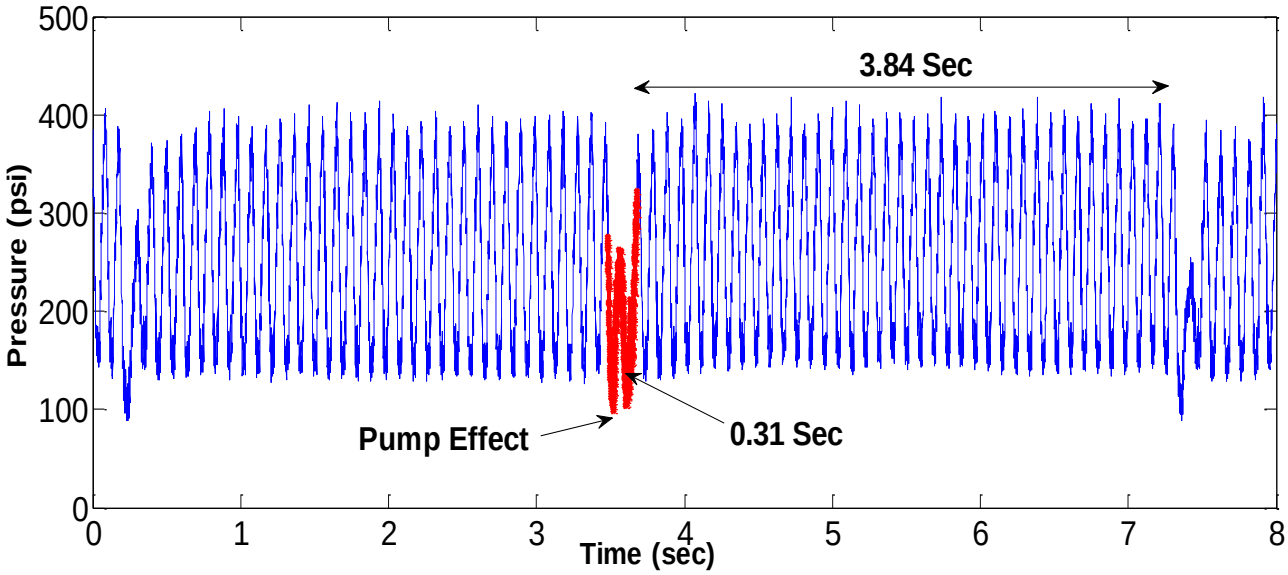

Figure 4.10- Inlet Pressure Data for the PPG tool at 151 LPM

The spectral analysis showed that the dominant frequency was 10.4 Hz while the other frequencies were harmonics of the dominant frequency, as shown in Figure 4.11.

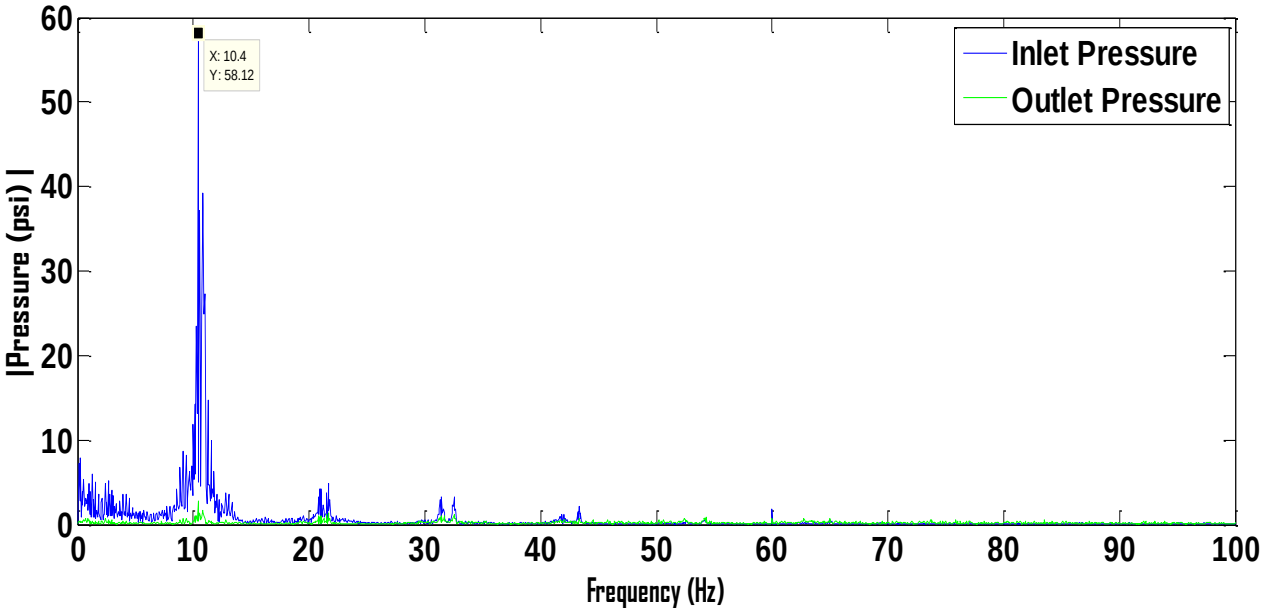

Figure 4.11- Spectral analysis of the pressure signals at 151 LPM

At 190 LPM, the pulse pressure increase was 300 psi peak to peak pressure as shown in Figure 4.12, the pumping unit effect was encountered with a pressure drop of 163 psi for a duration of 0.30 second and this effect occurred every 3.06 seconds.

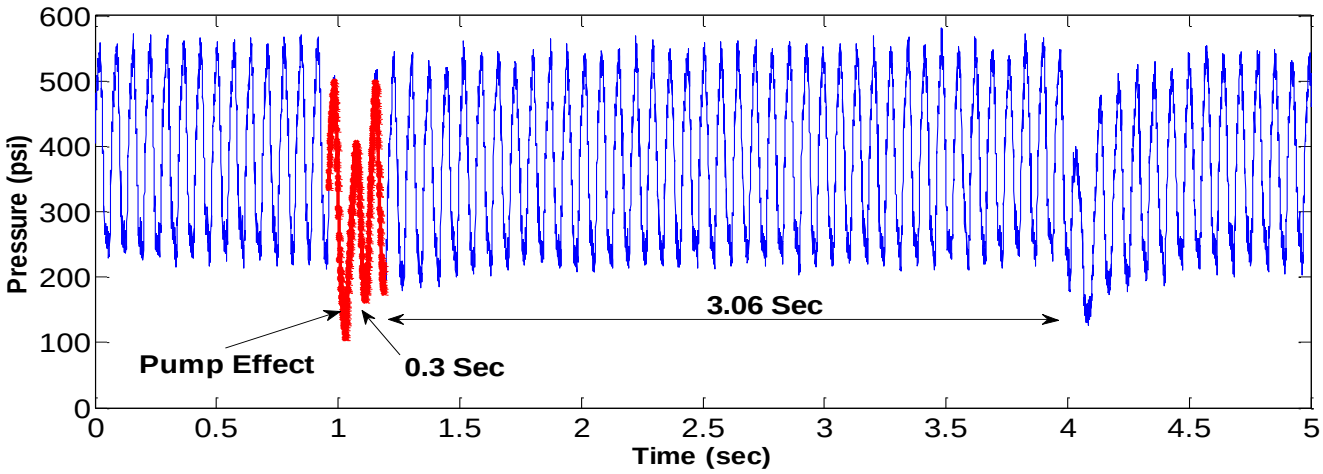

Figure 4.12- Inlet Pressure Data for the PPG tool at 190 LPM

The spectral analysis showed that the dominant frequency of the pulses was 14.5 Hz while the other frequencies were harmonics of the dominant frequency as shown in Figure 4.13.

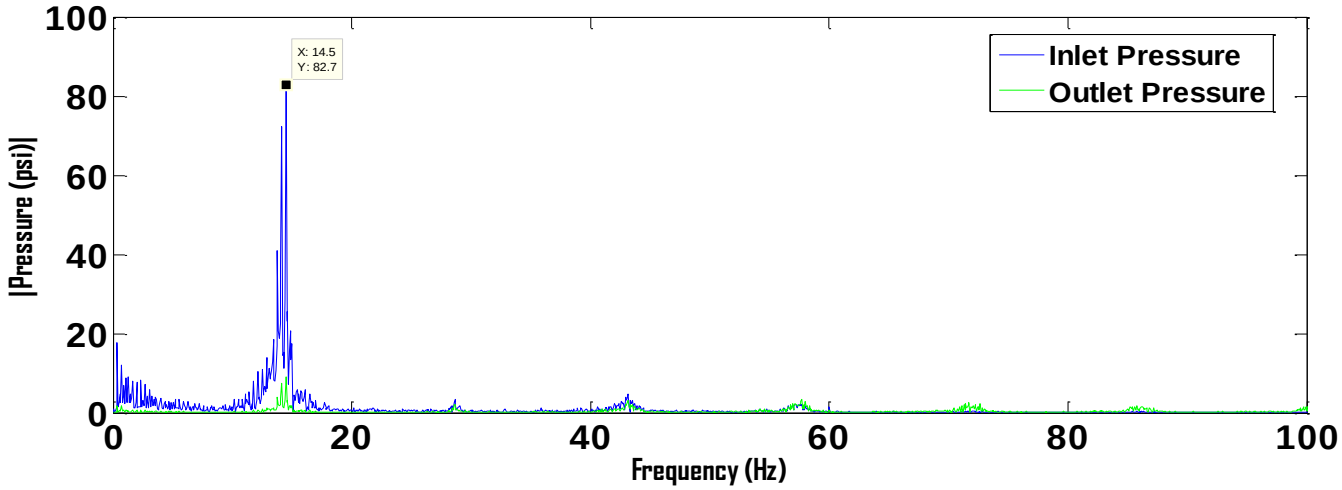

Figure 4.13- Spectral analysis of the pressure signals at 190 LPM

At 227 LPM, the pulse pressure increase was 410 psi peak to peak pressure as shown in Figure 4.14, the pumping unit effect was encountered with a pressure drop of 231 psi for a duration of 0.25 second and this effect occurred every 2.45 seconds.

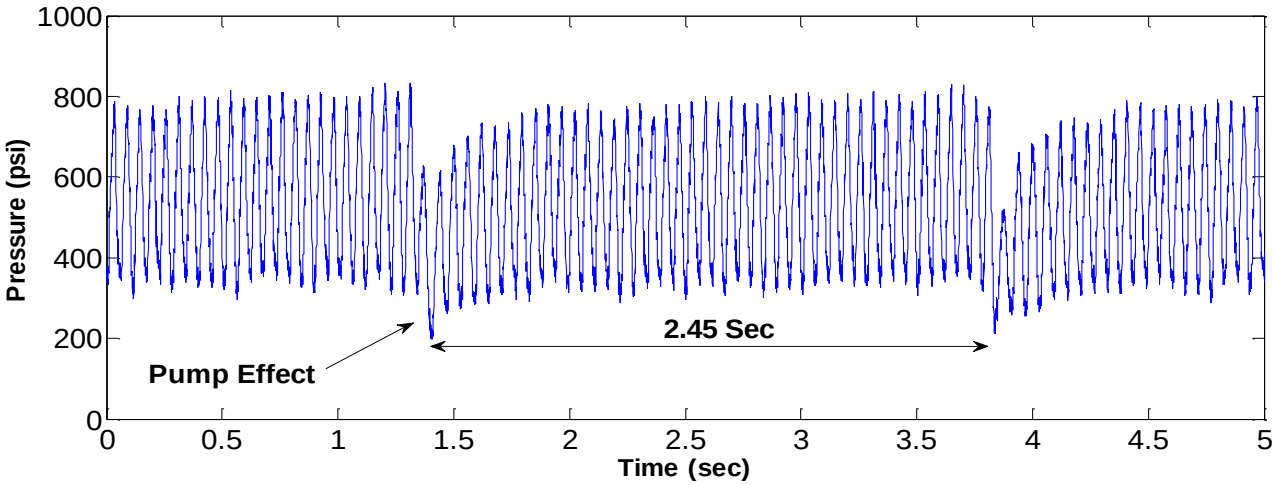

Figure 4.14- Inlet Pressure Data for the PPG tool at 227 LPM

In Figure 4.15, the spectral analysis showed that the dominant frequency of the pulses was 17.64 Hz while the other frequencies were harmonics of the dominant frequency.

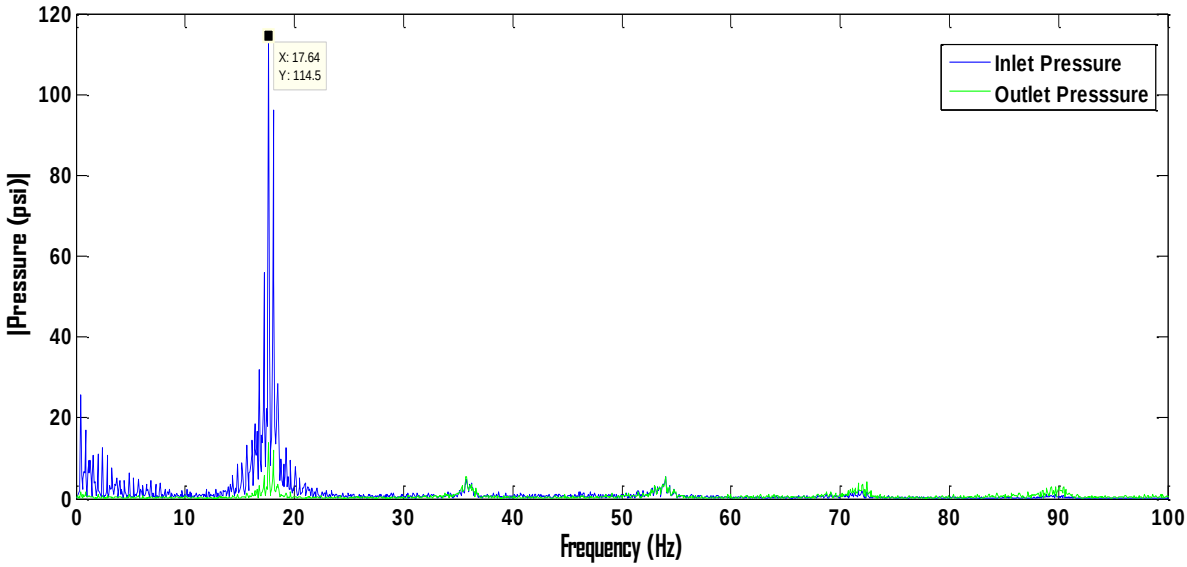

Figure 4.15- Spectral analysis of the pressure signals at 227 LPM

At 265 LPM, the pulse pressure increase was 570 psi peak to peak pressure as shown in Figure 4.16, the pumping unit effect was encountered with a pressure drop of 185 psi for a duration of 0.23 second and this effect occurred every 2.2 seconds.

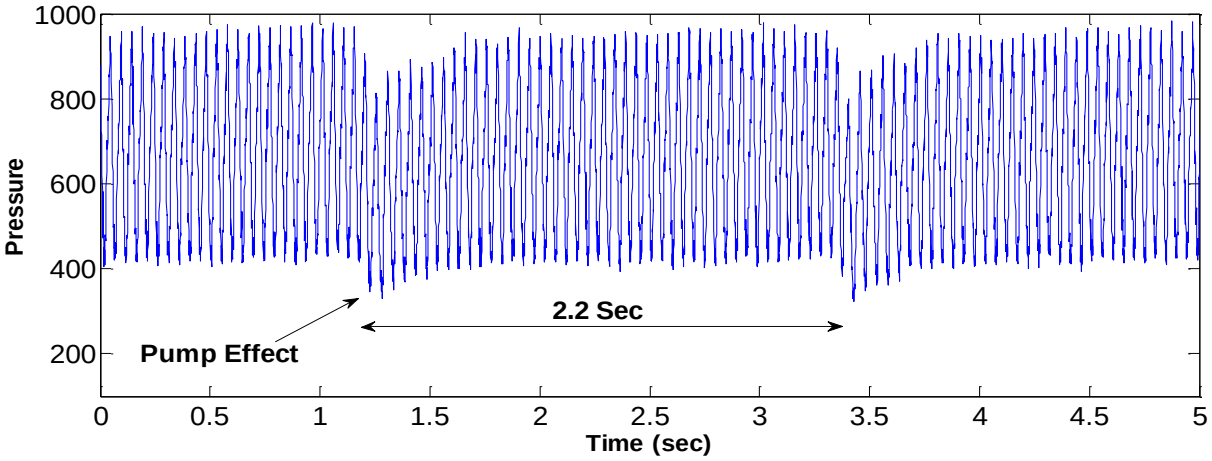

Figure 4.16- Inlet Pressure Data for the PPG tool 265 LPM

In Figure 4.15, the spectral analysis showed that the dominant frequency of the pulses was 20.5 Hz while the other frequencies were harmonics of the dominant frequency.

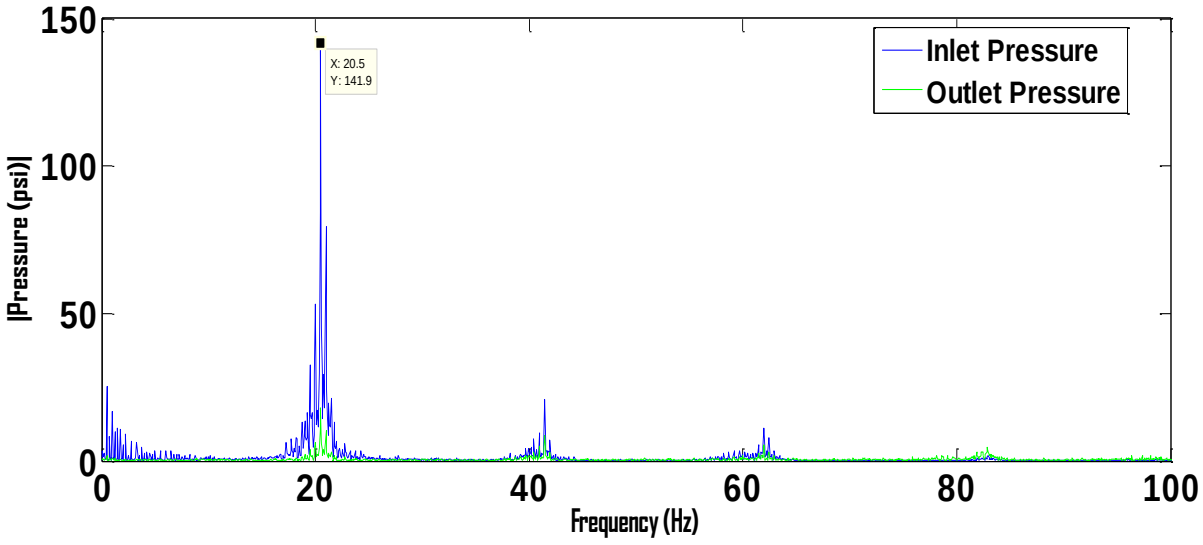

Figure 4.17- Spectral analysis of the pressure signals at 265 LPM

From the obtained data which is summarized in Table 4.2, a relationship among the pressure pulses frequency, pressure magnitude and the flow rate value could be derived. It was found that the pulsing frequency had a linear relationship with the flow rate used, as shown in Figure 4.18. while the pressure pulse magnitude was found to have a direct proportionality with the square value of the flow rate as shown in Figure 4.19.

Table 4.2- Summary of pressure and frequency data of the PPG

Flow Rate	Pressure pulse amplitude	Frequency of pulsation
LPM	psi	Hz
113	180	7.3
151	250	10.4
190	300	14.5
227	410	17.64
265	570	20.5

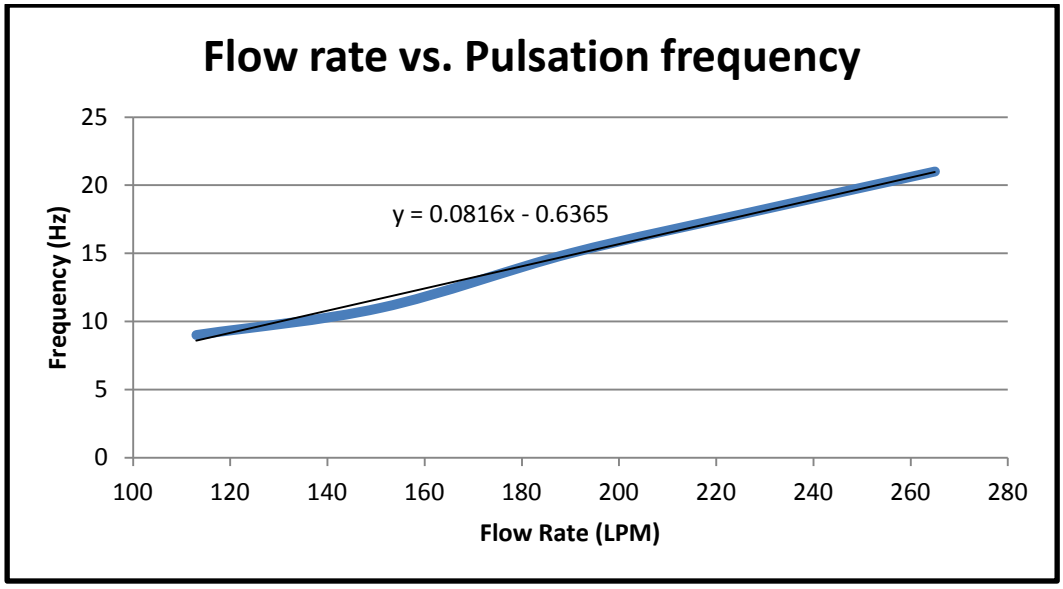

Figure 4.18- Relationship between pulsing frequency and flow rate used

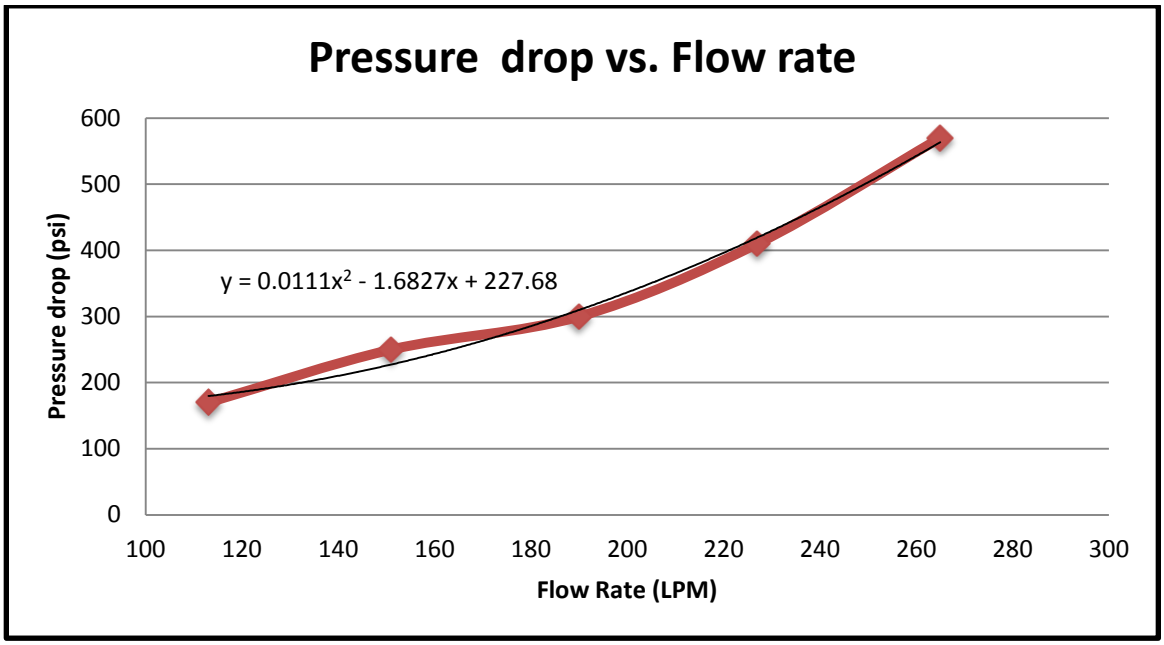

Figure 4.19- Relationship between the pressure drop and the flow rate used

4.2 Force Data analysis

When the empty pipe was installed there was practically no force encountered, even with the pump effect as the low frequency pulses coming from the pump did not introduce enough force to move the pipe or show any response on the data recorder. when the PPG was installed, at 113 LPM the pulses acting on a 1 square inch area applied forces on the load cells immediately. as mentioned in Chapter 3 the sum forces on the 3 load cells represented the overall value of force applied by the pressure pulse generated by the PPG. At 113 LPM the force generated was about 175 N considering the average 75% of peak values shown in Figure 4.20. While the spectral analysis of the 3 load cells showed that the forces dominant frequency totally agreed with the dominant frequency of the pulses at 7.3 Hz as shown in Figure 4.21.

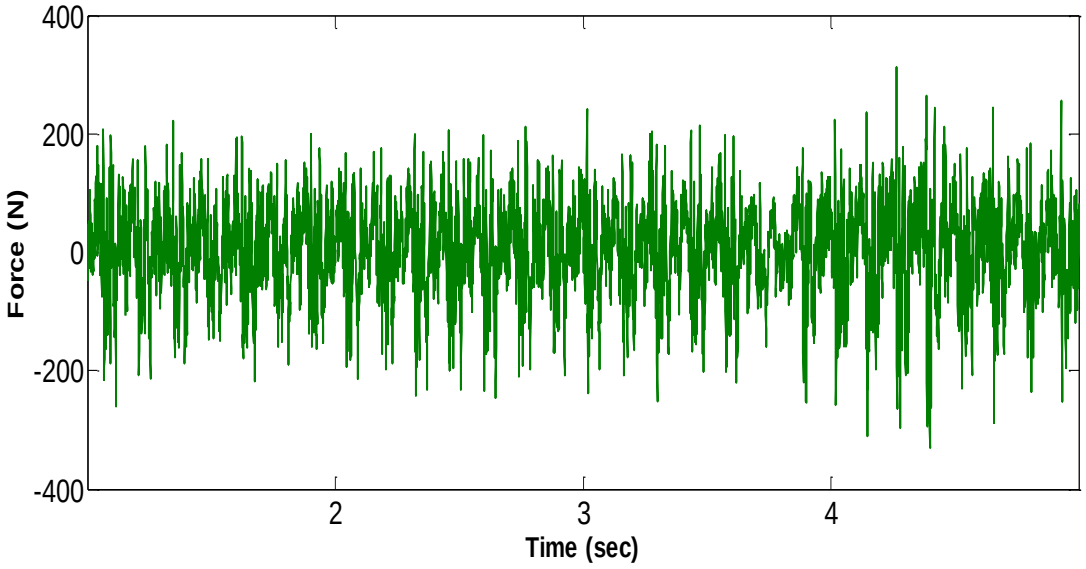

Figure 4.20- Forces generated by the PPG at 113 LPM

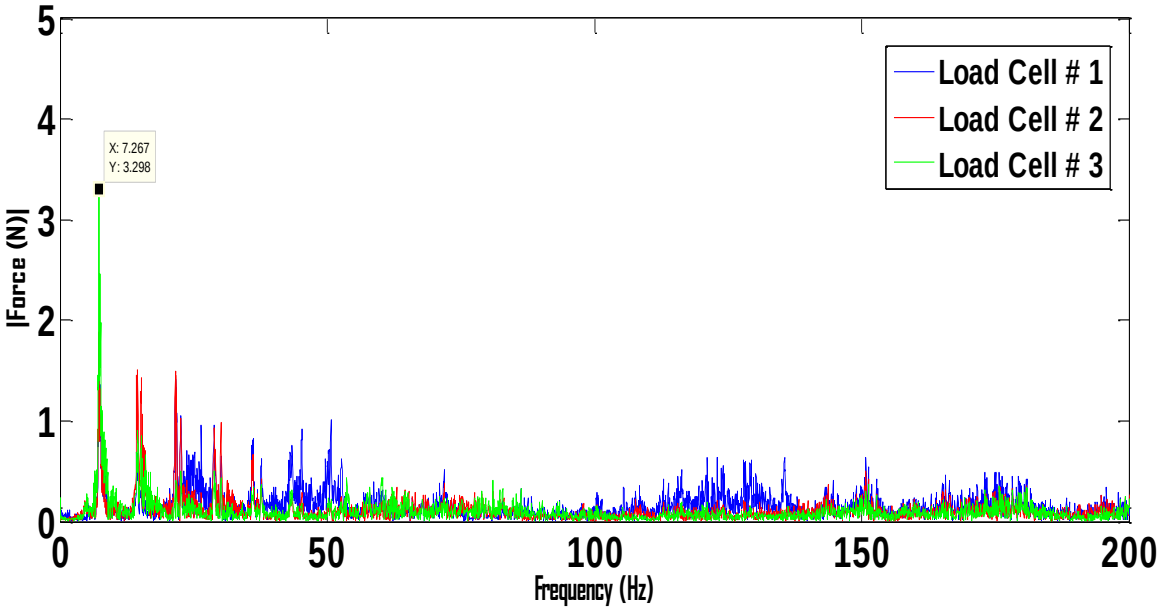

Figure 4.21- Spectral analysis of the forces encountered by the load cells at 113 LPM

At 151 LPM the force generated was about 330 N as shown in Figure 4.22. While the Spectral analysis of the 3 load cells showed that the forces dominant frequency totally agreed with the dominant frequency of the pulses at 10.4 Hz as shown in figure 4.23.

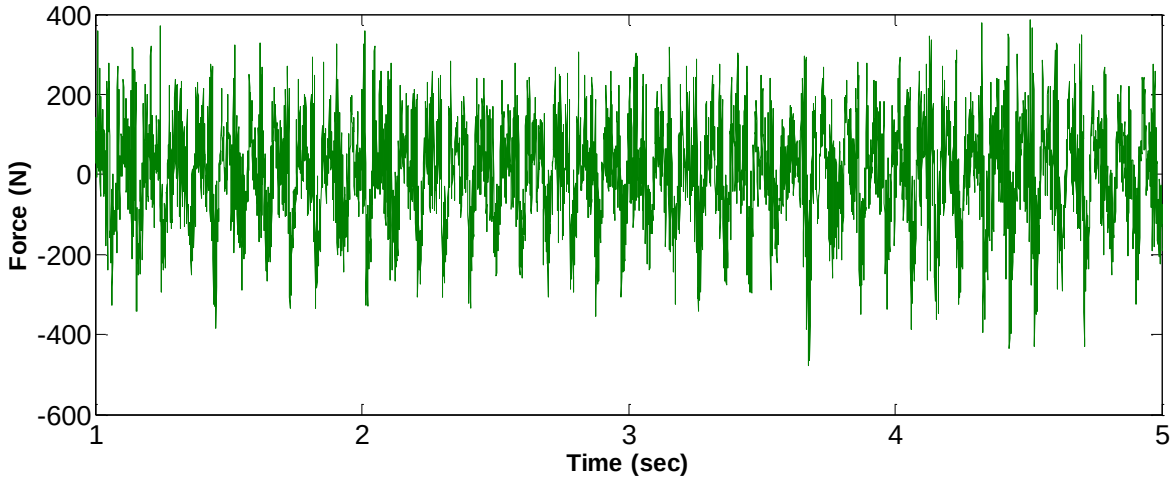

Figure 4.22- Forces generated by the PPG at 151 LPM

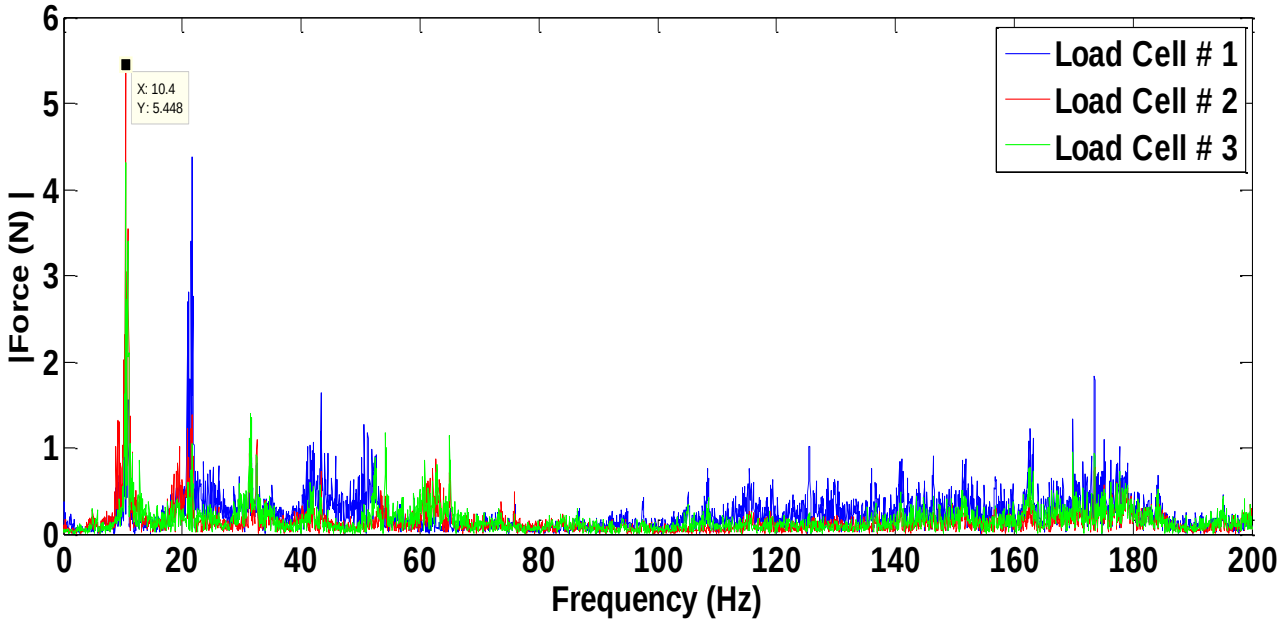

Figure 4.23- Spectral analysis of the forces encountered by the load cells at 151 LPM

At 190 LPM the force generated was about 660 N as shown in Figure 4.24. While the spectral analysis of the 3 load cells showed that the forces dominant frequency totally agreed with the dominant frequency of the pulses at 14.5 Hz as shown in Figure 4.25.

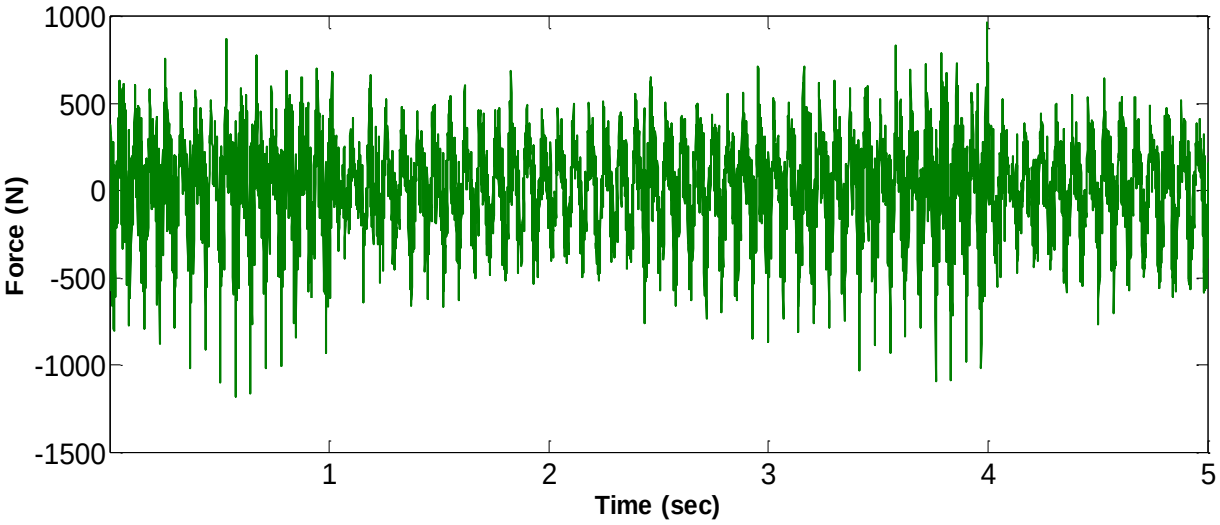

Figure 4.24- Forces generated by the PPG at 190 LPM

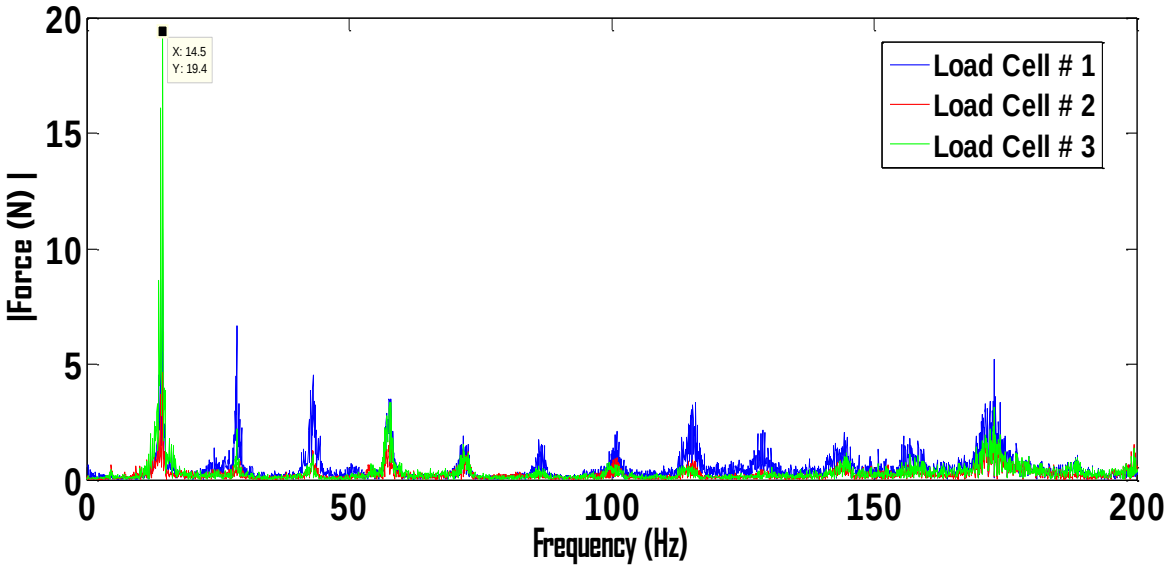

Figure 4.25- Spectral analysis of the forces encountered by the load cells at 190 LPM

At 227 LPM the force generated was about 1000 N as shown in Figure 4.26. While the spectral analysis of the 3 load cells showed that the forces dominant frequency totally agreed with the dominant frequency of the pulses at 17.64 Hz as shown in Figure 4.27.

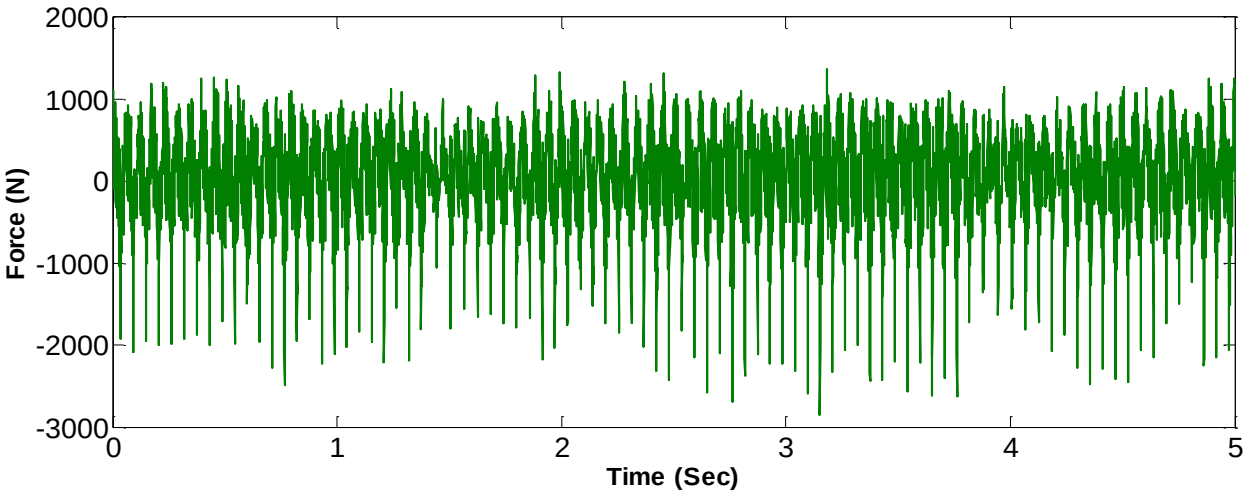

Figure 4.26- Forces generated by the PPG at 227 LPM

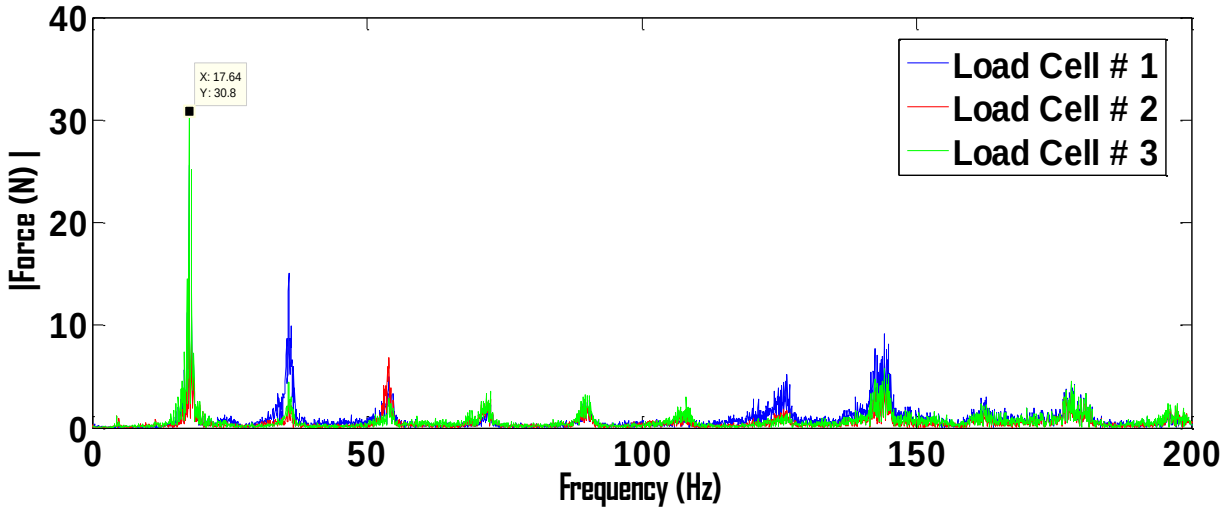

Figure 4.27- Spectral analysis of the forces encountered by the load cells at 227 LPM

At 265 LPM the force generated was about 1700 N as shown in Figure 4.28. While the spectral analysis of the 3 load cells showed that the forces dominant frequency totally agreed with the dominant frequency of the pulses at 20.5 Hz as shown in figure 4.29.

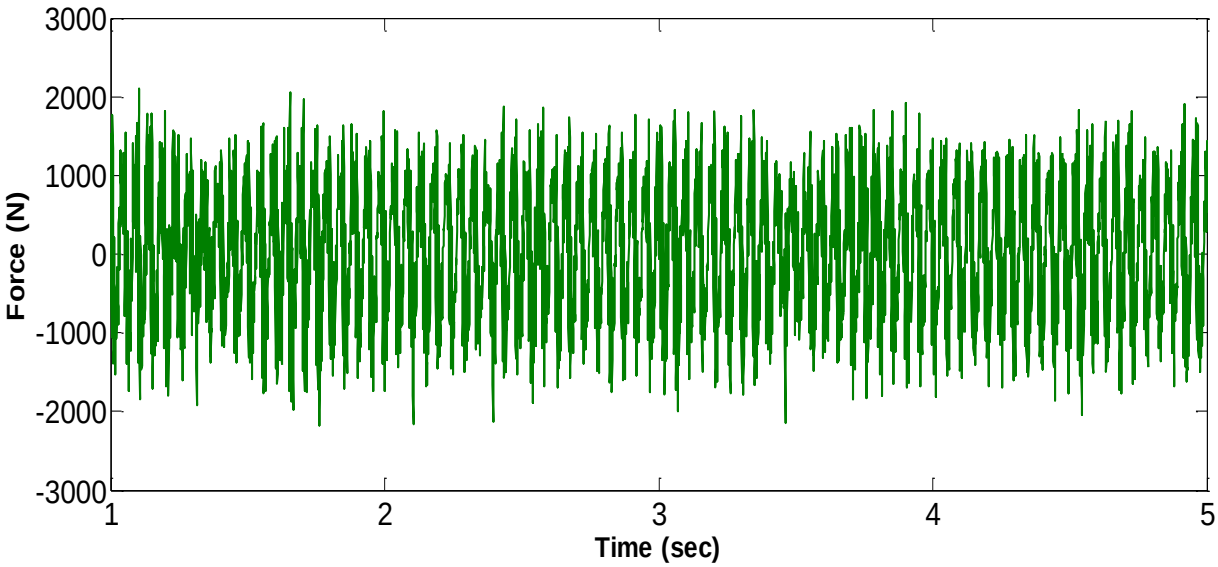

Figure 4.28- Forces generated by the PPG at 265 LPM

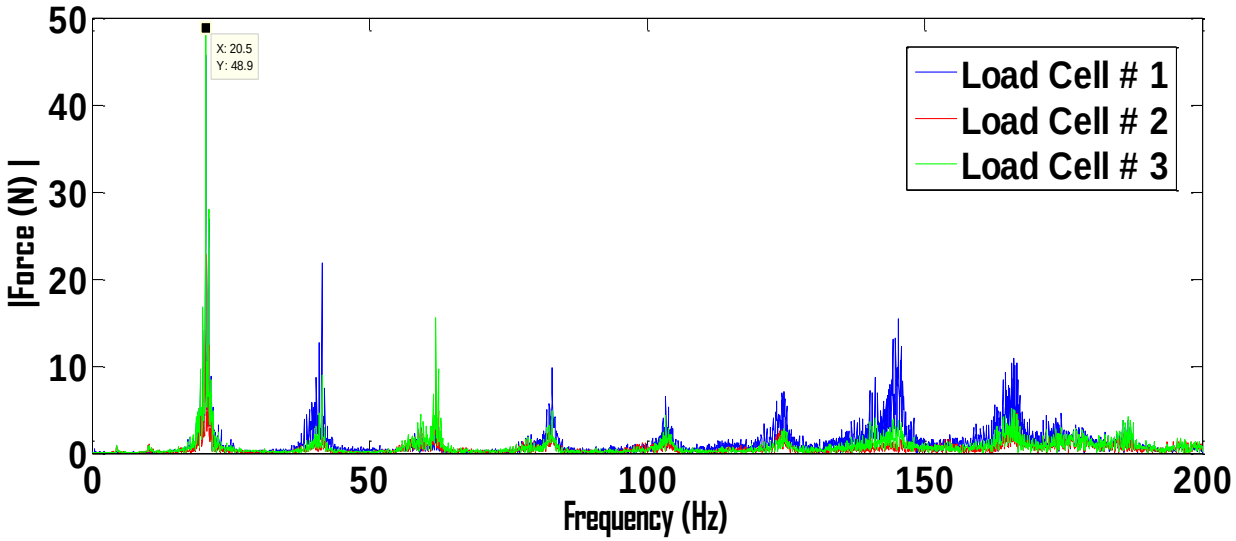

Figure 4.29- Spectral analysis of the forces encountered by the load cells at 265 LPM

The pump effect was seen for the same duration encountered with the pressure data with a magnitude similar to the pressure reduction. However the values mentioned for forces, (which are summarized in Table 4.3) were taken from the stable signal after the pump effect vanished.

Table 4.3- Summary of the forces data for the PPG

Flow Rate	Total Force	Frequency of forces
LPM	N	HZ
113	175	7.3
151	330	10.4
190	660	14.5
227	1000	17.64
265	1700	20.5

After conducting several characterization experiments, it was found that the PPG managed to introduce fluctuating forces by restricting the fluid flow through the tool. The frequency and intensity of the pressure pulses and forces were found proportional to one variable, which is fluid flow rate.

5 Experimental Setup and Plan for Drilling Experiments

After characterizing the PPG tool, and understanding the output pressures and forces introduced by the PPG. The next step was to investigate the effect of the generated pulses on drilling using PDC bits. In this chapter the setup used to conduct the laboratory drilling experiments is presented, along with the experimental plan designed to study the overall performance effect when using the PPG and when no PPG tool is introduced to the setup. In these drilling experiments, synthetic rock materials were used, which are also described in this Chapter.

5.1 Drilling Setup

The setup mainly consists of three main components, the pumping unit, the drill rig that has the drill motor and all the sensors mounted on, and the data acquisition system that collects all the information while drilling. The drill rig also has the capability of varying its system compliance from completely rigid into highly compliant. Each of these components is described thoroughly in the next few pages.

5.1.1 Pumping unit

The pumping unit includes a 20 kW motor installed on a triplex pump that can pump water with a maximum flow rate of 163 LPM and maximum pressure of 6900 kPa. which was considered sufficient enough to provide flow to operate the tool.

The pump also includes a Variable Frequency Drive (VFD) to control the flow rate by adjusting the rotary speed of the motor. A water tank, with a capacity of 1000 L, is put on top of the pump assembly to provide drilling fluid. The pumping unit is equipped with

sensors such as flow meter, and water tank level meter to control and record the flow conditions. Figure 5.1 shows the pump assembly which is connected to the rig by a flow line.

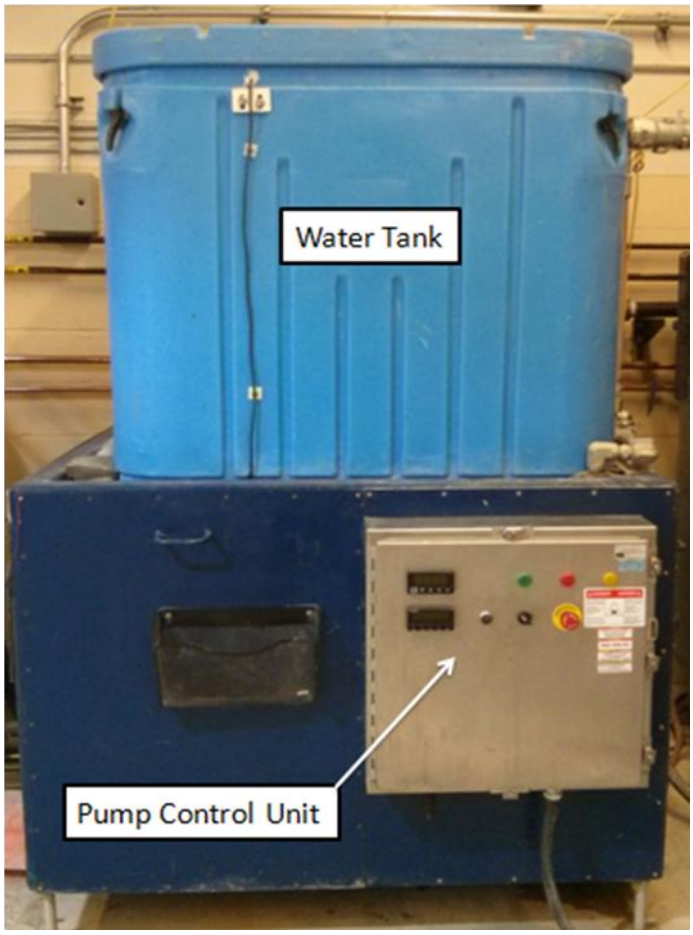

Figure 5.1- Pumping Unit

5.1.2 Drill Rig

The drill rig used for the experiments is shown in Figure 5.2. and as shown in the figure, the rig dimensions are relatively small (2m in height) and the PPG tool could not be mounted on the rig, but the pulses it generated were transferred to the bit through a flexible hose. The PPG was mounted on the ground with flexible hoses connecting it to the pump and the drill rig.

Detailed descriptions of each part of the rig is presented in this section, with figures to illustrate each component.

Figure 5.2- Drill Rig used for drilling experiments

As shown in Figure 5.3, the drill rig has a motor as a rotary head which can provide a maximum bit power of 4 kW. The maximum thrust and torque of the motor are 3500 N and 80 Nm respectively. The motor can provide two different rotary speeds, 300 and 600 RPM, the RPM can be chosen using a switch located on the side of the motor.

A current meter is attached to the motor to show the current drawn by the motor at all times. the rig has a wheel on which suspended load is placed to provide weight on bit required for drilling, providing a linear relationship between the suspended weight and the actual weight on bit given in Kg as:

$$WOB = 11.20 \times (Weight_{Suspended}) + 59.42. \quad (5\text{-}1)$$

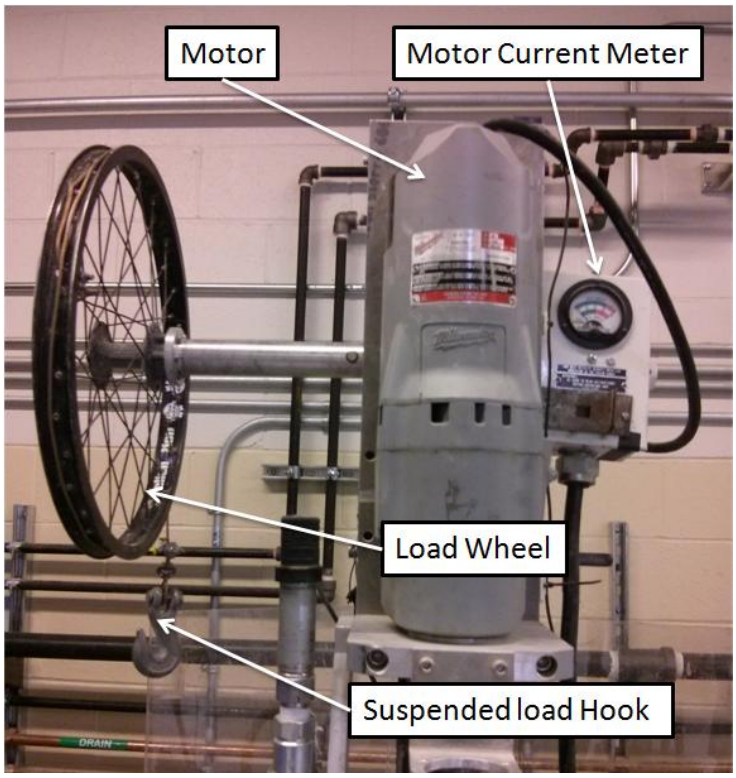

Figure 5.3- Drill Rig Motor

In Figure 5.4, the swivel that connects the drill motor to the drill string, and provides a connection to the triplex pump via a rubber hose is shown. The swivel also has a slot to mount a pressure sensor to record the inlet pressure of fluid before it goes to the bit. Water flows from the pump to a rubber hose then through the swivel then to the drill string and the PDC bit connected to its end.

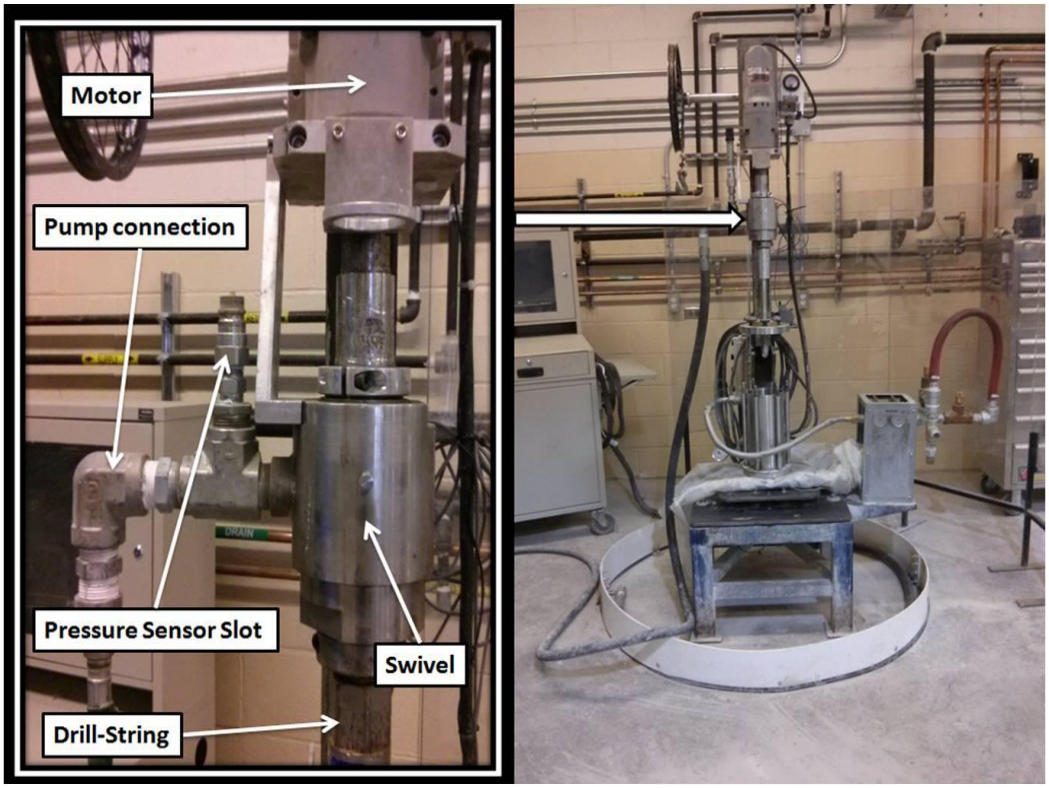

Figure 5.4- Swivel assembly

The drilling specimen is placed inside the pressure cell, which is used to control BHP. The length of the pressure cell is 12 inches and it can take 8 inches long rock specimens, the bit and drill string rotate inside the cell and the cell is sealed by a rotary seal installed at the top of the cell. Inside the pressure cell there are 3 metal bars to keep the rock centered and a disk that holds the rock in place.

Water and cuttings leave the cell through a flexible hose at its outlet then through a filter to collect the cuttings, the filter is equipped with pressure gauges to detect any clog. The pressure cell is connected to a pressure relief valve, which is pre-set to 300 psi, at which the valve opens to release the excess pressure.

The cell is also connected to a needle valve to control the bottom hole pressure value, and a slot for a pressure sensor to record the cell's pressure. Figure 5.5, shows the pressure cell, the drill string inside the cell, the flexible hose outlet, the way the sample is placed inside the pressure cell, and the water filter. In Figure 5.6, the valves connected to cell are shown as well as the system outlet from which the water is re-circulated back to the water tank.

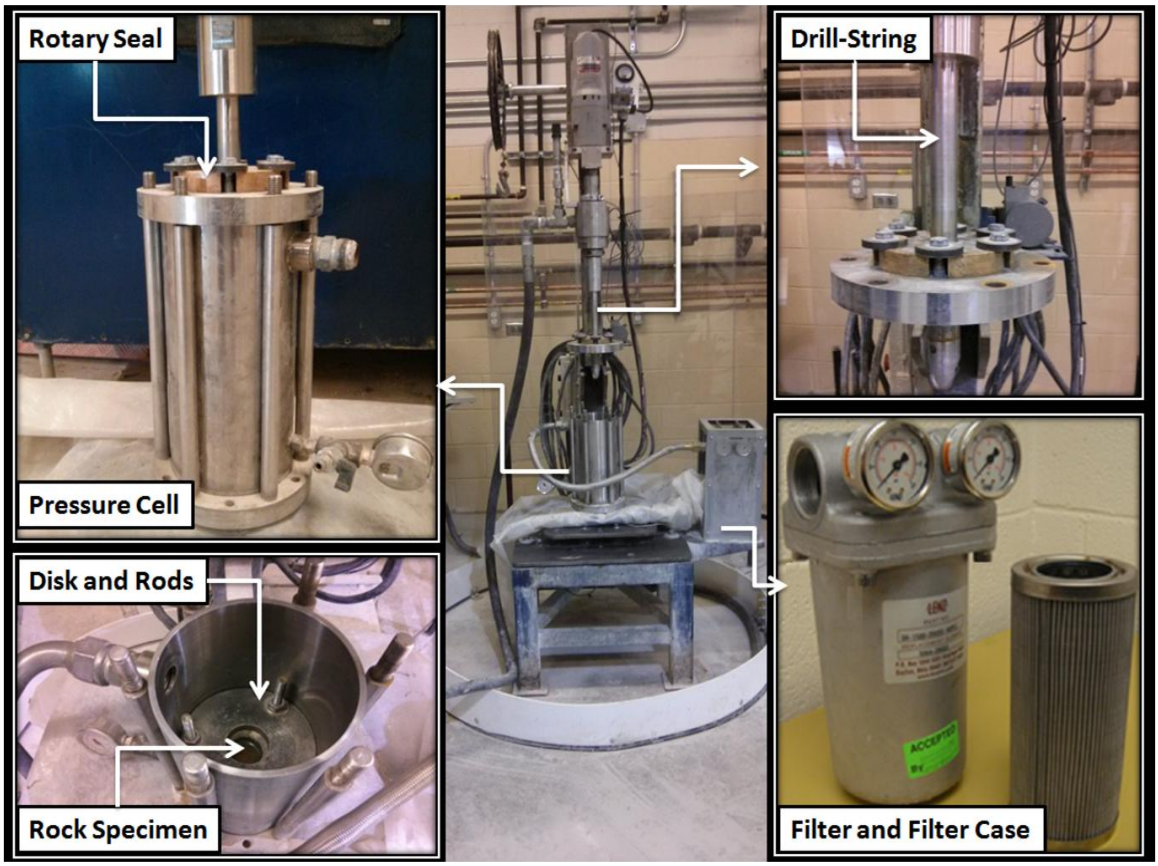

Figure 5.5- Pressure cell assembly

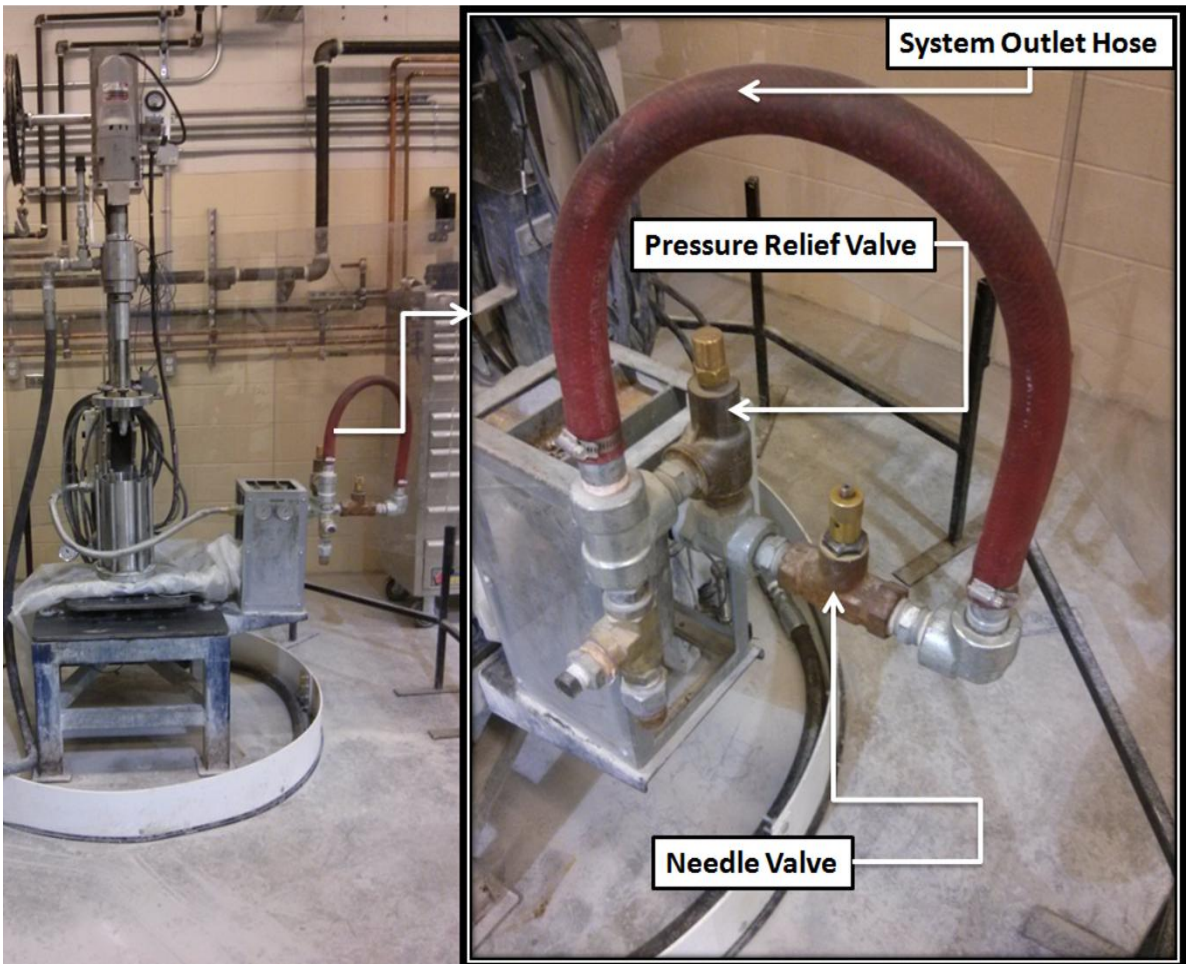

Figure 5.6- Pressure Cell Valves

In Figure 5.7, The direction of flow is illustrated by a simple diagram, starting from the triplex pump, flow travels to the swivel first and ends at the pump after the water is filtered. As shown in the figure, there are two pressure check points in the system at which clogs or higher pressure could be encountered. In case of clogged filter, the filter was disassembled and cleaned. while in the case of pressures higher than 300 psi, the relief valve would be opened to release the cell pressure.

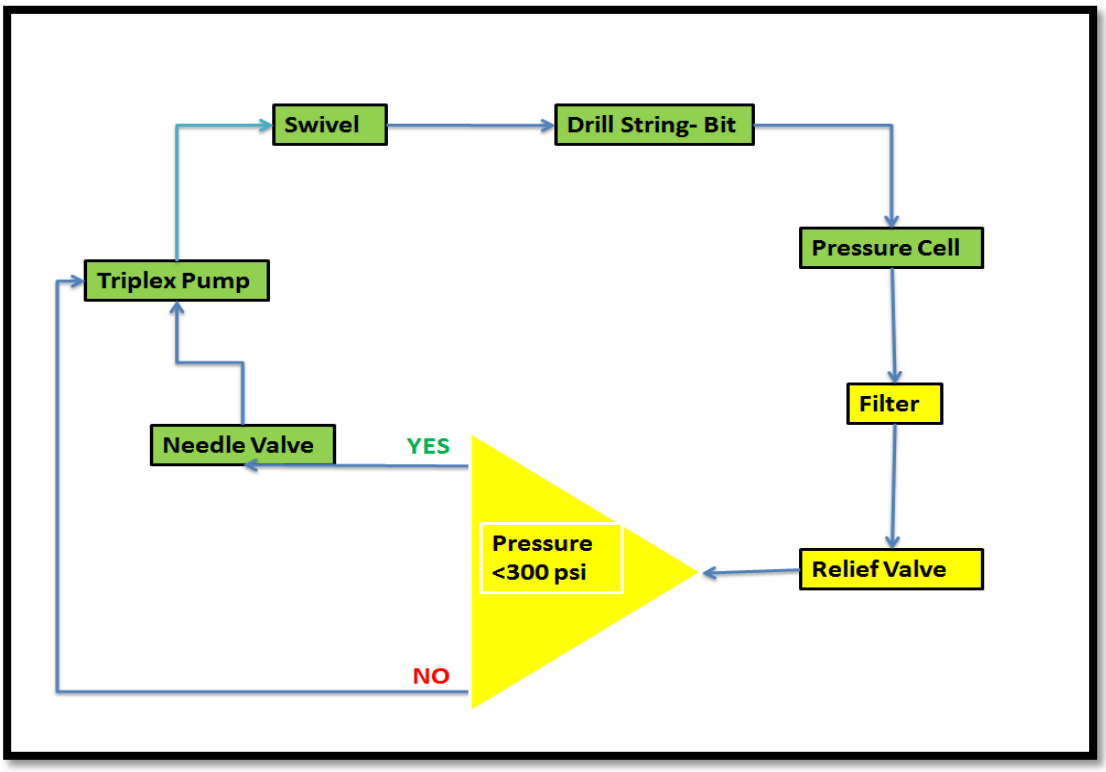

Figure 5.7- Flow Direction through the drilling setup

5.1.3 Drill Bit

A two cutter PDC bit with diameter of 35 mm was used for the drilling experiments.

The cutters are brazed to a shank that contains a single nozzle of 7 mm in diameter.

Each cutter has the face angle of 25° and back-rake angle of 25°. The cutters also constitute a chamfer with a back-rake angle of 70° and a depth of cut equals to 0.15 mm.

A schematic of the cutter is shown in Figure 5.8

Also from the figure each cutter has two regions of penetration with respect to the geometry of a rock-bit interface. The first region is the DOC1 when the chamfer is penetrating, and the second region is the DOC2 when the face of the cutter is penetrating.

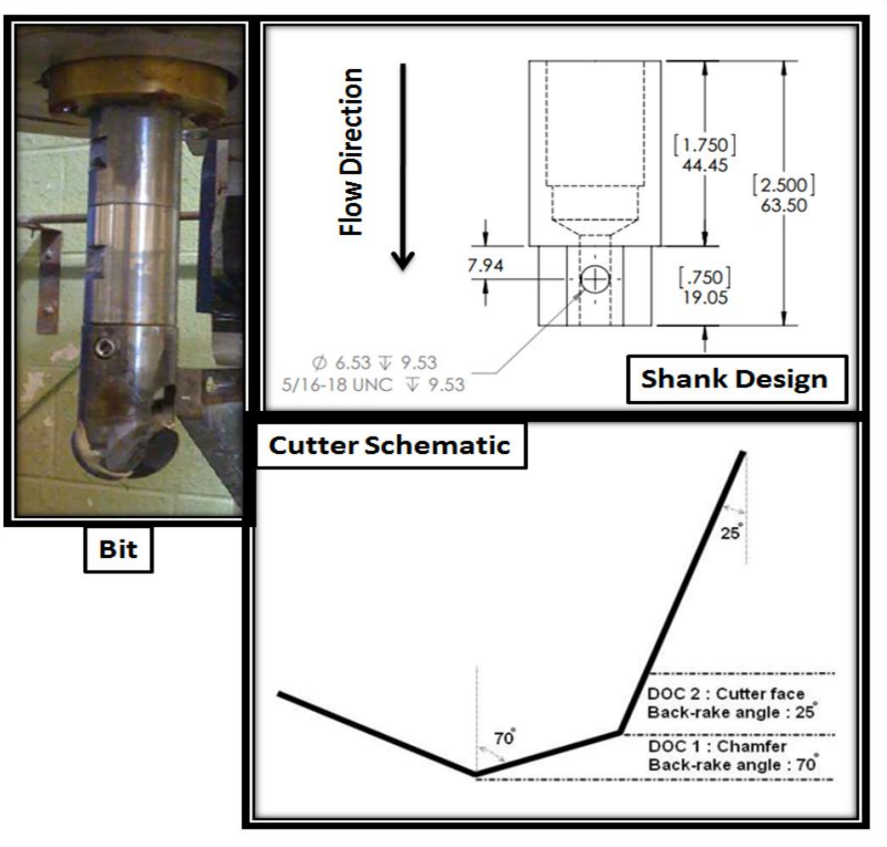

Figure 5.8- Bit, cutter schematic and shank design

5.1.4 Sensors and Data Acquisition System

In order to be able to analyze the drilling performance of the PPG, many parameters were needed to be recorded, including, ROP, WOB, inlet and outlet pressures, drill motor power consumption, BHP, and vibration magnitude and frequency. These parameters were measured using various sensors, as described below. To measure ROP, a tension cable Linear Variable Displacement Transducer (LVDT) was used to measure the displacement of the drill head downwards while penetrating the rock. WOB was measured by a pan cake load cell located beneath the pressure cell where the rock is set.

Inlet and outlet pressures were measured using two identical pressure sensors rated at 1500 psig. The drill motor power consumption was measured using a current meter which also had a gauge to show the current consumption at all times. The vibration of the whole setup was measured by an accelerometer attached above the drill motor. The rock vibration was measured by another LVDT placed beneath the plate to which the drill cell is attached. Figure 5.9, Shows all sensors used for the drilling experiments, while Figure 5.10, shows the computer/DAQ assembly used to record all data.

The DAQ used was a sophisticated multi channel DAQ with sampling frequency of 1000 Hz. The software used to record and monitor the measurements was Lab View V2.2.

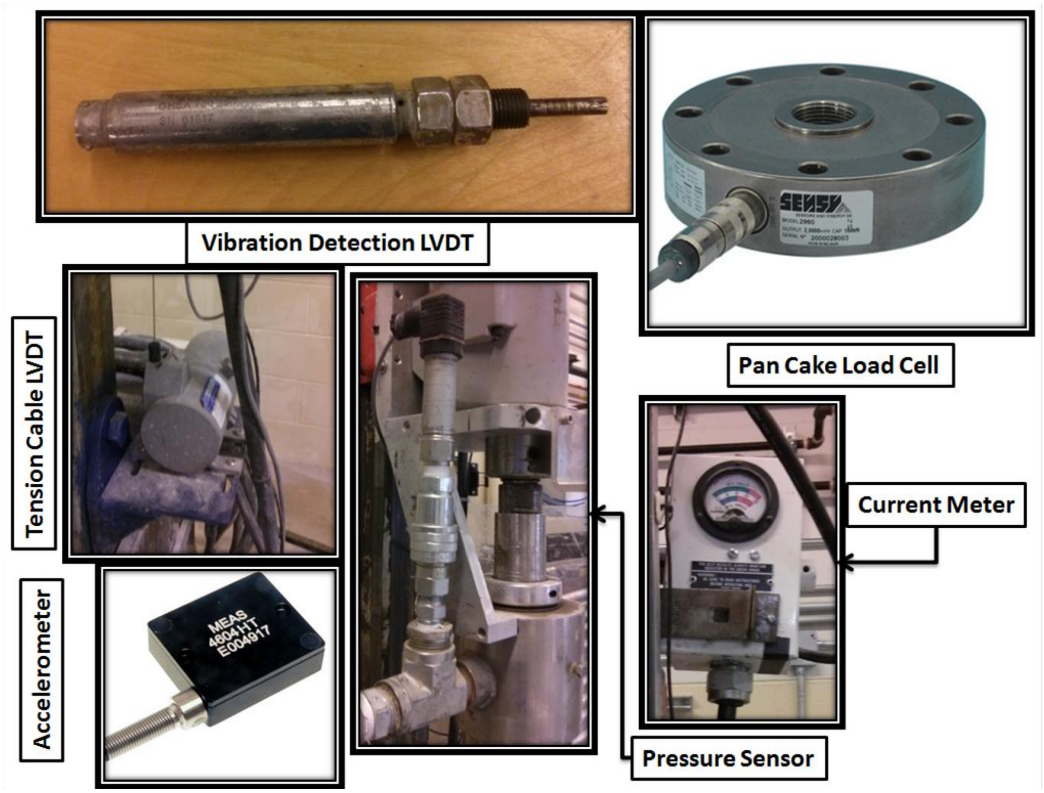

Figure 5.9- Sensors

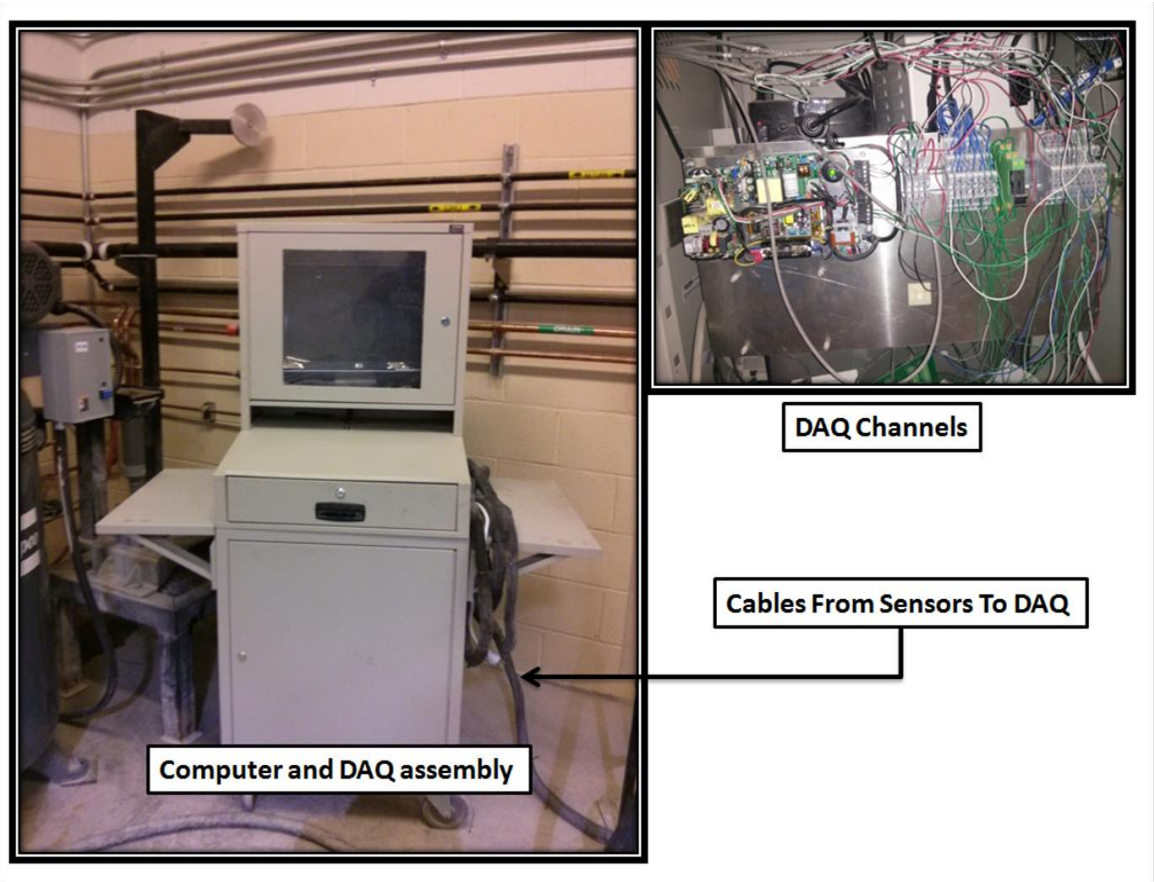

Figure 5.10- DAQ system and computer systems used for data recording

5.1.5 Compliance

While designing the drilling experiments and the setup to conduct them, it was necessary to give the system the axial compliance to vibrate responding to the axial forces introduced by PPG. The rig dimensions and limitations did not allow installing a compliant element behind the bit to transform the forces into axial vibrations. that lead to design a vibrating system beneath the rock to vibrate the rock instead of the bit.

The system is made up of two plates, one of them is fixed while the other is free to move. Between the two plates are rubber sandwich mounts used to connect the two plates, in other words the mounts act as springs that get compressed when loaded and are stretched when subjected to tension. The number of mounts and the design of each compliance pattern is based on the fact that parallel springs can be assumed as a single spring with higher stiffness.

The following formula shows how the total stiffness of each pattern is calculated.

$$K_{total} = K_1 + K_2 + \ldots + K_n \quad (5\text{-}2)$$

Where n, and K are the number of mount in each pattern and stiffness respectively. Since all used mounts in each pattern are identical, the above formula can be rewritten as

$$K_{total} = n \times K \quad (5\text{-}3)$$

In order to calculate the K value of a single rubber mount, an experiment using a loading INSTRON Machine-Model 5585H was conducted to measure the amount of reduction in the mount height (displacement) when subjected to increasing load force. The setup used is shown in Figure 5.11, while the results of the test are shown in Figure 5.12 .

The K value which is the slope of the curve obtained when plotting the load Vs displacement values was found to be 0.1877 KN/mm.

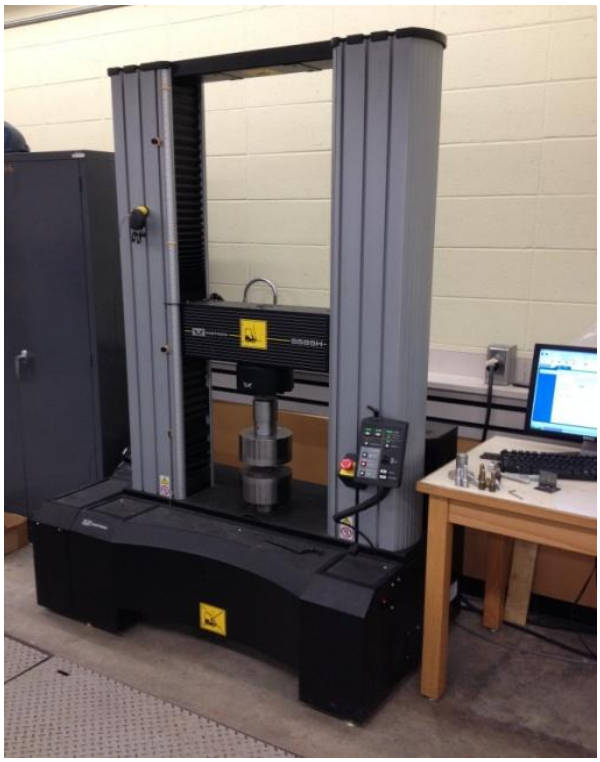

Figure 5.11- INSTRON Machine-Model 5585H

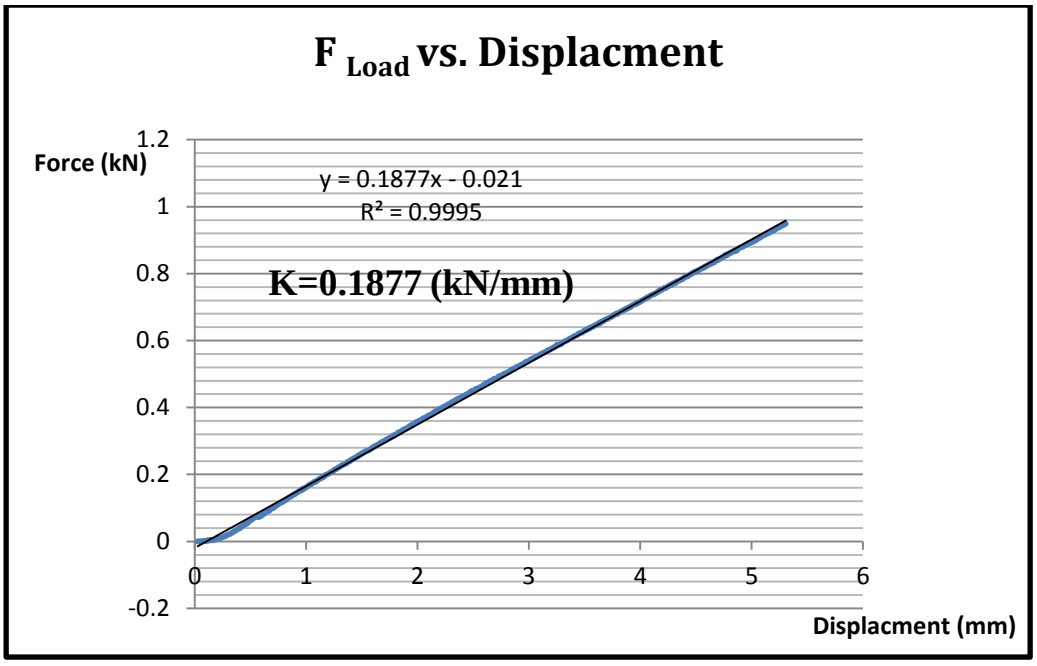

Figure 5.12- Load versus Displacement Curve

During the drilling experiments, a rigid pattern and two different compliance patterns were used. the compliance patterns were 6 mounts and 8 mounts with a total K values of 1.1262 KN/mm and 1.5016 KN/mm respectively. Figure 5.13, shows the different compliance element patterns used in the drilling experiments.

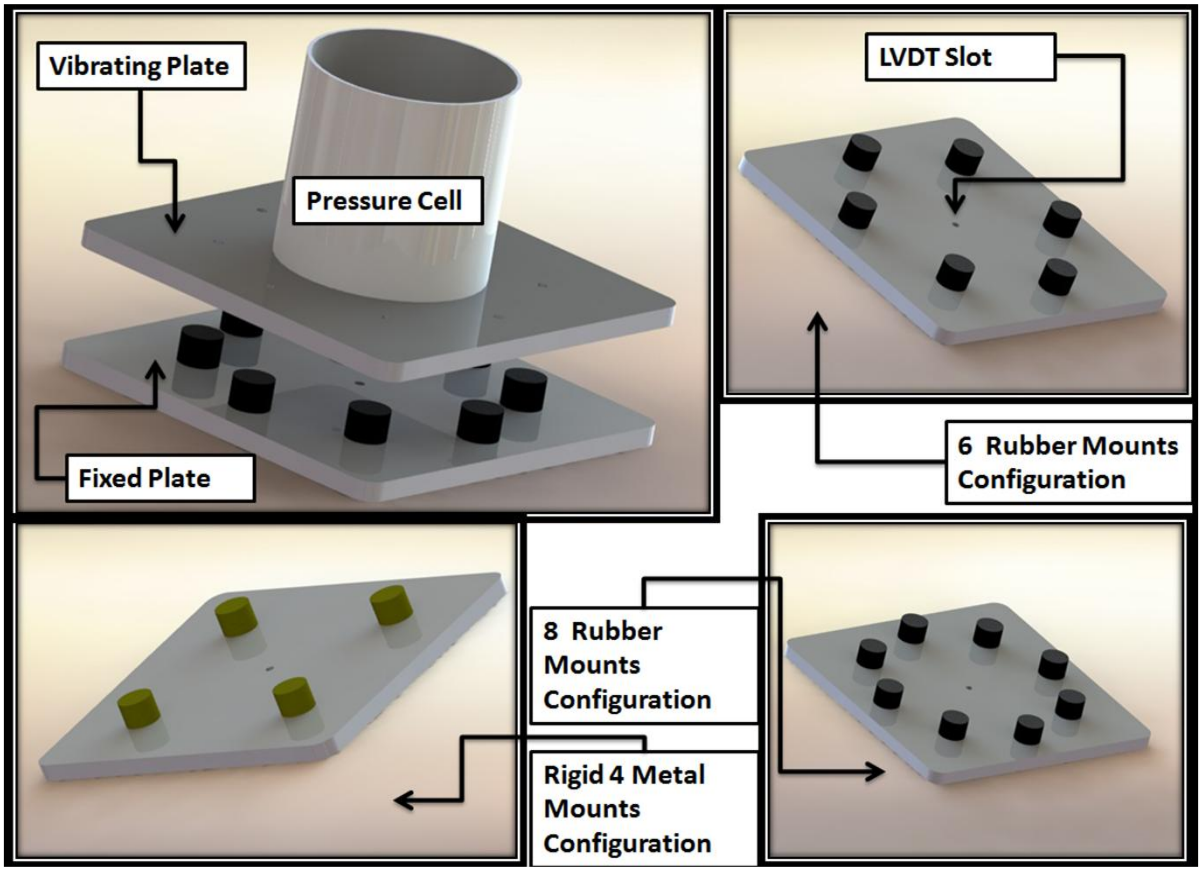

Figure 5.13- Different compliance patterns used.

5.1.6 Synthetic Rock Specimens

In order to prepare a rock sample for drilling tests, concrete slurry was molded in cylinders with a diameter of 100 mm. The concrete slurry included aggregates, cement, super plasticizer and water. The ratio of each component is mass based and is determined from unpublished study done by ADG member Zhen Zhang. The samples were left to cure in custom tanks submerged in water for about 45 days before the experiments, as shown in Figure 5.14 The physical properties of the rock were determined using core plugs with a diameter of 46 mm, which were extracted from the center of the prepared rock specimen using an NQ diamond coring bit. The elastic moduli and strength of the intact specimen were measured according to the ASTM standard D7012-10 [40].

Table 5.1 shows properties of the rock specimens tested. Figure 5.15 the surface of the rock after surface grinding. The surface represents the distribution of the aggregates in the matrix of the specimen. On the day of the experiments a rock sample was tested under unconfined compression in a stiff loading frame, and provided a UCS of 51 MPa.

Figure 5.14- 4" drilling specimens curing in water tanks

Table 5.1- Physical Properties of the rock samples

Property	Value
UCS	51 MPa
Tensile Strength	5.4 MPa
Young's Modulus	29 GPa
Poisson Ratio	0.15
Effective Porosity	29%
Internal Friction Angle	40°

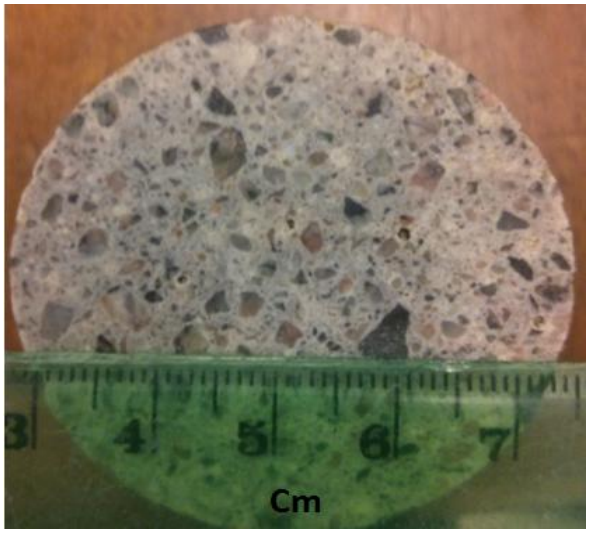

Figure 5.15- Rock surface after grinding

5.2 Experimental Plan

The drilling experiments were designed to investigate the effect of the pressure pulses on drilling, by varying drilling parameters and by comparing the performance data with and without utilizing the PPG tool. All drilling parameters were varied during the experiments except for the Motor RPM, considering that the PPG mechanism doesn't depend on RPM in all cases, it was assumed that the motor RPM is not directly related to the effect of the pressure pulses. Three rounds of experiments were conducted to study the effect of pressure pulses. The first round was designed to study the PPG performance with no system compliance introduced, at both atmospheric pressure and 150 psig BHP. Table 5.2 shows the matrix of the 28 runs conducted in the first round.

In the second round, 27 runs were conducted to study the effect of the two different compliance setups with 6 and 8 rubber mounts installed, these are shown in Table 5.3.

Table 5.2- First round of drilling Experiments

Run Number	Flow Rate(LPM)	WOB (N)	Tool	Compliance (mm/KN)	Back Pressure (psi)
1	160	1152	PPG	Rigid	Minimum
2	160	1428	PPG	Rigid	Minimum
3	160	1481	PPG	Rigid	Minimum
4	160	1650	PPG	Rigid	Minimum
5	160	1802	PPG	Rigid	Minimum
6	160	1966	PPG	Rigid	Minimum
7	160	2295	PPG	Rigid	Minimum

8	160	1152	PPG	Rigid	150
9	160	1428	PPG	Rigid	150
10	160	1481	PPG	Rigid	150
11	160	1650	PPG	Rigid	150
12	160	1802	PPG	Rigid	150
13	160	1966	PPG	Rigid	150
14	160	2295	PPG	Rigid	150
15	160	1152	None	Rigid	Minimum
16	160	1428	None	Rigid	Minimum
17	160	1481	None	Rigid	Minimum
18	160	1650	None	Rigid	Minimum
19	160	1802	None	Rigid	Minimum
20	160	1966	None	Rigid	Minimum
21	160	2295	None	Rigid	Minimum
22	160	1152	None	Rigid	150
23	160	1428	None	Rigid	150
24	160	1481	None	Rigid	150
25	160	1650	None	Rigid	150
26	160	1802	None	Rigid	150
27	160	1966	None	Rigid	150
28	160	2295	None	Rigid	150

Table 5.3- Second round of drilling experiments

Run Number	Flow Rate(LPM)	WOB (N)	Tool	Compliance (mm/KN)	Back Pressure (psi)	
29	160	1152	PPG	0.888	Minimum	Compliance effect - 6 Mounts
30	160	1428	PPG	0.888	Minimum	
31	160	1481	PPG	0.888	Minimum	
32	160	1650	PPG	0.888	Minimum	
33	160	1802	PPG	0.888	Minimum	
34	160	1966	PPG	0.888	Minimum	
35	160	2295	PPG	0.888	Minimum	
36	160	1152	None	0.888	Minimum	
37	160	1428	None	0.888	Minimum	
38	160	1481	None	0.888	Minimum	
39	160	1650	None	0.888	Minimum	
40	160	1802	None	0.888	Minimum	
41	160	1966	None	0.888	Minimum	
42	160	2295	None	0.888	Minimum	
43	160	1152	PPG	0.666	Minimum	Compliance effect - 8 Mounts
44	160	1428	PPG	0.666	Minimum	
45	160	1481	PPG	0.666	Minimum	
46	160	1650	PPG	0.666	Minimum	
47	160	1802	PPG	0.666	Minimum	

48	160	1966	PPG	0.666	Minimum
49	160	2295	PPG	0.666	Minimum
50	160	1152	None	0.666	Minimum
51	160	1428	None	0.666	Minimum
52	160	1481	None	0.666	Minimum
53	160	1650	None	0.666	Minimum
54	160	1802	None	0.666	Minimum
55	160	1966	None	0.666	Minimum
56	160	2295	None	0.666	Minimum

For the third round, 15 runs were conducted to study the effect of changing the flow rate and the bottom hole pressure bringing the total number of runs to 70 runs with some repetition in between, these are shown in Table 5.4.

Table 5.4- Third round of drilling experiments

Run Number	Flow Rate(LPM)	WOB (N)	Tool	Compliance (mm/KN)	Back Pressure (psi)	
57	113	1966	PPG	**0.666**	Minimum	Flow Rate Effect
58	129	1966	PPG	**0.666**	Minimum	
59	144	1966	PPG	**0.666**	Minimum	
60	113	1966	None	**0.666**	Minimum	
61	129	1966	None	**0.666**	Minimum	
62	144	1966	None	**0.666**	Minimum	
63	160	1966	PPG	**0.666**	100	Back Pressure Effect
64	160	1966	PPG	**0.666**	150	
65	160	1966	PPG	**0.666**	200	
66	160	1966	PPG	**0.666**	250	
67	160	1966	None	**0.666**	100	
68	160	1966	None	**0.666**	150	
69	160	1966	None	**0.666**	200	
70	160	1966	None	**0.666**	250	

6 Analysis of the Drilling Experiments

In this chapter, the overall results of the experiments are thoroughly discussed. As mentioned earlier in Chapter 2, the drilling performance parameters are not only limited to ROP and MSE results, but other parameters like CPF, bore-hole quality and overall FPD cannot be determined in the laboratory environment. That made the analysis of the experiments data focused on ROP and MSE trends. the formulas used for the analysis are explained before the results are discussed.

6.1 Formulas used in Data Analysis

For ROP calculations, the slope of the LVDT sensor displacement curve with time was used directly as the ROP value. For qualitative MSE, the formula mentioned earlier in Chapter 2 was used to calculate MSE. where;

$$\text{Total MSE (Pa)} = \frac{Power\ Consumption\ of\ Drill\ Head\ (\frac{Nm}{s})}{Bit\ Area\ \ (m^2) X\ ROP(\frac{m}{s})} + \frac{WOB\ (N)}{Bit\ Area\ (m^2)} \qquad (6.1)$$

The power consumption of the drill head was directly acquired from the current sensor data by subtracting the RMS value of the off-bottom current consumption from the RMS value of the on-bottom current consumption.

For some data analysis, the hydraulic horse power per square inch (HSI) was calculated based on the formula below;

$$\text{HSI} = \frac{Horse\ Power\ of\ the\ Bit}{Area\ of\ drill\ Bit} \qquad (6.2)$$

$$\text{Where the Horse power (HP)} = \frac{Pressure\ at\ the\ bit(psi)\ x\ Flow\ rate\ (USGPM)}{1174} \qquad (6.3)$$

6.2 The Effect of PPG with No Compliance

In the 1st round, the effect of the PPG was investigated based on its ability to create pressure pulses only, which only affects the hydraulic horse power at the bit and the hole cleaning. In other words, no compliance was introduced to the setup to transform the sinusoidal forces generated by the pressure pulses into impact forces and vibration displacement. It can be seen in Figure 6.1, that the PPG did not affect the ROP positively. On the contrary the ROP acquired when no tool was placed, was better in particular at higher WOB provided that the BHP was kept at minimum of 30 psi.

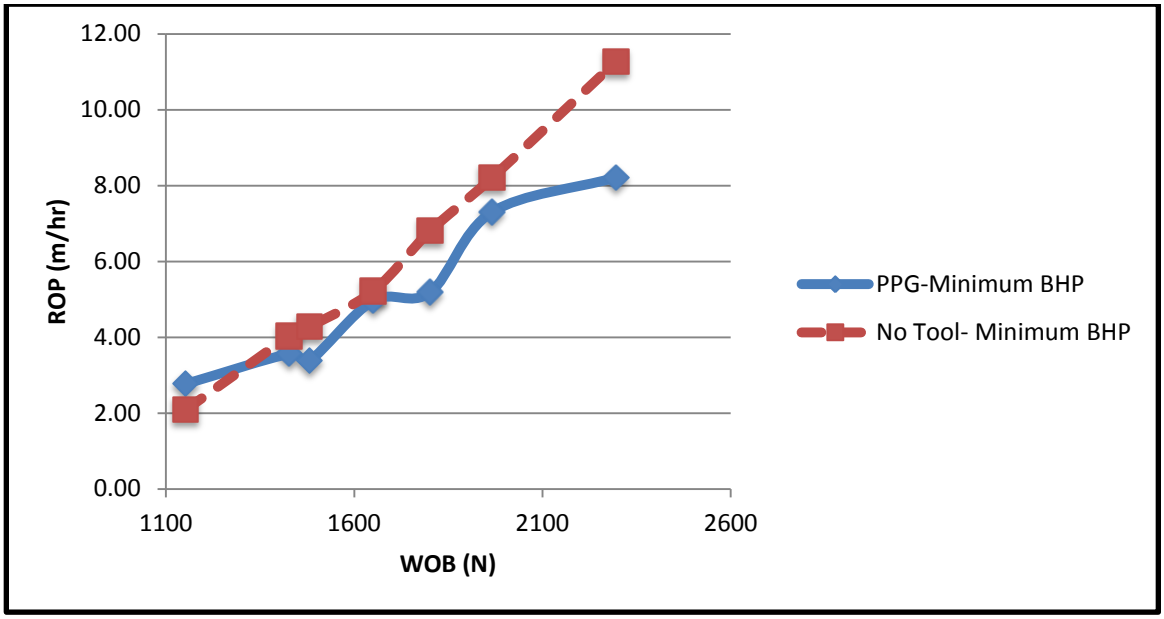

Figure 6.1- ROP curves with minimum BHP of 30 psi applied.

It can be observed as well, that for the 1st four weights applied on bit, ROP was almost identical. The explanation for that can be seen in Table 6.1, showing the Depth Of Cut (DOC) for the 1st four points.

It was observed that the depth of cut was either less than 0.15 mm or close to it, which means that at these low WOB, the cutter was not fully engaged with the rock sample and only the chamfer was interacting with the rock.

Table 6.1- Depth of Cut vs. WOB

WOB (N)	DOC (mm) using PPG	DOC (mm) without PPG
1152	**0.009**	**0.007**
1428	**0.012**	**0.013**
1481	**0.011**	**0.014**
1650	**0.017**	**0.017**
1802	**0.017**	**0.023**
1966	**0.024**	**0.027**
2295	**0.027**	**0.038**

For the higher three weights, the decrease in ROP when using the PPG could be explained by studying the pressure profile for both cases. It was observed that, when using the PPG, the pressure fluctuated between 440 psi to 520 psi as shown in Figure 6.2. Which means the HSI fluctuated between 6.884 and 8.136. while in the case of drilling without the PPG tool connected, the pressure was averaging 515 psi as shown in Figure 6.3, leading to an HSI value of 8.058. That means, the overall hydraulic power was higher when not using the PPG, providing that the hole cleaning was sufficient in both cases, and the pressure pulses could not introduce any effective force due to the lack of compliance that converts the force into vibration displacement. In Figure 6.4, the spectral analysis of the pressure data shows the pulsing frequency of the tool, which was about 9 Hz. The spectral analysis of the load cell data shows the same frequency when the tool was used, as shown in Figure 6.5.

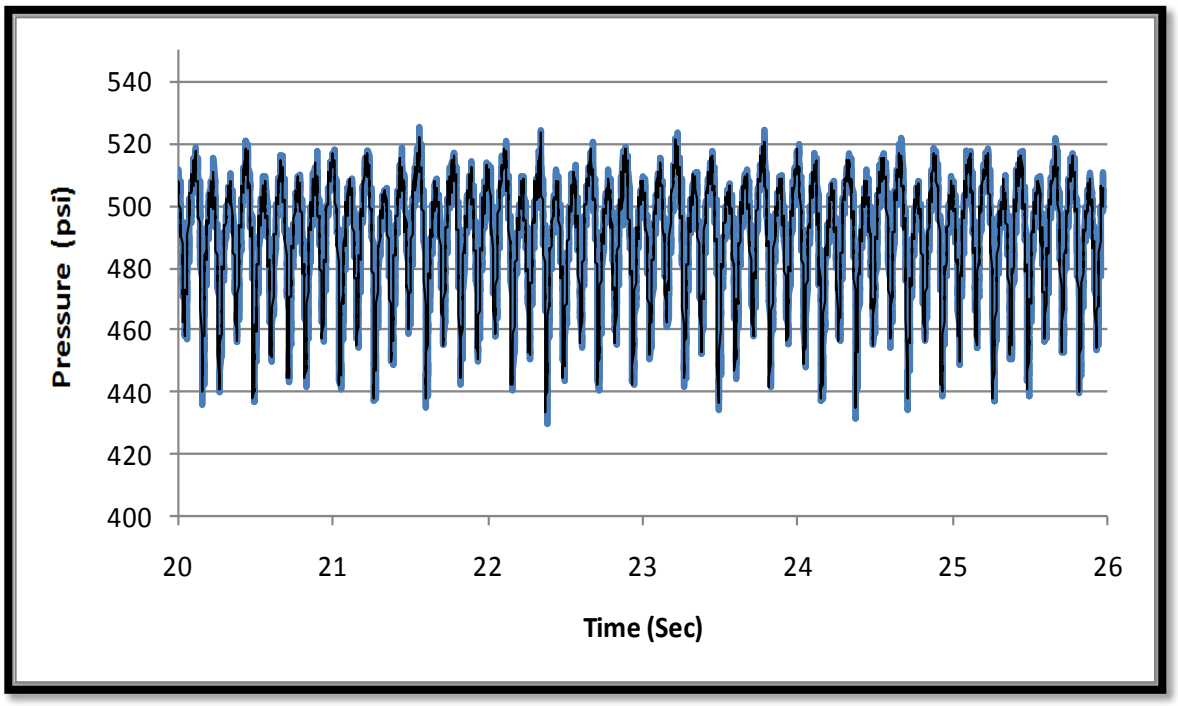

Figure 6.2- Pressure profile of the PPG

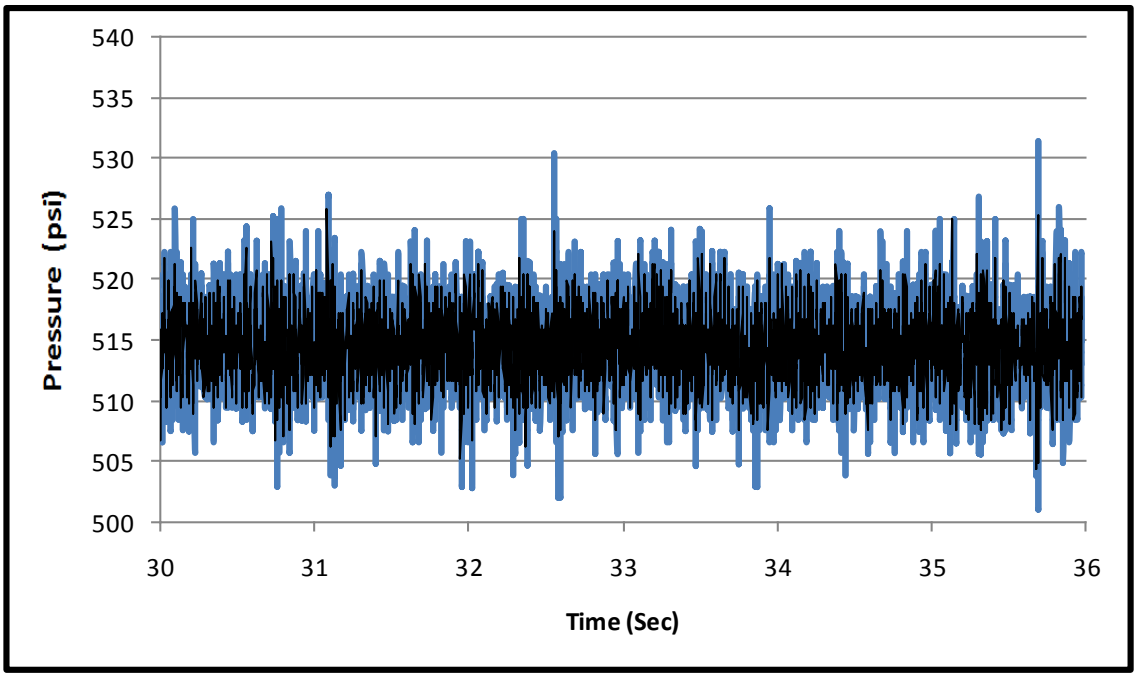

Figure 6.3- Pressure Profile for drilling without the PPG

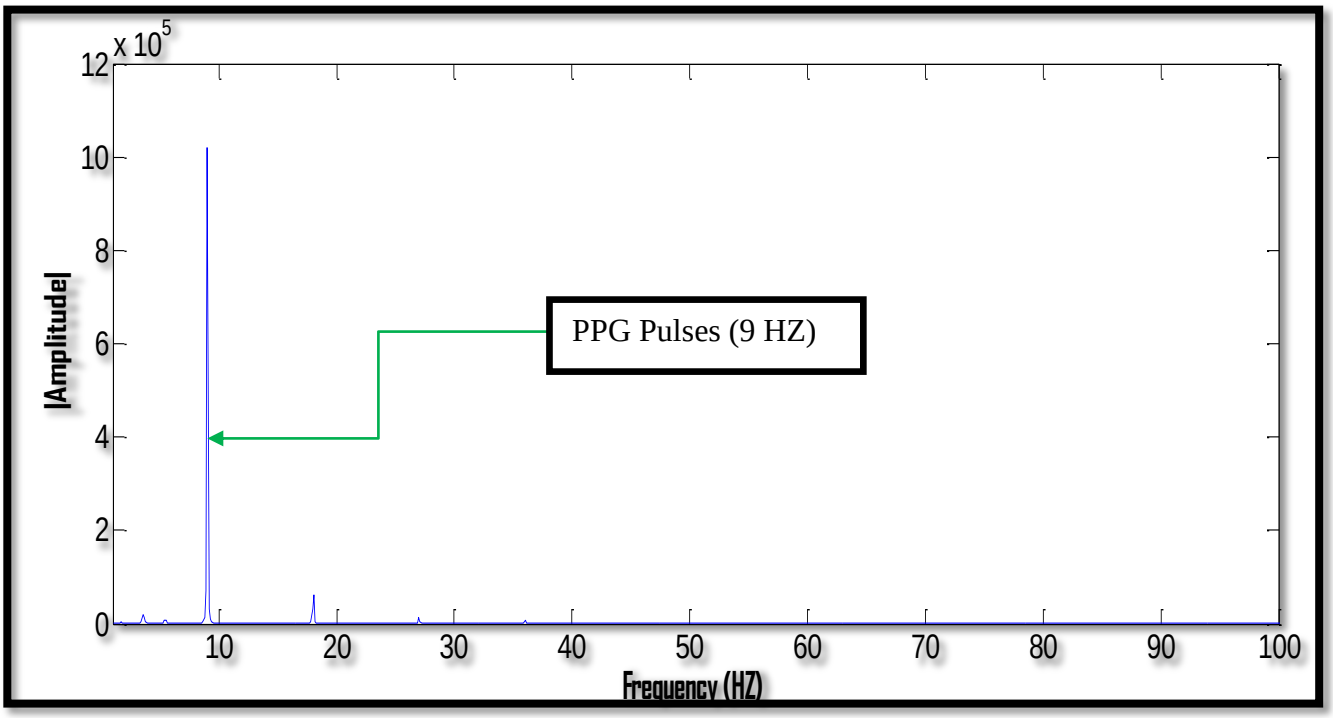

Figure 6.4-Spectral analysis of the Pressure Data while drilling with the PPG

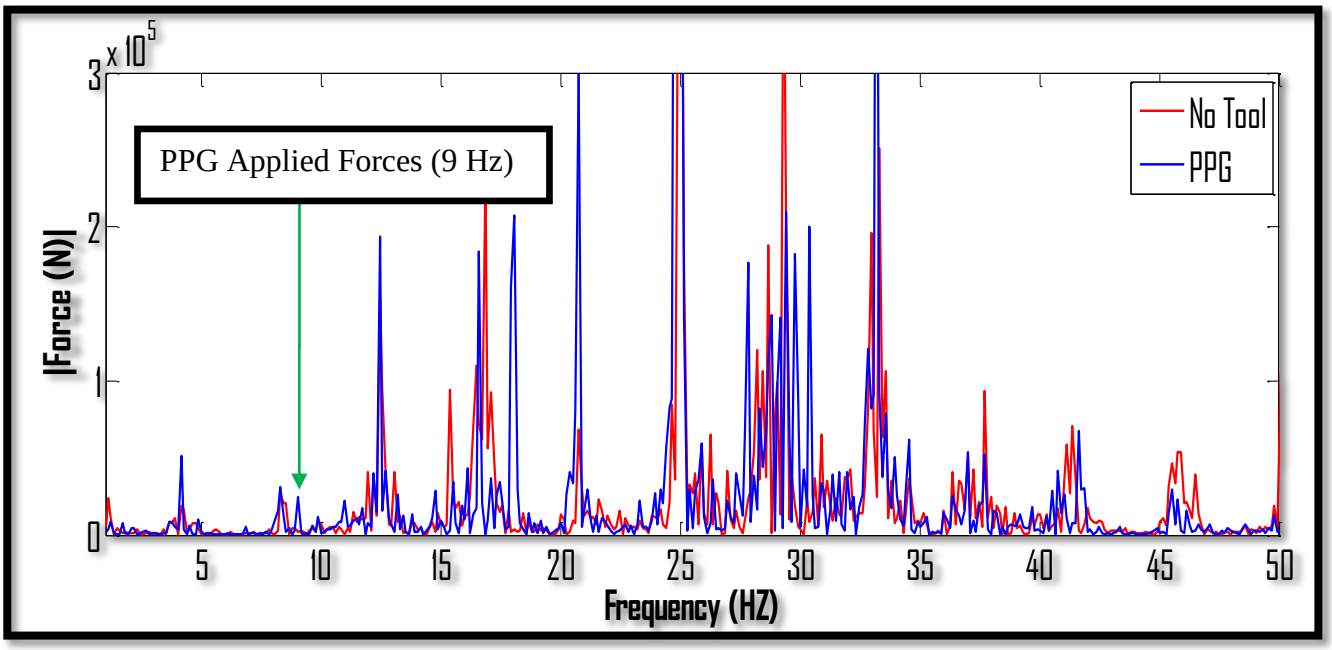

Figure 6.5- Spectral analysis for Load Cell

From the spectral analysis figures shown, it can be seen that there are several signal frequencies showing the rock bit interaction and the pulses. it can be seen that the interaction done by one cutter is shown at 4 Hz, and the interaction between the rock and both cutters is shown at 8 Hz, while the tool pulsing is shown at 9 Hz. Given that the actual RPM is not constant at 300 RPM, the actual RPM could be estimated from the spectral analysis as 240 RPM, although the measurement was not made.

For the MSE analysis, the output curves agreed with the pattern in the ROP data. Practically the 1st four runs had the close power consumption, while the last 3 runs showed that the No-Tool configuration consumed less motor power and had lower MSE as shown in Figure 6.6.

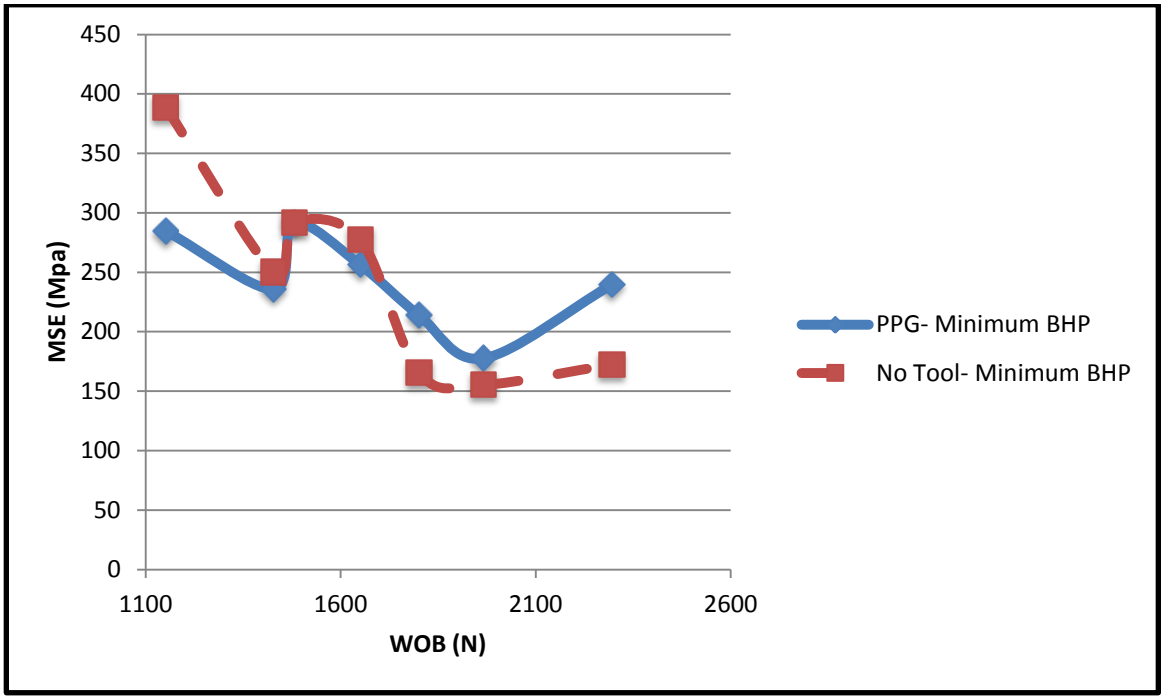

Figure 6.6- MSE Curves for Rigid (no compliance) configuration

When the same experiments were repeated while applying a constant BHP, the results showed that the effect of the pulses on HSI was almost negligible. Which could be explained as a negligible change of pressure as an effect of the added BHP. The ROP curves for drilling with the PPG and without the PPG at minimum BHP and applied 150 BHP are shown in Figure 6.7, showing also the decrease of ROP when the 150 psi was applied.

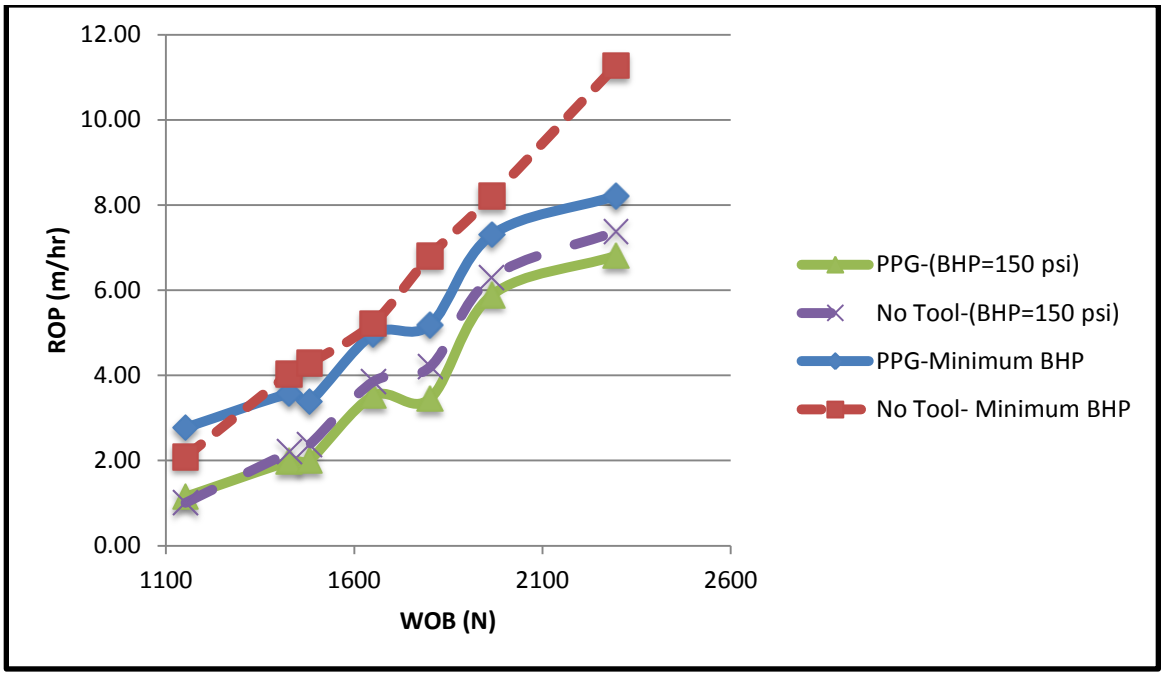

Figure 6.7-Combined ROP curves for Rigid Configuration

6.3 The Effect of PPG with Compliance

As mentioned earlier, two different compliances were introduced to the system, as described in Chapter 5. Some experiments were done with 8 mounts, with an equivalent compliance of 0.666 mm/KN, while other experiments were done using 6 rubber mounts, with an equivalent compliance of 0.888 mm/KN. The results were quite opposite to the results shown with the rigid configuration. As shown in Figure 6.8 when 8 mounts were used, it was observed that the PPG affected the ROP positively when the forces generated by the PPG were transformed into vibration displacements and acted on the rock as a result of having compliance, except for one point at which using the tool lead to a slower ROP compared to no-tool when the WOB was 1650 N.

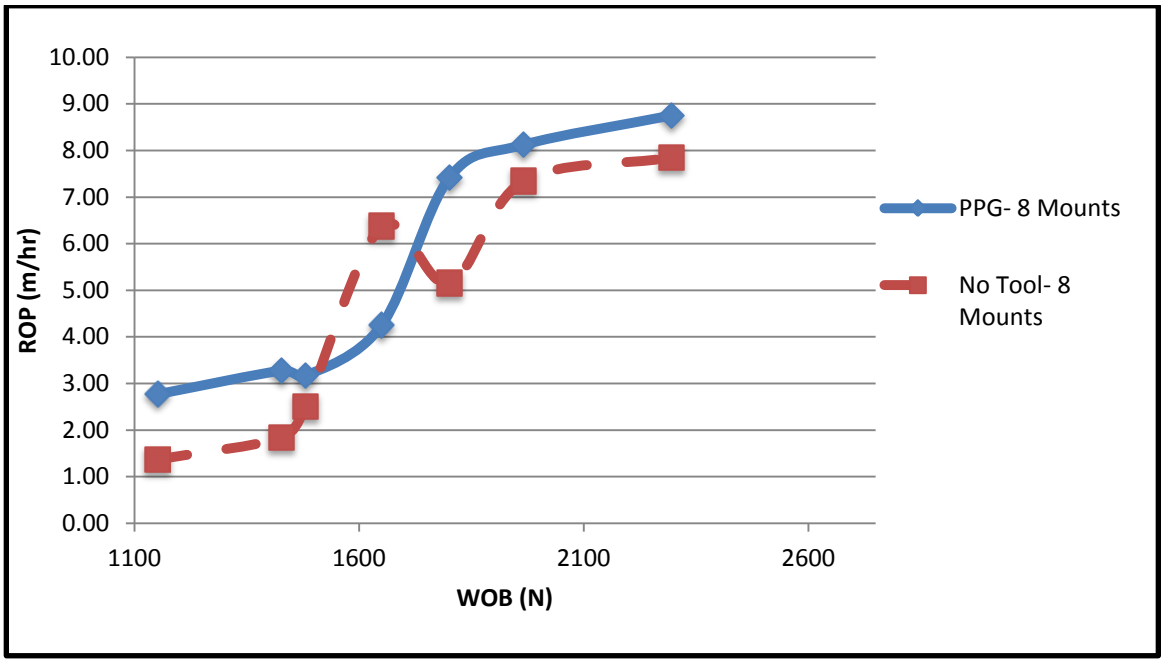

Figure 6.8- ROP results with 8 mounts configuration

To explain the better results and the unique behavior at 1650 N, the data from the LVDT vibration sensor and the load cell were thoroughly analyzed. It was observed as shown in Figure 6.9, that the vibration displacement when using the PPG tool was actually higher. However, for that single point at 1650 N applied WOB, the displacement was higher when no PPG was attached, the reason for that couldn't be accurately determined but an assumption was made that at that particular WOB the combination of drilling parameters lead to more vibration without using the PPG. From the results, it was clear that within a particular compliance configuration, the ROP had a direct proportional relationship with the magnitude of displacement, which practically increases with adding more force on the bit. However, it's assumed that the direct proportional relationship is functional until a maximum vibration displacement is reached, after which the bit cutters have less contact with the rock surface, leading to less cutting area and slower ROP.

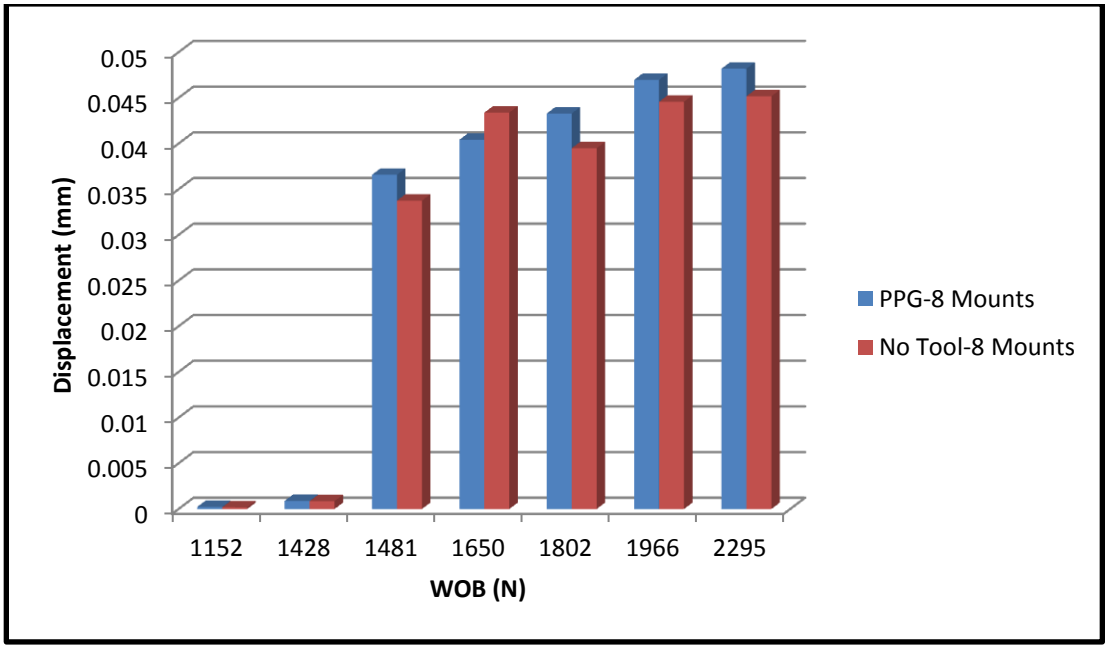

Figure 6.9- Vibration displacement vs. WOB for the 8 mounts configuration

The data from the load cell was analyzed as mentioned before, to see the role of the PPG that lead to a higher vibration displacement. In Figures 6.10 and 6.11, the force profiles recorded by the load cell when drilling with and without the PPG are shown. The applied WOB was 1802 N in both cases.

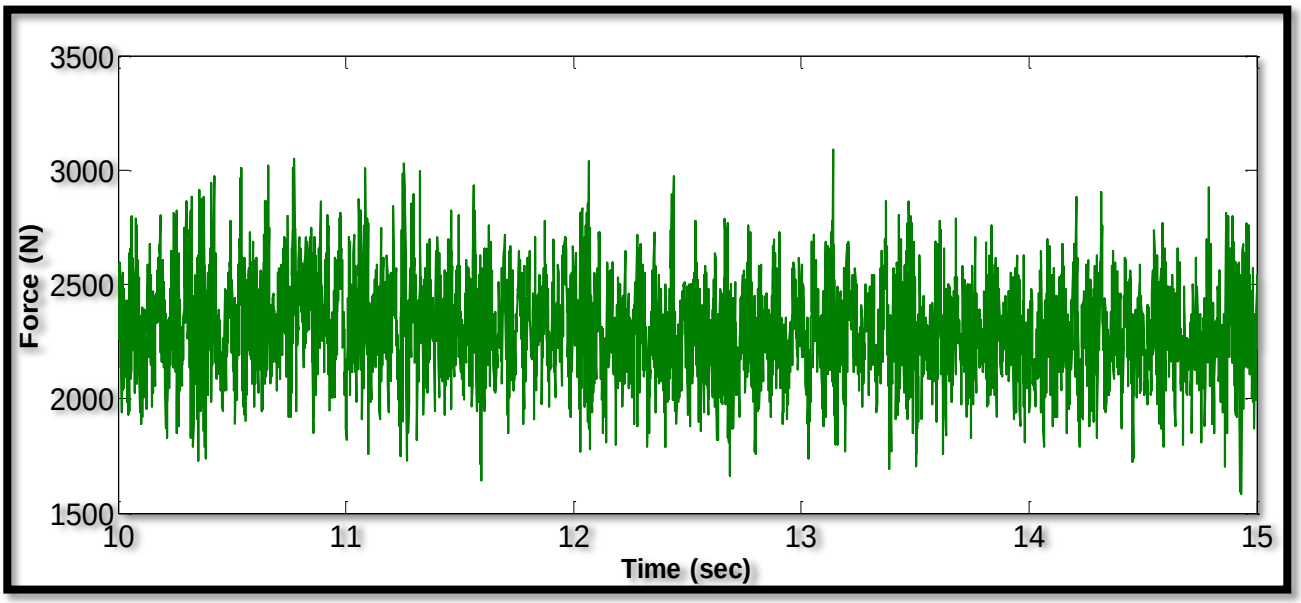

Figure 6.10- Force Profile at 1802 N when no PPG was attached

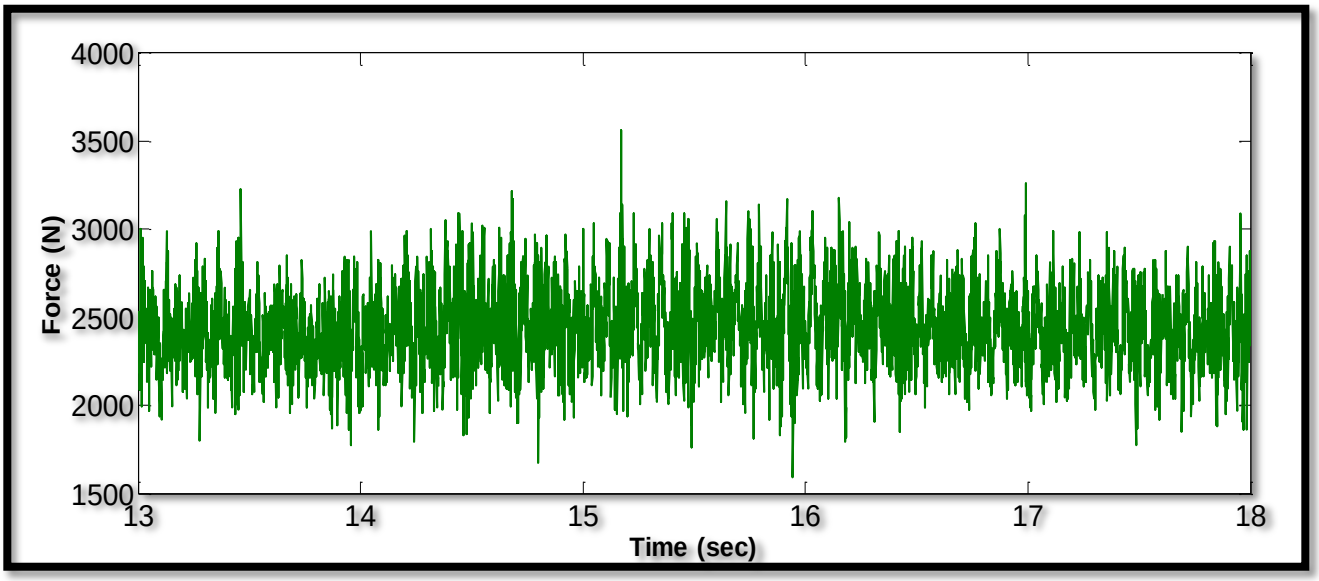

Figure 6.11- Force profile at 1802 N when the PPG was attached

Figure 6.10 shows that the average force is 2250 N with peaks reaching 2900 N and a deviation of ±200 N from the average value at different points. Considering that the load cell reads an extra WOB due to the weight of the pressure cell, the movable plate and the rock sample. Where in Figure 6.11, the forces increase with pulses to reach peaks of 3250 N, the overall average was 2600N with a deviation of ±400N from the average value at different points. That means that the PPG actually introduced an addition force of about 400 N, which contributed to the higher displacement and the higher ROP. The spectral analysis of the LVDT shown in Figure 6.12, also shows the presence of the PPG force signal at 9 Hz.

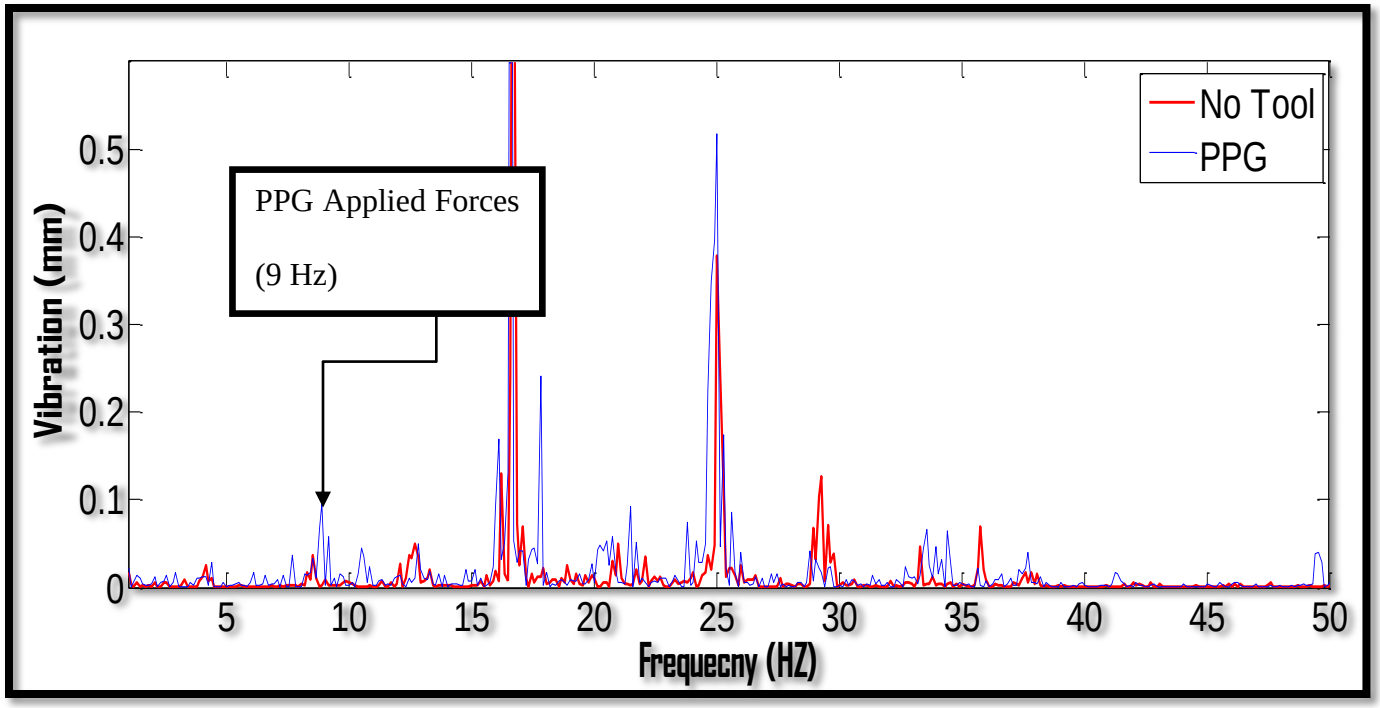

Figure 6.12- Spectrum analysis of vibration displacement with 8 mounts configuration

The MSE analysis also agreed with the ROP results as shown in Figure 6.13, where drilling with the PPG showed less power consumption and less MSE, except at the anomaly where 1650 N were applied.

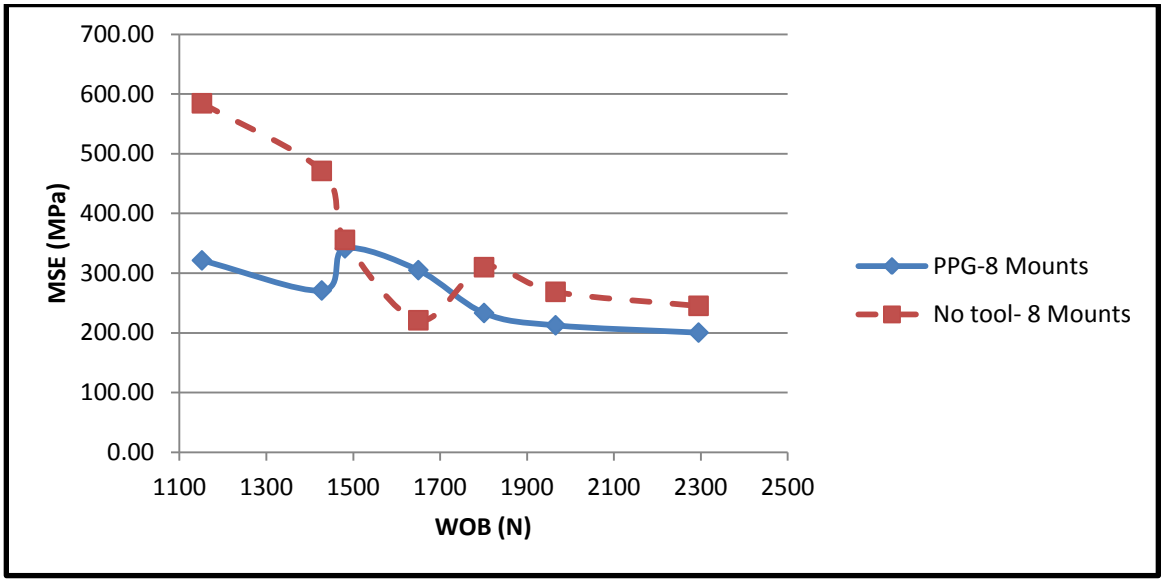

Figure 6.13- MSE vs. WOB for 8 mounts configuration

When the compliance was then changed to 0.888 mm/KN by replacing the 8 Mounts octagonal configuration to a 6 mounts hexagonal configuration, the results came out as shown in Figure 6.14. The ROP with the PPG tool installed was better except at one point when 442 Lbs WOB was applied. The displacement data is shown in Figure 6.15, confirming the relationship obtained from previous runs, and again it was observed that ROP has a direct proportional relationship with the magnitude of vibration displacement within the same compliance configuration. The maximum displacement at which the theory is no longer applicable could not be reached due to the limitations of the experimental setup.

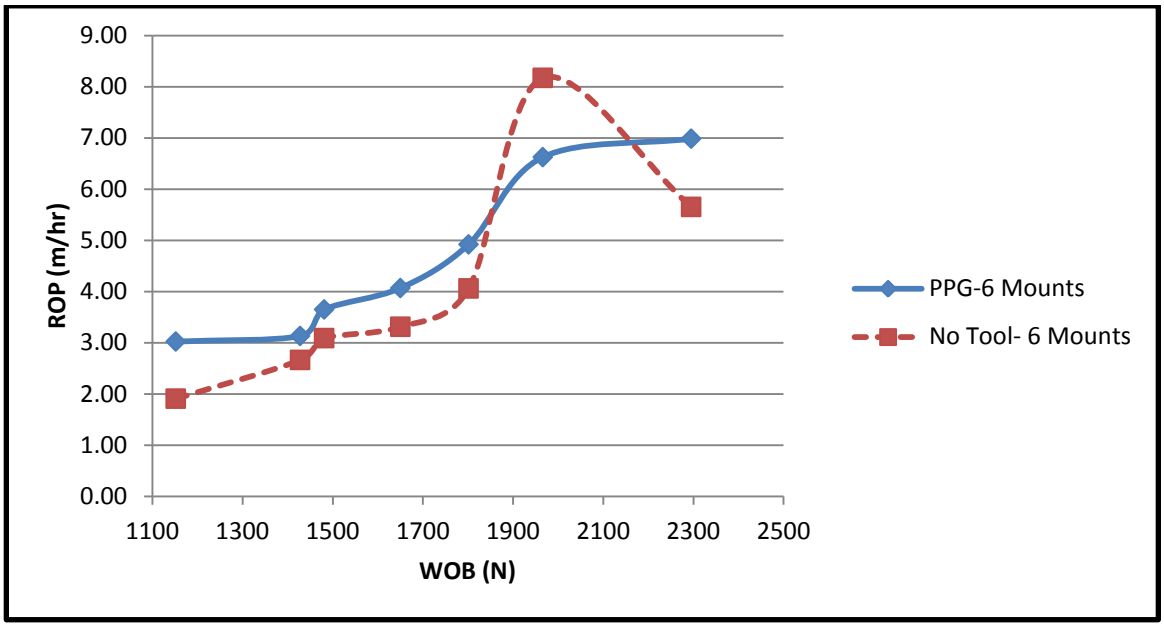

Figure 6.14- ROP vs. WOB for 6 mounts configuration

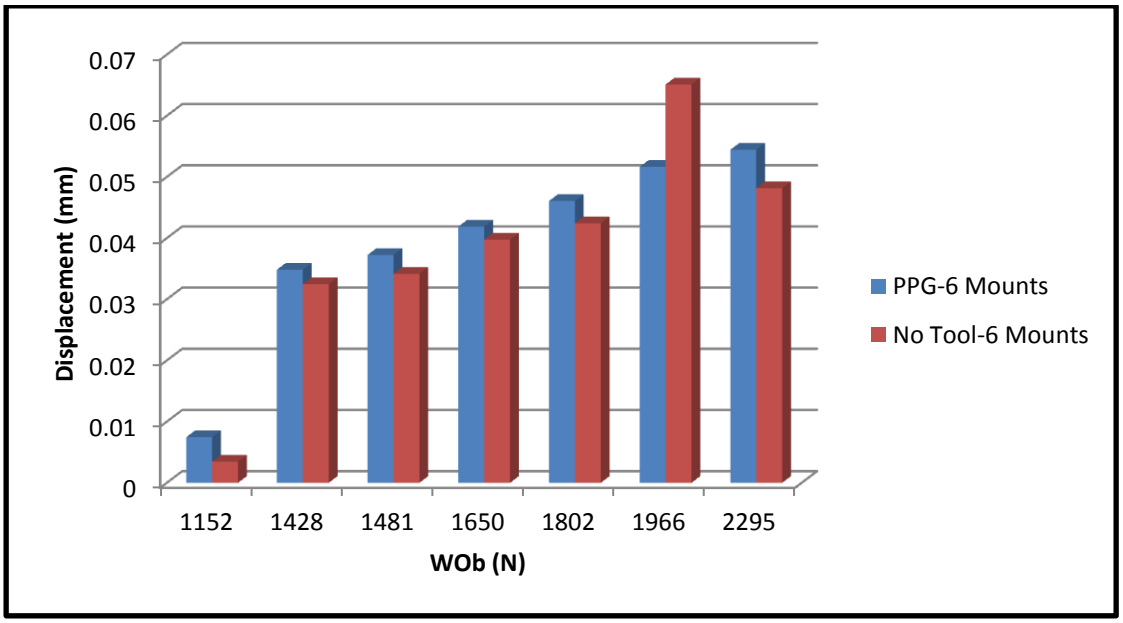

Figure 6.15-Vibration displacement vs. WOB for the 6 mounts configuration

The forces generated by the PPG are similar to the forces shown with the 8 mounts, considering that the only parameter that changes the forces of the PPG is varying the flow rate. The spectral analysis of the LVDT data shows the contribution of the PPG pulses in generating the observed vibration displacement, as shown in Figure 6.16.

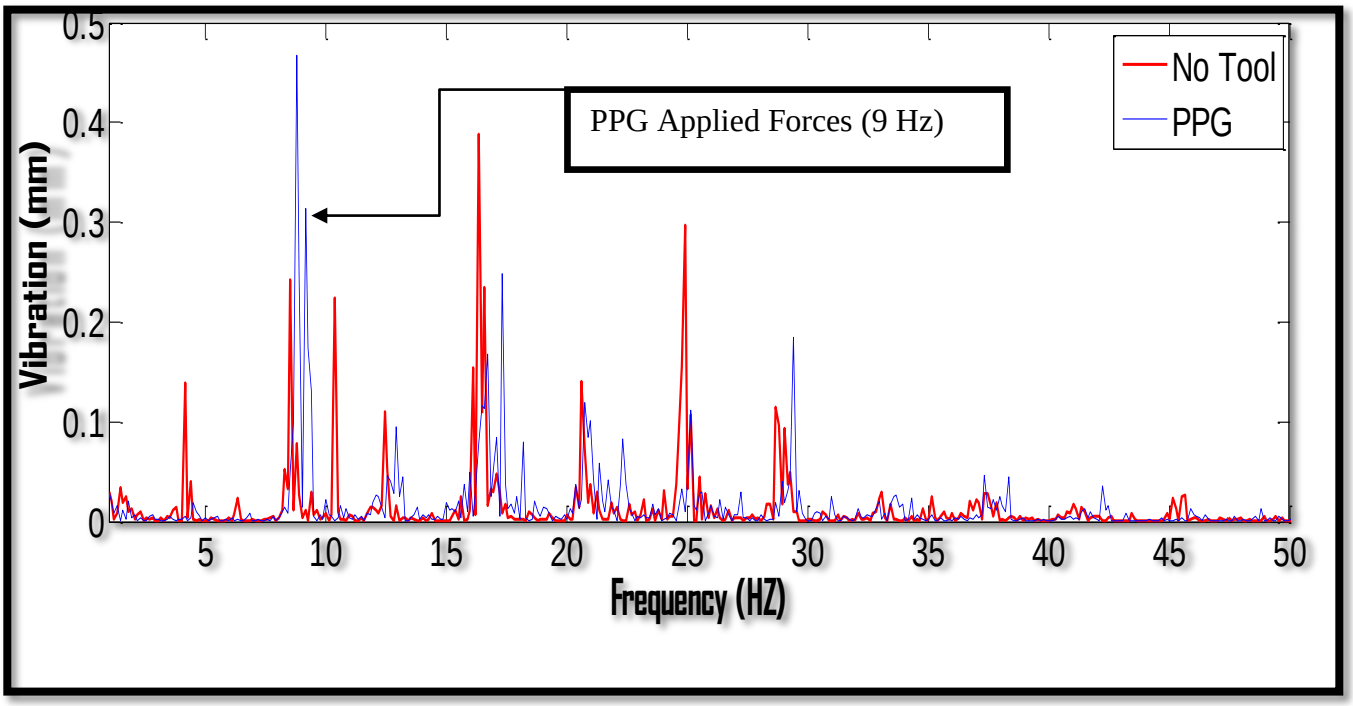

Figure 6.16- Spectral analysis of vibration displacement with the 6 mounts configuration

The MSE results also agreed with the ROP results as shown in Figure 6.17, showing that the PPG used less power and less MSE while drilling except for one point when 442 Lbs were applied on the bit.

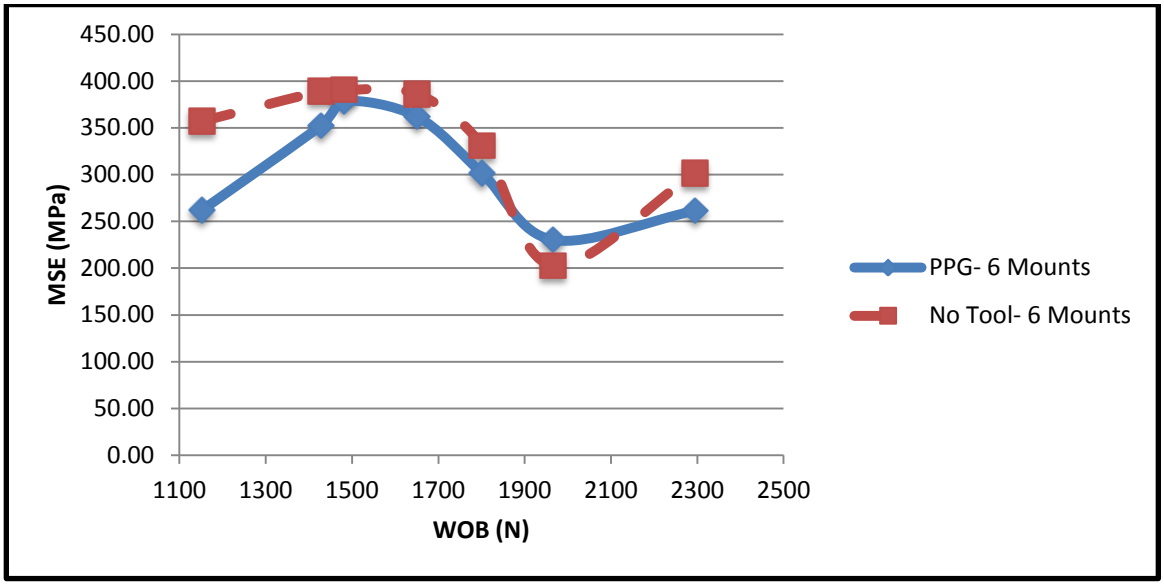

Figure 6.17- MSE vs. WOB for the 6 mounts configuration

It was also observed that although using 6 mounts provided higher vibration displacement than the 8 mounts configuration, the ROP with 8 mounts was higher. It is hypothesized that this is due to the broader interaction area between the PDC cutters and the rock due to the smaller displacement range. This theory is shown conceptually in Figure 6.18, which shows an illustration of the displacement versus the cutting area concept, while Figure 6.19 shows a comparison between the ROP of the different compliance configurations while using the PPG. It is assumed that slight compliance showed better performance as a result of utilizing the PPG additional force, while using higher compliance reduced the instantaneous cutting area of the cutter resulting in slower ROP than both slight compliance configuration and rigid configuration.

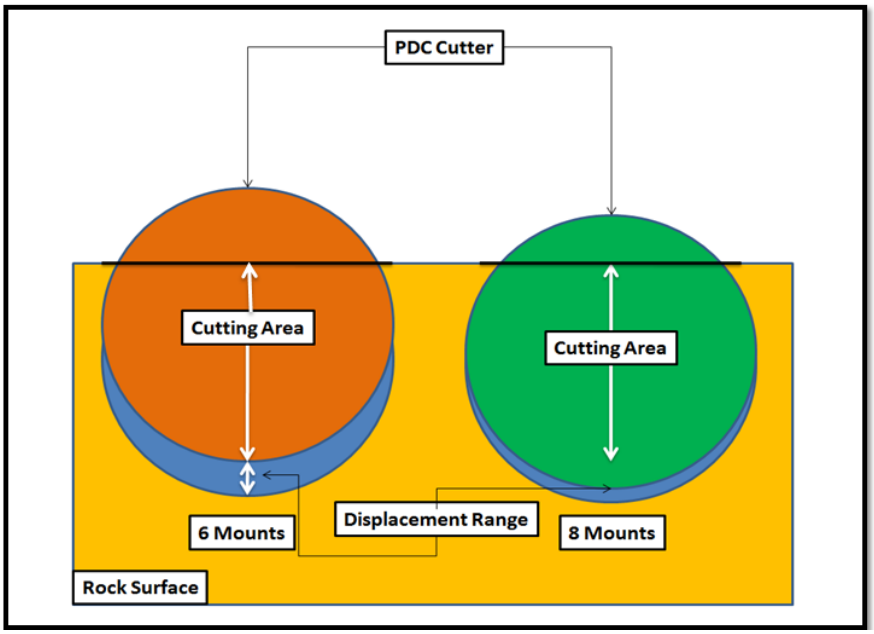

Figure 6.18- An illustration of the relationship between cutting area and displacement range

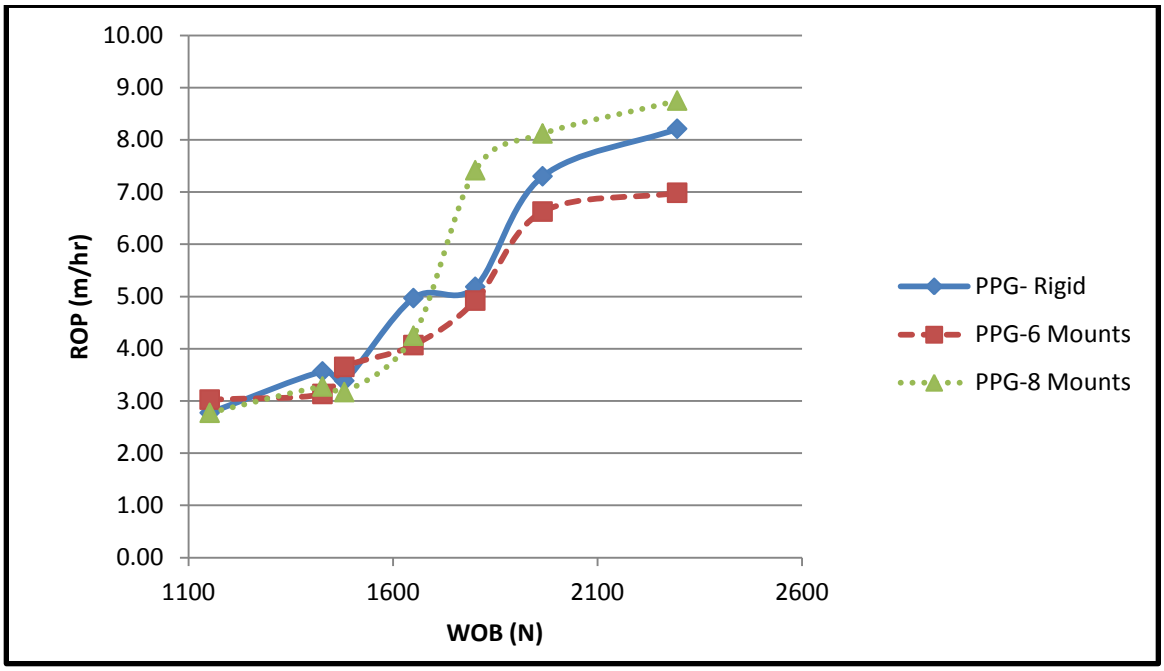

Figure 6.19- ROP of the different compliance configuration of the PPG

Additional experiments were done to investigate the effect of varying the BHP and the flow rate on the effect of the pressure pulses while maintaining 0.666 mm/KN compliance (8 Mounts) and a constant WOB of 1966 N. The results were quite as expected, when the flow rate was reduced, the forces applied by the PPG were weakened as well as the BHC efficiency when using the PPG and when not using it. Figure 6.20 shows the reduction of ROP as a result of reducing the flow rate. When the BHP was increased, the ROP dropped in both cases, which is explained as a gradual reduction in the BHC efficiency as well as a reduction of the HSI at the bit. These results are shown in Figure 6.21.

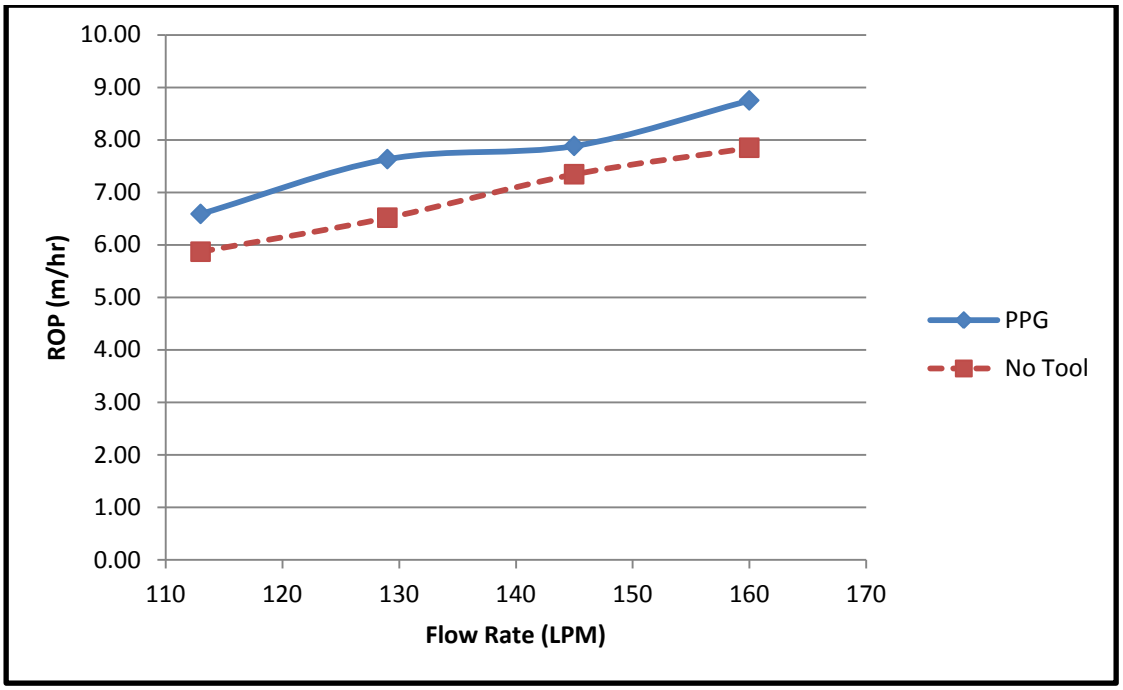

Figure 6.20- Effect of varying the flow rate on ROP

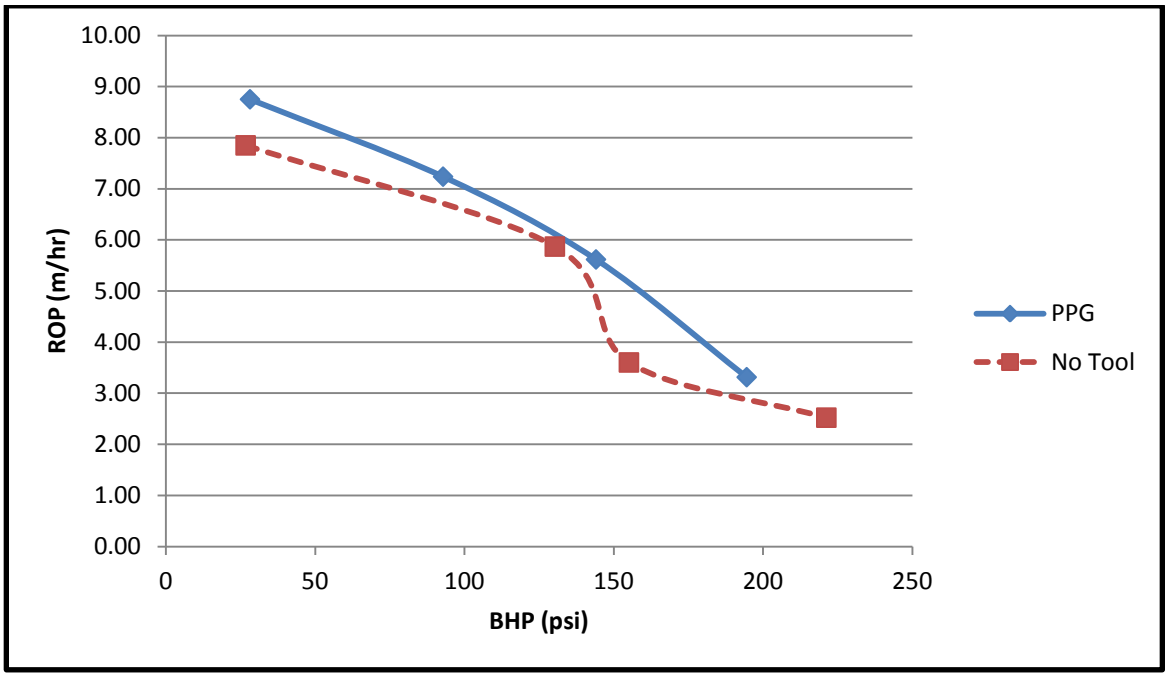

Figure 6.21- The Effect of Varying BHP on ROP

The MSE results also agreed with the results from the ROP curves and are shown in Figures 6.22, and 6.23 respectively.

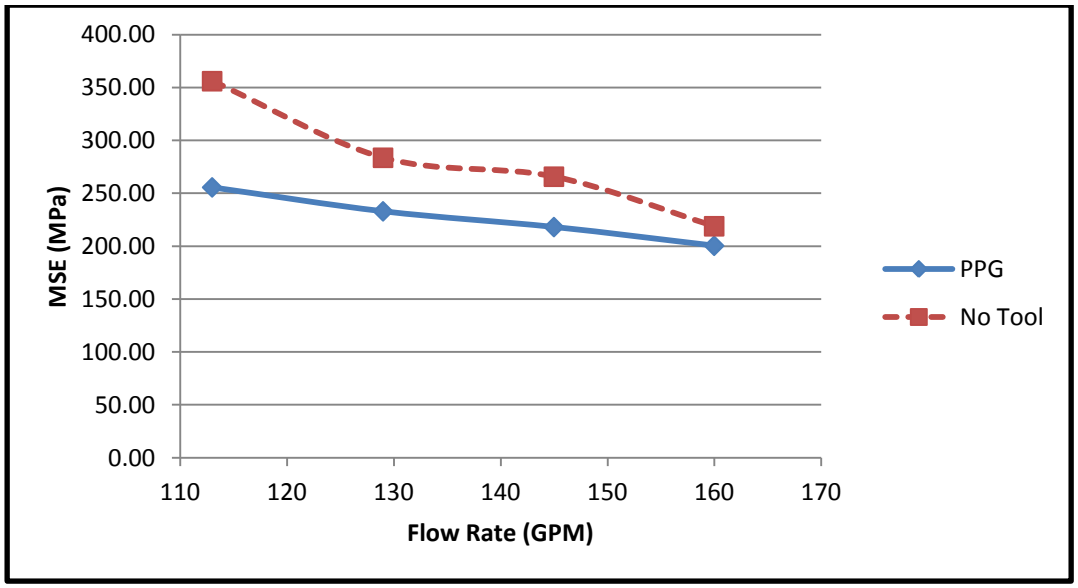

Figure 6.22- MSE vs. Flow Rate for the 8 mounts configuration

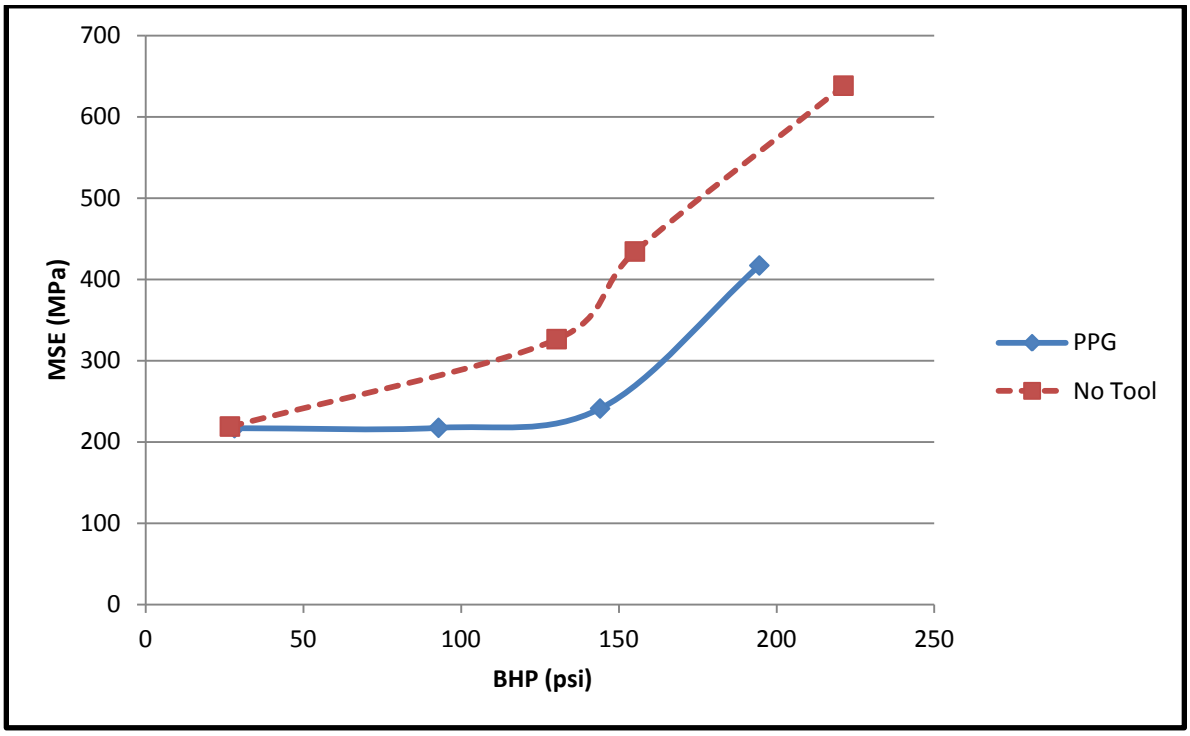

Figure 6.23- MSE vs. BHP for the 8 Mounts configuration

After conducting all sets of experiments, several significant conclusions were made, and the effect of the pressure pulses on drilling efficiency became understandable.

The conclusions are all mentioned in the next chapter.

7 Summary, Conclusion and Future Work Recommendations

In this chapter, a summary of the study is presented, including the research done on both phases of experiments, namely the characterization of the PPG and the drilling experiments. followed by the conclusion for the obtained results. Finally the issues that need to be investigated and focused on in future in that area of research are addressed and highlighted.

7.1 Research summary

The research started as an approach to widen the study of the vibration assisted rotary drilling (VARD) technology, as a part of the research done by the Advanced Drilling Group (ADG) of the Memorial University of Newfoundland. Using an existing technology to create down-hole pressure pulses, the pressure pulse generating tool was considered a potential vibration source when placed above the bit. Several sets of experiments were conducted to characterize the PPG tool given by a sponsor company to support the undergoing research in the related area.

For these experiments, the ADG developed a sophisticated experimental setup to accurately monitor the outputs from the PPG at different operational conditions. That included a reaction frame, and a comprehensive Data Acquisition and sensor setup.

It was found from the characterization experiments that the PPG introduced enough hydraulic impact forces to be an efficient VARD tool candidate.

Based on that conclusion, drilling experiments were designed to see the effect of the created pressure pulses on simulated down-hole conditions. For these experiments, the work done by the ADG to develop a laboratory scale drilling rig, experimental setup and reliable synthetic rock highly contributed to the efficiency of the conducted experiments .

The data acquired from the drilling experiments was thoroughly analyzed and the research then came to several conclusions, and given below

7.2 Conclusion

After conducting several characterization and drilling experiments, it was found that the pressure pulses and the vibration they create do affect the drilling performance. The frequency and amplitude of the pressure pulses were found proportional to one variable, which is flow rate.

In drilling, it was found that compliance played a major role in drilling performance. In other words, the pressure pulses had no effect when the system was rigid and the forces they generated were unable to create vibration by displacing the bit from the rock surface. In fact, the variation in pressure at the bit reduced the overall hydraulic horse power, which in turn affected the rate of penetration negatively, meaning that the use of the PPG without compliance actually reduced drilling performance compared to when no tool was used. When compliance was introduced to the drilling setup to match the real drilling conditions (where no rigid system exist due to the drill string flexibility), it was found that the pressure pulses positively affected the ROP and reduced the MSE used.

It was also found that when the displacement was high enough to reduce the contact between the cutter and the rock surface, the cutting area became smaller, and the effect was negative on the drilling performance.

It was also observed, that within the same compliance system, the ROP is directly proportional to the rock displacement. The result of varying flow rates, showed that the performance effect of the pressure pulses is directly proportional to the flow rate, where the frequency and amplitude of pulses are directly related to the flow rate used to operate the tool. Increasing BHP negatively affected the performance in all cases. However, the drilling performance when the pressure pulses were generated was still higher than when no pressure pulses existed. After all, the overall conclusion is that whenever there was axial compliance within the drilling system, the pressure pulses lead to better performance.

7.3 Future Work Recommendations

Due to the limitations of the drilling setup used, including the capacity of the pump and the range of weights that could be applied on the drilling bit, the experiments could not reflect the effect of the pressure pulses at higher flow rates and higher weights on bit. Further laboratory experiments can be carried on to study the effect of the pressure pulses at these high end conditions, to see the effect of higher dynamic to static load ratio which could not be achieved with the current setup. Also, it's highly recommended to use the PPG tool as a VARD tool coupled to a full scale bottom-hole assembly to test it under actual field conditions to move the technology to a higher readiness level, and prove the technology as an industry performance improvement.

8 References

[1] Drilling history article (2014). Retrieved from http://www.rigsinternational.com/our-offer/history-of-drilling/

[2] Ruehl, C., & Giljum, J. (2011). BP energy outlook 2030. *Energy, 2030*, 2.

[3] Offshore rig day rates (2014). Retrieved from http://www.rigzone.com/data/dayrates

[4] Vieira, P., Lagrandeur, C., and Sheets, K. (2011). Hammer drilling technology-the proved solution to drill hard rock formations in the middle east. Paper presented at the *SPE Middle East Oil and Gas show and Conference*,

[5] Taylor, M., Murdock, A., and Evans, S. (1996). High penetration rates and extended bit life through revolutionary hydraulic and mechanical design in PDC drill bit development, SPE 36435. *Society of Petroleum Engineers, Inc*, , 191-204.

[6] Mensa-Wilmot, G., Langdon, S. P., and Harjadi, Y. (2010). Drilling efficiency and rate of penetration: Definitions influencing factors relationships and value. Paper presented at the *IADC/SPE Drilling Conference and Exhibition*,

[7] Pessier, R. C., Wallace, S. N., and Oueslati, H. (2012). Drilling performance is a function of power at the bit and drilling efficiency. Paper presented at the *IADC/SPE Drilling Conference and Exhibition*,

[8] Brantly, J., and Clayton, E. H. (1939). A preliminary evaluation of factors controlling rate of penetration in rotary drilling. Paper presented in the *Drilling and Production Practice, 1 January, New York, New York*, API-39-008

[9] Garnier, A., and Van Lingen, N. (1959). Phenomena affecting drilling rates at depth, SPE-1097-G, Published in *The Petroleum Transactions, AIME, Volume 216, 1959, pages 232-239.*

[10] Garner, N. (1967). Cutting action of a single diamond under simulated borehole conditions. *Journal of Petroleum Technology, 19*(07), 937-942.

[11] Black, A., Dearing, H., & DiBona, B.Effects of pore pressure and mud filtration on drilling rates in a permeable sandstone" paper SPE 12117. *JPT (Sept.1985), 1671*

[12] Maurer, W. (1962). The" perfect-cleaning" theory of rotary drilling. *Journal of Petroleum Technology, 14*(11), 1,270-1,274.

[13] Wells, M., Marvel, T., and Beuershausen, C. (2008). Bit balling mitigation in PDC bit design. Paper presented at the *IADC/SPE Asia Pacific Drilling Technology Conference and Exhibition,*

[14] Feenstra, R., and Van Leeuwen, J. (1964). Full-scale experiments on jets in impermeable rock drilling. *Journal of Petroleum Technology, 16*(03), 329-336.

[15] Yaveri, M., Damani, K., and Kalbhor, H. (2010). Solutions to the down hole vibrations during drilling. Paper presented at the *Nigeria Annual International Conference and Exhibition*,

[16] Ashely, D., McNary, X., and Tomlinson, J (2001). Extending bit life with multi-axis vibration measurements. Paper presented in the *SPE/IADC Drilling Conference, 27 February-1 March, Amsterdam, Netherlands* SPE/IADC, 67696

[17] Eskin, M., Maurer, W. C., and Leviant, A. (1995). In Maurer Engineering (1st Ed.), *Former-USSR R&D on novel drilling techniques Pages 8-21*

[18] Barkap, D. D. e. a. (1957). In Maurer Engineering (1st Ed.), *Former-USSR R&D on novel drilling techniques page.22*

[19] Baidyuk, B.V. e. a. (1993). In Maurer Engineering (1st Ed.), *Former-USSR R&D on novel drilling techniques pages 18-22*

[20] Izosimov, A.M., Volokhin, A.V. and Khacharuridze, Ya. F., (1980): ``*Well Drilling Device*," USSR Authorship Certificate No. 899836, applied for January 23, 1980.

[21] Sintsov, Ye. A. et al., 1985: ``Drilling Tool," USSR Authorship Certificate No. 1469086, applied for November 27, 1985.

[22] Pennington, J. V. (1953). Some results of DRI investigation-rock failure in percussion. Paper presented in the *Drilling and Production Practice, 1 January, New York, New York*, API-53-329

[23] Li, H., Butt, S., Munaswamy, K., and Arvani, F. (2010). Experimental investigation of bit vibration on rotary drilling penetration rate. Paper presented at the *44th US Rock Mechanics Symposium and 5th US-Canada Rock Mechanics Symposium, Salt Lake City, UT, June,* 27-30.

[24] Li, H. (2011). *Experimental investigation of the rate of penetration of vibration assisted rotary drilling.* Unpublished manuscript, available at the Memorial University Library and the ADG Laboratory.

[25] Babatunde, Y., Butt, S., Molgaard, J., and Arvani, F. (2011). Investigation of the effects of vibration frequency on rotary drilling penetration rate using diamond drag bit. Paper presented at the *45th US Rock Mechanics/Geomechanics Symposium (ARMA), San Francisco, CA, Paper,* (11-527)

[26] Babatunde, Y. (2011). *The effect of varying vibration frequency an amplitude for drilling optimization.* Unpublished manuscript, available at the Memorial University Library and the ADG Laboratory.

[27] Khorshidian, H., Mozaffari, M., and Butt, S. (2012). The role of natural vibrations in penetration mechanism of a single PDC cutter. Paper presented at the *46th US Rock Mechanics/Geomechanics Symposium,*

[28] Gharibiyamchi, Y. (2013). *Evaluation and characterization of hydraulic pulsing drilling tools and potential impacts on penetration rate* ,Unpublished manuscript, available at the Memorial University Library and the ADG Laboratory.

[29] Ledgerwood III, L. (2007). PFC modeling of rock cutting under high pressure conditions. Paper presented at the *1st Canada-US Rock Mechanics Symposium*,

[30] Babapour, S., and Butt, S. D. (2014, August). Investigation of Enhancing Drill Cuttings Cleaning and Penetration Rate Using Cavitating Pressure Pulses. In *48th US Rock Mechanics/Geomechanics Symposium*. American Rock Mechanics Association.

[31] Pronin, O. (2012). *Pulse-Cavitation vibrating drilling prototype development and evaluation* , Unpublished manuscript available at the Memorial University Library and the ADG Laboratory.

[32] Hustrulid, W. A., and Fairhurst, C. (1971). A theoretical and experimental study of the percussive drilling of rock part I—theory of percussive drilling. Paper presented at the *International Journal of Rock Mechanics and Mining Sciences & Geomechanics Abstracts, , 8*(4) 311-333.

[33] Han, G., Bruno, M., and Lao, K. (2005). Percussion drilling in oil industry: Review and rock failure modelling. Paper presented at the *American Association of Drilling Engineers Paper AADE-05-NTCE-59, AADE National Technical Conference & Exhibition, Houston, April 2005,*

[34] Cheng, R., Ge, Y., Wang, H., Ni, H., Zhang, H., and Sun, Q. (2012). Self-oscillation pulsed percussive rotary tool enhances drilling through hard igneous formations. Paper presented at the *IADC/SPE Asia Pacific Drilling Technology Conference and Exhibition*,

[35] Kolle, J.J., "*Hydraulic Pulse Drilling: Final Report*" Presentation for GTI Natural Gas Technology II Conference, February 8 – 11, 2004.

[36] McCarthy, J., Stanes, B., Clark, K., and Kollker, C.A sten change in drilling efficiency: Quantifying the effects of adding an axial oscillation tool within challenging wellbore environments" SPE/IADC 119958 presented at the 2009 SPE/IADC drilling conference and exhibition.

[37] Skyles, L., Amiraslani, Y., and Wilhoit, J. (2012). Converting static friction to kinetic friction to drill further and faster in directional holes. Paper presented at the *IADC/SPE Drilling Conference and Exhibition*

[38] Robertson, L., Mason, C., Sherwood, A., and Newman, K. (2004). Dynamic excitation tool: Developmental testing and CTD field case histories. Paper presented at the *SPE/ICoTA Coiled Tubing Conference and Exhibition,*

[39] Rasheed, W. (2001). Extending the reach and capability of non rotating BHAs by reducing axial friction. *SPE/ICoTA Coiled Tubing Roundtable, 7-8 March, Houston, Texas*

[40] Standard, A.D7012–10 (2010) standard test method for compressive strength and elastic moduli of intact rock core specimens under varying states of stress and temperatures. *Annual Book of ASTM Standards, American Society for Testing and Materials, West Conshohocken, PA,*

Appendix A: Drill Bit Shank Design

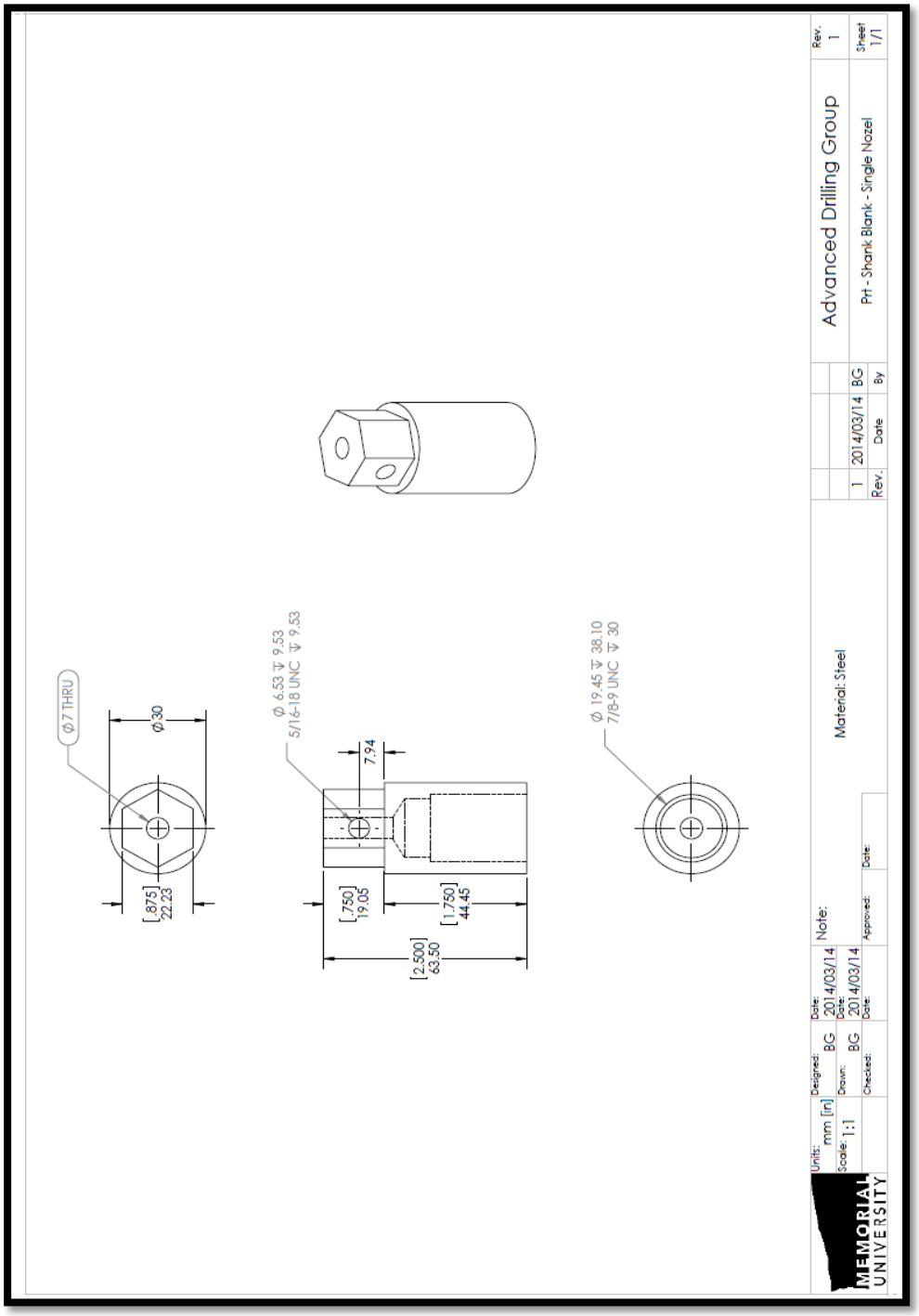

Appendix B: Petro-graphic Information of the Aggregates in Rock Specimens

The following table, shows the petro-graphic information of the aggregates, which were used for the preparation of the rock specimens.

Table - Petro-graphic Information of rock aggregates

Rock/Mineral Types	Total per sieve fraction (%)					
	5-2.5 mm	2.5-1.5 mm	1.25-0.63 mm	0.63-0.315 mm	0.315-0.16 mm	Weighted Content
	17.40%	19.10%	18.20%	18.30%	16.10%	-
Granit	80%	72%.5	27.40%	6.30%	0	38.10%
Volcanic	17.30%	8.40%	7.90%	1.20%	0.60%	7%
Quartz	1.40%	10%	34%	76.20%	86.40%	40.60%
Feldspar	0	8.20%	30%	12%	7.60%	11.70%
Biotite	0	0	0	2.80%	3.80%	1.30%
Weathered Particles	1.30%	0.90%	0.70%	1.50%	1.60%	1.20%
Total	100%	100%	100%	100%	100%	99.90%